Bulletin 658

COMPUTER SIMULATION OF PARTICULATE SYSTEMS

UNITED STATES DEPARTMENT OF THE INTERIOR

BUREAU OF MINES

1971

Bulletin 658

COMPUTER SIMULATION OF PARTICULATE SYSTEMS

By Lindsay D. Norman and others

BUREAU OF MINES
Elbert F. Osborn, Director

UNITED STATES DEPARTMENT OF THE INTERIOR
Rogers C. B. Morton, Secretary

This publication has been cataloged as follows:

Norman, Lindsay D

Computer simulation of particulate systems, by Lindsay D. Norman and others. [Washington] U.S. Dept. of the Interior, Bureau of Mines [1971]

55 p. (U.S. Bureau of Mines. Bulletin 658)

1. Bulk solids. 2. Digital computer simulation. I. Title. (Series)

TN23.U4 no. 658 622.06173

U.S. Dept. of the Int. Library.

For sale by the Superintendent of Documents, U.S. Government Printing Office
Washington, D.C. 20402 - Price 60 cents
Catalog No. I 28.3:658
Stock Number 2404–0946

CONTENTS

ILLUSTRATIONS

TABLES

COMPUTER SIMULATION OF PARTICULATE SYSTEMS

by

Lindsay D. Norman [1] and others [2]

ABSTRACT

Computer models for simulating the construction and for calculating the properties of particulate solids in two- and three-dimensional systems (coverings of circles and packings of spheres, respectively) were developed. By simulating the physical process of constructing circle coverings and sphere packings, in which the circles or spheres were randomly selected from many different distributions of sizes, physically realizable loose random assemblies were simulated whose physical and geometrical properties were predictable with the computer. Many of these properties, such as the number of contacts, are extremely difficult to measure accurately, or considerable ingenuity is required in their determination. All of these properties were easily and accurately calculated by the computer models for many different coverings and packings constructed from equal, discrete, uniform, and log-normal distributions of particles. In addition to the loose random assemblies, dense random covering and packing constructions were simulated whose properties are ideal upper limits for those of the loose random coverings and packings. The properties of the dense random coverings and packings, heretofore only obtainable by theoretical analysis, were also simply obtained.

The statistical geometry of loose random coverings and packings was studied, and several new interpretations of the area-covering or space-filling requirements in these systems were made. In two dimensions, it was found that the properties of all loose random coverings are predictable by taking suitably weighted averages of the corresponding properties of just four kinds of polygons whose edges are defined by connecting the centers of mutually tangent circles in the covering. The distributions of these polygons that permit area-covering were determined, and empirical equations for predicting the density, average coordination number, and average pore area in loose and dense random coverings were formulated.

The properties of loose packings were determined by performing a simplicial division of the computer-simulated assemblies to produce a unique set of minimum volume, space-filling tetrahedra whose edges connected the sphere centers in each packing. A simple empirical equation was formulated that permits the calculation of the average number of contacts in any sphere packing, random or regular.

Some of the statistical geometrical properties of the simplicial tetrahedra in

[1] Staff assistant to the Deputy Director—Mineral Resources and Environmental Development, Bureau of Mines, Washington, D.C.

[2] The two other authors who contributed to this bulletin are identified in the chapters in which their work first appears.

the computer-simulated packings were analyzed. The tetrahedron edge length distributions in all the loose random packings were nearly identical when the edges were presented in terms of sphere diameters, regardless of the sphere population in the packing. Moreover, the gap lengths in the loose packings were to an excellent approximation representable by a uniform distribution of sizes. The distributions of spheres in tetrahedra resulting from the simplicial division of the loose random packings also existed in the tetrahedra in dense random packings. These observations were employed in developing a unique method for predicting the geometrical properties of loose random packings without simulating the assembled packing. Instead, the space-filling simplicial graph could be predicted for any given density of packing of any sphere population. The cumulative packing properties of these tetrahedra were shown to be nearly identical to those calculated by all loose random packing simulations attempted in this investigation. The simplicial tetrahedra completely describe a packing and can therefore be used to predict all properties of interest.

INTRODUCTION

Over the past century considerable interest in particulate systems has been revived owing to their importance in many technologies and industries. These systems are composed of discrete, solid particles whose mean diameter usually exceeds 0.1 micron. The volume of these systems is comprised partly of contacting particles and partly of voids, which may or may not be filled with another material. The behavior of particle assemblies is important in powder metallurgy and ceramics; in studies of sedimentation, seepage, and flow through porous media and packed beds; in defect and surface structures; and in describing ideal liquid structures, sintering, bulk flow of granular materials, compaction, and grinding, to name a few.

In virtually all systems of particulate solids, the configuration of the particles directly influences the observed properties of the system. Frequently, whether or not the particles are packed efficiently is of paramount importance. However, there is but meager published information on either the internal geometry of such systems or precise analytical formulations that would permit the optimization or prediction of packing characteristics. If such formulations are to be developed to any degree of general applicability, the configurational geometry, or statistical geometry, of particulate systems must be elucidated. Most of the data that does exist is empirical, it having been developed to solve specific technological problems. Such data have only limited applicability in solving problems of how particles pack and how, in general, bulk properties may be analytically predicted and interpreted.

Problems of this nature have been of concern to the Bureau of Mines since the 1920's, when Furnas (*1*) [3] was among the first to study aggregate packings. Since that time, many packing studies have been made. However, understanding of packing geometry and the ability to predict particulate system properties remain in almost the same state as existed 40 years ago. In an effort to improve this situation, the Bureau reinitiated studies of particulate packings in 1967 in the belief that the complexities heretofore encountered in attempting to describe particulate assemblies could be solved by the use of modern electronic data processing techniques. The initial part of this research consisted of a thorough review of the literature to provide a framework for subsequent studies. A summary of the results of this review is presented in chapter 1.

The first objective of the present Bureau research was the development of a means to model random assemblies of circles and spheres that would accurately

[3] Italicized numbers in parentheses refer to items in the list of references at the end of the "Introduction."

simulate actual particulate systems. Circles and spheres were chosen to simplify the development. This was not considered a serious limitation, because the majority of real three-dimensional packings are composed of nearly spherical particles or of particles that can be statistically treated as spheres. Similar reasoning was applied to the two-dimensional case. The myriad arrangements and sizes of particles existing in irregular random assemblies, which precluded the successful development of earlier models, called for new and novel approaches to the problems of model building. In this investigation these problems were largely solved by the use of electronic data processing techniques. Computer-simulated constructions of random coverings and packings from any distribution of particles were made possible by the immense capacity for performing mathematical calculations in existing computers. In addition to simulating the construction of particulate systems, the computer was also employed to calculate their statistics and properties. The computer programs developed for these purposes were written in FORTRAN IV computer language and were compiled and run on an IBM 7094 machine.

The second objective of this research was to develop the computer simulations to the point where they could be used to predict real packing or covering properties and to develop a body of data that could be used to improve and add to what is currently known about the statistical geometry of random particulate systems. In chapter 2 the computer model developed to simulate dense random coverings of circles is described. Chapters 3, 4, and 5 are given over to computer simulation models of dense random packings of spheres, loose random coverings of circles, and loose random packings of spheres, respectively. A method for predicting the properties of loose random packings of spheres that does not require the simulation of assembled packings is described in chapter 6.

REFERENCE

1. Furnas, C. C. Flow of Gases Through Beds of Broken Solids. BuMines Bull. 307, 1929, 144 pp.

— 1 —

PREVIOUS ATTEMPTS TO CHARACTERIZE PARTICULATE SYSTEMS

by

Lindsay D. Norman

In the past two and a half centuries, many physicists, mathematicians, and engineers have studied with varying degrees of rigor the geometrical problems associated with the packing of particles. Almost all of these investigations were based on filling space with the most regular body, the sphere, repeated in a regular pattern. In 1883 the early crystallographer Barlow (*1*) [1] showed that the densest space-filling packings were the close-packed hexagonal and face-centered cubic forms of crystal structures. As other crystal structures were identified, their use in describing the geometry of particulate systems became widespread. This was particularly true in the 1930's after Graton and Fraser (*16*) published their detailed account of the five ways that equal, hard spheres could be regularly arranged to fill space. Some relevant properties of unit cells arranged these five ways with equal spheres are listed in table 1; their plane sections are shown in figure 1.

The simplest of all the regular arrangements is the cubical packing, formed by stacking cubes having sides equal to twice the sphere radius. Each unit cell of volume $8R^3$ contains one octant of each of eight spheres; thus, it contains one sphere and has a packing density of $\pi/6=0.5236$, as shown in table 1. Similarly, the cubical-tetrahedral, or single-stagger, unit cell has a volume of $4R^3\sqrt{3}$ and a packing density of $\pi/3\sqrt{3}$. The tetragonal-sphenoidal, or double-stagger, packing is similar to the cubical-tetrahedral packing except that each sphere in a given layer rests in the depression between adjacent spheres in adjoining layers. Its unit cell volume is $6R^3$, and it has a density of $2\pi/9$. In pyramidal packings spheres rest in the holes formed by four tangent spheres in adjoining layers. Each sphere contacts four others in each of three adjacent layers to give a unit cell volume of $4R^3\sqrt{2}$ and a density of $\pi/3\sqrt{2}$. Tetrahedral packings have the same coordination number (the number of spheres in contact with a given sphere) and density as pyramidal packings, but in this case, each sphere rests in triangular holes in the adjacent layers. In all regular packings of large volumes of equal particles (large enough to eliminate electrostatic forces, air films, boundary effects, etc.), packing density is independent of the size of the particles.

Table 1.—Characteristics of regular packings of equal spheres

Regular packing	Coordination number [1]	Layer spacing	Density
Cubical (simple cubic)	6	2	0.5236
Cubical-tetrahedral	8	2	.6046
Tetragonal-sphenoidal	10	$\sqrt{3}$	.6981
Pyramidal (rhombohedral)	12	$\sqrt{2}$	.7405
Tetrahedral (rhombohedral)	12	$2\sqrt{2}/\sqrt{3}$	.7405

[1] The number of spheres in contact with any given sphere.

For years, many investigators used regular structures having relatively simple geometries to describe actual particle packings, even though these structures were impossible to approach in experiments on real particle packings. Smith, Foote, and Busang (*39*) were among the first to

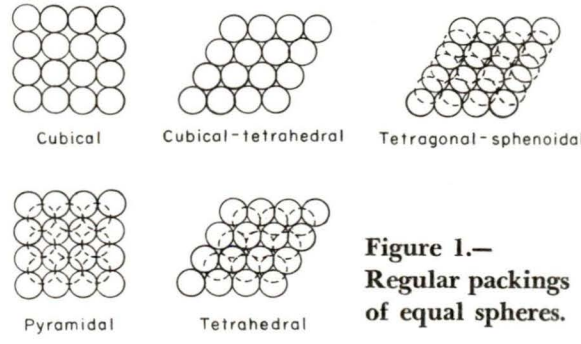

Figure 1.— Regular packings of equal spheres.

[1] Italicized numbers in parentheses refer to items in the list of references at the end of this chapter.

report on experimental packings of hard spheres. Their measurements showed that lead shot poured into a container formed an irregular array with a density of about 0.553. Shaking the container resulted in successive improvements to 0.628. Measured coordination numbers at these densities were 6.9 and 9.4, respectively. They demonstrated that the irregular arrays could, to a fair approximation, be treated as separate tetrahedral and cubical arrangements. By a judicious mixing of the two regular structures, they were able to find the proper proportion of each that yielded the experimentally observed packing density and coordination. The empirical equations

$$\Phi=0.5236+0.2169X \quad (1)$$

and

$$N=(6+10.968X)/(1+0.414X) \quad (2)$$

were developed from these data. The equations describe density Φ and coordination N as functions of the fraction X of particles that are packed tetrahedrally. The shaken density obtained by Smith, and coworkers is in excellent agreement with the 0.631 found later by Westman and Hugill (*43*) and the 0.634 found by White and Walton (*44*). The effects on packing density of particle shape and size and of adding filler spheres in the voids of the five theoretically possible regular arrangements were also reported by White and Walton. Additions of very fine filler spheres gave a maximum density of 0.961. Packing eliptically shaped particles did not significantly increase density, whereas irregularly shaped particles having greater departures from sphericity than ellipsoids actually decreased packing density below 0.63.

From the aforementioned experiments, it is clear that equal, hard, spherical particles in real packings tend to pack to densities not far from 0.63. This value is considerably lower than that of the most stable regular packing, the tetrahedral, or close-packed, array. However, this is not surprising if one considers the randomness with which particles are introduced into most particulate systems; in fact, in a system subject only to gravitational forces and free of other constraints such as container walls, a diversity of geometrical forms is always formed. This realization led to the designation of two distinct types of particle assemblies: regular packings, in which the particles form a repeating pattern in space, and random packings, which usually have some statistical particle size distribution randomly arranged in a nonregular structure. This distinction became particularly important in the early 1950's with the initiation of extensive studies in powder metallurgy and ceramics. Ceramic and metal packings are invariably produced from multisize particles. Thus, predicting packing characteristics based on interpretations of regular arrangements of equal particles was impossible. Other than the empirical work of Furnas (*14*) and Westman and Hugill (*43*), no significant research was conducted before 1950 to determine how particle size distribution affects packing properties.

It is convenient to distinguish two types of random packing: dense and loose. Dense random packing describes an arrangement in which each particle is tangent to all of its nearest neighbors, with no gaps between adjacent particles. The ideal situation of gapless assemblages and therefore high densities in dense packing serves as a useful upper limit for the more realistically obtainable packings in which gaps exist between some particles. These latter packings are considered loose random packings.

The ideal nature of the dense randomly packed structure and the seeming inability to obtain it experimentally have fascinated many scientists for years. Since Barlow (*1*) described close-packed regular structures having densities of 0.7405, it has been assumed that these had the maximum attainable density for any packing of equal spheres. Investigation of less systematic, or random, packings in the past two decades, however, has revealed the possibility of packings with greater densities. Although the question of whether or not dense random packings can exist has not been completely resolved, several mathematicians have made theoretical estimates of the geometrical packing properties that equal-sphere packings of this nature would have. In 1947 Hudson (*19*), while studying the clustering of equal spheres of radius R around a central sphere, showed that dense packing of the 12 neighbors in the close-packed structures would occur if the central sphere had a radius of $0.90215R$. If the central sphere had a radius R, Boerdijk (*7*) and Rogers (*31*) proved that theoretical densities as high as 0.7797 could exist, and Coxeter (*8*), among others, proved that the corresponding number of contacting spheres would be greater than 13. For one accustomed to the idea that tetrahedral packings are the densest possible, the paradox of the 13th sphere was conceptually very difficult. However, as far back as 1939 Marvin (*25*) had compressed random packings of lead shot to form bodies with an average of 14 faces,

the equivalent of 14 contacts. Later, Matzke (*26*) microscopically examined 600 central bubbles in a froth and found the average number of contacts was 13.7.

The statistics of dense random particle packings were first considered by Wise (*45*). He considered the characteristic sphere size distributions of many real particle assemblies. General statistical equations for calculating density and number of contacts were developed for a dense random packing that was mathematically cut into tetrahedra, with each tetrahedron having its vertices at the centers of four mutually tangent spheres. For a log-normal distribution of spheres with a standard deviation of 1.685, Wise estimated the packing density at 0.8. Wise's nonrigorous work was the first of its kind for multisize particle distributions, but his equations could only handle very special continuous particle distributions. In 1963, Hogendijk (*18*) reported similar results for dense random packings of discrete radii distributions with one, two, three, four, and five different sphere sizes. Numerical evaluations of several geometric properties of the dense-packed heaps of spheres were made, and for equal spheres, these gave density estimates in agreement with the theoretical value of 0.7797 obtained by Rogers (*31*).

The second type of random packing, loose random packing, occurs in almost all real particle packings, and for this reason it is perhaps the most interesting, if least understood, of all the particle assemblies. In 1959 the geometry of loose random packings of equal particles was proposed by Bernal (*2*) to represent the structure of ideal, liquids. The essential proposition in Bernal's theory was that liquids are "homogenous, coherent, and essentially irregular assemblages of molecules containing no crystalline regions or holes large enough to admit another molecule." The radial distribution functions of simple liquids such as liquid argon were used by Bernal to construct ball-and-spoke models of the corresponding irregular loose packings. From these models he was able to measure the number of balls that would theoretically contact each ball. This number was near 10 in his models, and he called it the number of physical neighbors. In another experiment balls of plasticene were packed together irregularly and pressed into a solid mass. Topological analysis of the resulting polyhedra showed the predominance of pentagonal faces on a wide variety of polyhedra. Bernal called the number of faces on each polyhedron the geometrical coordination, or the number of geometrical neighbors, of that polyhedron. In the ball-and-spoke model equivalent polyhedra were examined by constructing the planes that bisected the distances between each ball and any other close to it. A convex polyhedron formed by these planes surrounded each ball so that the number of geometrical neighbors could be calculated. In the ball-and-spoke model this number was 13.6; in the plasticene model it was 13.3. This number is necessarily higher than the number of physical neighbors, because in addition to the contacting balls, nearly contacting balls were also considered. The maximum estimated density in the Bernal ball-and-spoke model was some 10 percent less than regular close-packing. These data confirmed the earlier observations of Smith, Foote, and Busang (*39*), among others, that regular close-packing and irregular packing are arrangements of quite different local coordination and of different density.

Applying topological considerations to the problem of filling space with ideal bodies, Smith (*36–37*) proved that space-filling irregular polyhedra sharing faces with as many as 20 neighbors were theoretically possible. However, 14 geometrical neighbors were shown to be the most probable. Similarly, Meijering (*28*) developed two intricate statistical models describing the isotropic formation of space-filling polyhedra from nuclei distributed at random. One of these models predicted that irregular polyhedra would on the average have 13.28 faces, in excellent agreement with Bernal's plasticene model. Smith and Meijering also noted the predominance of pentagonal faces on all of the irregular polyhedra, the average number of edges per face being somewhat greater than 5.1. These data invalidated Lord Kelvin's (*20*) long-held proposition that close-packing of bodies always arose from the packing of tetrakaidecahedrons. These polyhedra are related to the truncated octahedron and have eight doubly curved hexagonal faces and six quadrilateral faces with bowed edges, for a total of 14 faces.

Prompted by the possibility that irregular arrays of equal spheres might have packing densities higher that the regular close-packed structures, Scott (*33*) poured thousands of ball bearings into spherical flasks of various sizes. He observed a range of packing densities lying between two well-defined limits, 0.637 and 0.601. The packings represented by these limits were called dense random packing and loose random packing, respectively, Scott's choice of a title for the higher density packing was unfortunate because pack-

ings having densities higher than 0.7405 had earlier been referred to as dense random packings. The convention adopted in the present study is to call Scott's maximum density packings "random close-packings;" the lower density packings "loose random packings;" and the idealized packings "dense random packings." Bernal and Mason (*6*) used a special marking technique to obtain the physical coordination of Scott's random close-packings and found it to be approximately 8.5. This value was subsequently improved upon by Scott (*34*), who devised a method for calculating random close-packing radial distributions from which an average physical coordination of 9.3 was obtained by considering all spheres within a radial distance of 1.1 sphere diameters as contacting spheres.

Bernal's theory that the holes in random packings of equal spheres could not be large enough to admit another sphere led to his determination (*3–4*) of five polyhedra having triangular faces formed by tangent spheres. The general class of polyhedra to which these belong is known as deltahedra (*9*). The five polyhedra, subsequently called the Bernal polyhedra, are shown in figure 2. Bernal found that if strict tangency of the face spheres was enforced the polyhedra could not be made to fill space. However, if the polyhedral edges were allowed to be distorted or extended up to 15 percent, he was able to show the existence of these five polyhedra in his physical models of loose random packing. The frequency of occurrence of each polyhedron in a large ball-and-spoke model was obtained; these data are listed in table 2. The number of alternate positions and coordinations offered a sphere in the five polyhedra was considered by Bernal to qualitatively explain the effects of temperature on the packing characteristics of simple liquid molecules. For the data in table 2, dense-packed tetrahedra predominate. Bernal proposed that increases in temperature would increase the probability of forming the less dense polyhedra at the expense of the tetrahedra and result in lower densities and coordination.

Table 2.—Bernal polyhedra in a large ball-and-spoke model [1]

Type of polyhedra	No. of faces	Number frequency	Volume frequency
Tetrahedra	4	0.730	0.484
Half octahedra	8	.203	.269
Trigonal prisms	14	.032	.078
Archimedean antiprisms	16	.004	.021
Tetragonal dodecahedra	10	.031	.148

[1] From Bernal (*4*, p. 309).

The geometrical properties of the Bernal polyhedra were presented by Smith (*38*), who also pointed out how they could be divided to form the simplicial graph of random close-packings of equal spheres. The simplicial graph of any aggregate of points or particles is formed by first con-

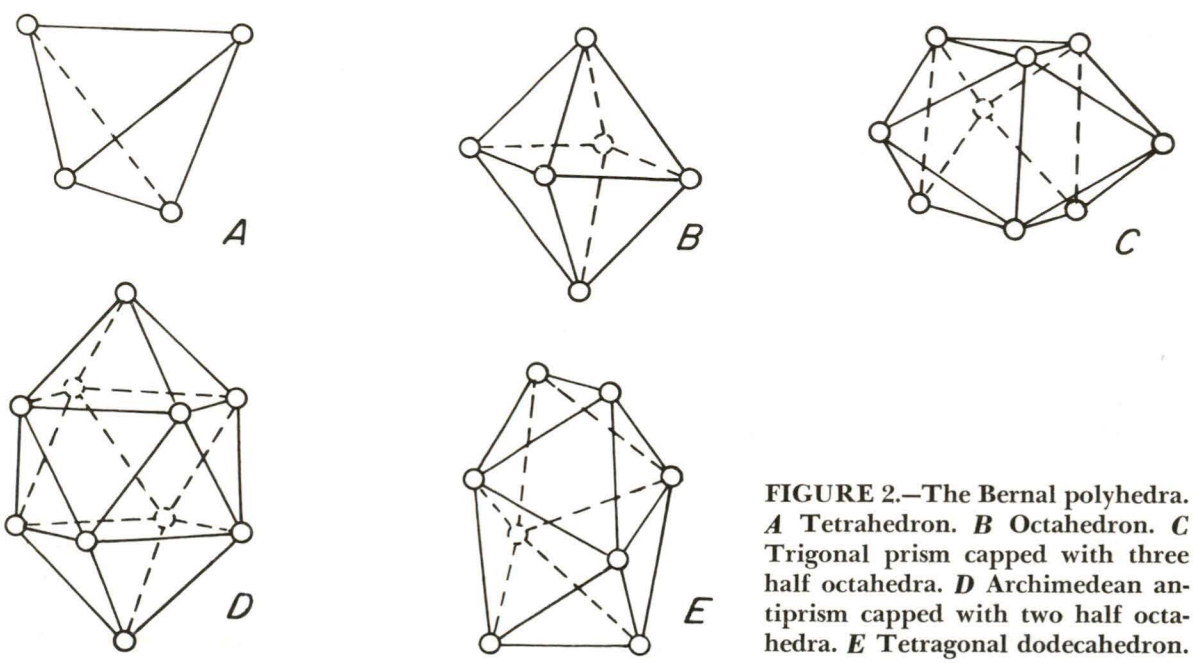

FIGURE 2.—The Bernal polyhedra. *A* Tetrahedron. *B* Octahedron. *C* Trigonal prism capped with three half octahedra. *D* Archimedean antiprism capped with two half octahedra. *E* Tetragonal dodecahedron.

structing the Dirichlet region, or Voronoi polyhedron (*10, 31, 42*), for each point or sphere center in the packing. For the special case of points arranged in regular arrays, this figure is called the domain in complex alloy structures, and it is known as the Wigner-Seitz cell in solid-state physics. Contained within each Voronoi polyhedron are all the locations in the system closer to the particular point element than to any other. These polyhedra are equivalent to those constructed by Bernal when he dissected his ball-and-spoke models to determine the geometrical neighbors of each ball. The three-dimensional array of Voronoi polyhedra in a packing also define an inverse array whose zero-, one-, two-, and three-dimensional elements correspond respectively to the three-, two-, one-, and zero-dimensional elements of the Voronoi polyhedra. The inverse array is known as the simplicial graph, or Delaunay simplice, of the aggregate. It is a unique construction for any irregular or regular array of points and consists of a system of space-filling tetrahedra (simplices) formed between each of the geometrical neighbors of each point in the packing. Because of its uniqueness, the properties of the simplicial tetrahedra in any particle packing can be studied to yield information on the statistical geometry of the packing. Unfortunately, only cursory work (*5, 22, 24*) has been done, and then only for packings of equal spheres.

In addition to the work already mentioned, theoretical studies of the random filling or division of one-, two-, and three-dimensional spaces and higher by equal units have recently received attention by a number of authors. A summary of this work is given by Solomon (*41*). Similarly, Gilbert(*15*) and Larman (*23*) have discussed the theoretical ramifications of filling space of any arbitrary number of dimensions with unequal units. However, this information is of the nature of pure geometry, and it has little direct applicability to the statistics associated with actual loose random packings. An exception is the statistical study published by Higuti (*17*), who performed a number of measurements on random packings of steel balls, whose size distribution was chosen to represent a log-normal distribution. Local packing characteristics, such as number of contacts, were measured on cross sections of the packing. These data were compared with the corresponding values predicted by a simple statistical mathematical model in which the particles were assumed to penetrate one another freely. Boundary effects and the inability to fully describe the random structure in the bulk of the packing from plane sections led to many error-producing approximations. Thus, the predicted densities and number of contacts for general log-normal packings of spheres were rarely observed experimentally.

Experiments for determining the effect of particle size distribution on packing density were recently reported by Sohn and Moreland (*40*), who correlated the variation of packing density in a number of Gaussian and log-normal random packings with the corresponding standard deviation, size ratio, etc., of the distributions. These data should provide an empirical foundation for predicting densities of packings having these types of particle distributions. Empirical studies (*13, 27, 30*) aimed at predicting densities of packings made from fewer numbers of particle sizes, usually less than four, have been made. However, these studies lack the generality required to make them useful for packings containing numbers and sizes of particles other than those considered.

It is obvious from the preceding review that a considerable amount of both theoretical and experimental research has been done on interpreting the geometry and properties of particulate systems. Almost without exception, the experimental research resulted in empirical interpretations of packing phenomena based on macroscopically observable packing parameters, to the exclusion of important local properties. In almost all cases theoretical development was ultimately forced to rely on the use of simplified packing schemes that did not accurately depict the particle arrangements in real particulate systems, notably the random packing arrangements. Furthermore, the use of equal particles in most of this research limits its application in solving most problems of packing unequal particles. Because of the diversity of irregular geometrical forms and particle sizes that normally exist in real particulate systems, optimizing and predicting packing characteristics remains an empirical art, and statistical, geometrical descriptions of randomly packed structures must still rely on fictitious assemblages of particles. Bernal's prelimiary work with equal spheres and that of Wise and Higuti with unequal spheres are possibly the only investigations reported in the literature that were nearly devoid of the limitations mentioned above. However, no published work extending Bernal's liquid structure theories (1967) could be found. Similarly, no further theoretical work on packings of unequal particles has been

reported, a result of the extremely tedious and complex mathematics heretofore encountered in calculations of packing geometries and properties.

An allied area of random particulate packings for which there is no, or inadequately developed, statistical geometry is that of two-dimensional dense and loose random coverings. While research on coverings has paralleled in many ways that done in three dimensions, there has been considerably less of it. For example, the purely geometrical implications of covering an area with regular bodies such as circles, in regular and in limited irregular arrangements, have been reported by Fejes Tóth *(11–12)* and others *(21, 32, 35)*. Except for the brief mention *(44)* of how regular tetrahedral and cubic covering arrangements can be formed with glass rods, experimental studies on coverings are not reported in the literature. Similarly, no research has been published on the development of models for predicting random covering properties or for determining statistical geometry within random coverings. Hence, development of these models offers considerable opportunity for making many new contributions to the statistical geometry of two-dimensional random structures. The practical implications of covering an area are fewer in number than those proposed for the three-dimensional models. One particularly interesting idea is found in the work of Miller *(29)*, who suggested that random covering models would be useful for predicting random surface-packing parameters in solids undergoing unidirectional growth from liquids.

Probably the greatest single problem faced in past research has been the inability to accurately construct general models of random dense and loose coverings and packings in which the spatial arrangements of equal or unequal particles are precisely known. If these models could be developed, they would immediately find use in detailing the statistical geometry that exists within these arrangements. Furthermore, by avoiding the crippling assumptions inherent in previous three-dimensional models, they could be used to accurately predict both local and bulk packing and covering properties in real particle assemblies. Many of these properties are impossible to measure experimentally or considerable experimental ingenuity is required in their determination. In addition, the models could predict the particle size distribution required to optimize specific packing or covering properties, in lieu of the hit-or-miss approach now in use. Accurate predictions of density, number of geometrical and physical neighbors, surface area, pore size and shape, etc., made in lieu of experimental measurements on actual particulate assemblies having any size or number distribution of particles, would undoubtedly be a great boon to powder metallurgists and ceramists wishing to increase the green density or sinterability in their particle compacts, to chemical process engineers in improving packed-bed performance, and in the development of theories describing the behavior of particulate systems in other technologies. In the present study, dense and loose random covering and packing models were developed whose properties were accurately predicted with a computer.

REFERENCES[2]

1. Barlow, W. Probable Nature of the Internal Symmetry of Crystals. Nature, v. 29, Dec. 20, 1883, p. 186.
2. Bernal, J. D. A Geometrical Approach to the Structure of Liquids. Nature, v. 183, Jan. 17, 1959, pp. 141–147.
3. ——. Geometry of the Structure of Monoatomic Liquids. Nature, v. 185, Jan. 9, 1960, pp. 68–70.
4. ——. The Structure of Liquids. Proc. Roy. Soc. (London), Ser. A, v. 280, No. 1382, July 28, 1964, pp. 299–324.
5. Bernal, J. D., and J. L. Finney. Random Close-Packed Hard Sphere Model. II. Geometry of Random Packing of Hard Spheres. Disc. Faraday Soc., No. 43, 1967, pp. 62–69.
6. Bernal, J. D., and J. Mason. Coordination of Randomly Packed Spheres. Nature, v. 188, Dec. 10, 1960, pp. 910–911.
7. Boerdijk, A. H. Some Remarks Concerning Close-Packing of Equal Spheres. Philips Res. Rept., v. 7, January 1952, pp. 303–313.
8. Coxeter, H. S. M. Close Packing and Froth. Ill. J. Math., v. 2, No. 4B, 1958, pp 746–758.
9. Cundy, H. M. Deltahedra. Math. Gaz., c. 36, 1952, pp. 263–266.
10. Dirichlet, G. L. Uber die Reduktion der positiven quadratischen Formen mit drei unbestimmten ganzen Zahlen (Concerning the Reduction of Positive Quadratic Forms With Three Indefinite Whole Numbers). J. reine angew. Math., v. 40, 1850, pp. 209–227.
11. Fejes Tóth, L. Some Packing and Covering Theorems. Acta Univ. Szeged. Acta Sci. Math., v. 12A, 1950, pp. 62–67.
12. ——. An Arrangement of Two-Dimensional Cells. Ann. Univ. Sci. Budapest. Polando Eotvos Nominatae, Sect. Biol., v. 2, 1959, pp. 61–68.

[2] Titles enclosed in parentheses are translations from the language in which the item was originally published.

13. Fuerstenau, D. W., and J. Fouladi. Degree of Mixedness and Bulk Density of Packed Particles. Am. Ceram. Soc. Bull., v. 46, September 1967, pp. 821–823.
14. Furnas, C. C. Flow of Gases Througs Beds of Broken Solids. BuMines Bull. 307, 1929, 144 pp.
15. Gilbert, E. N. Randomly Packed and Solidly Packed Spheres. Can. J. Math., v. 16, No. 1, 1964, pp. 286–298.
16. Graton, L. C., and H. J. Fraser. Systematic Packing of Spheres, With Particular Relation to Porosity and Permeability. J. Geol., v. 43, November–December 1935, pp. 785–909.
17. Higuti, I. A Statistical Study of Random Packing of Unequal Spheres. Ann. Inst. Stat. Math. (Tokyo), v. 12, No. 3, 1961, pp. 257–271.
18. Hogendijk, M. J. Random Dense Packing of Spheres With a Discrete Distribution of the Radii. Philips Res. Rept., v. 18, March 1963, pp. 109–126.
19. Hudson, D. R. Close-Clustering of Spheres Round a Kernal. Proc. Leeds Phil. Soc., v. 5, 1947, pp. 65–74.
20. —— Kelvin, William Thomson, *1st baron*. On Homogeneous Division of Space. Proc. Roy. Soc. (London), v. 55, No. 331, 1894, pp. 1–16.
21. Kershner, R. The Number of Circles Covering a Set. Am. J. Math., v. 61, No. 3, 1939, pp. 665–671.
22. Kiang, T. Random Fragmentation in Two and Three Dimensions. Z. Astrophys., v. 64, No. 5, 1966, pp. 433–439.
23. Larman, D. G. On Packings of Unequal Spheres in Rn. Can. J. Math., v. 20, No. 4, 1968, pp. 967–969.
24. Levine, M. M, and J. Chernick. A Numerical Model of Random Packing of Spheres. Nature, v. 208, Oct. 2, 1965, pp. 68–69.
25. Marvin, J. W. The Shape of Compressed Lead Shot and Its Relation to Cell Shape. Am. J. Botany, v. 26, No. 5, 1939, p. 280.
26. Matzke, E. B. Three-Dimensional Shape of Bubbles in Foam—An Analysis of the Role of Surface Forces in Three-Dimensional Cell Shape Determination. Am. J. Botany, v. 33, No. 1, 1946, p. 58.
27. McGeary, R. K. Mechnical Packing of Spherical Particles. J. Am. Ceram. Soc., v. 44, October 1961, pp. 513–522.
28. Meijering, J. L. Interface Area, Edge Length, and Number of Vertices in Crystal Aggregates with Random Nucleation. Philips Res. Rept., v. 8, April 1953, pp. 270–290.
29. Miller, W. A. Surface Packing Parameters and Rectilular Densities in Solids and Liquids. Appendix in A Hard Sphere Model of Crystal Growth by G. A. Chadwick. Metal Sci. J., v. 1, September 1967, pp. 132–138.
30. Ridgeway, K., and K. J. Tarbuck. Particulate Mixture Bulk Densities. Chem. Process Eng., v. 49, February 1968, pp. 103–105.
31. Rogers, C. A. The Packing of Equal Spheres. Proc. London Math. Soc., v. 8, 1958, p. 609.
32. ——. The Closest Packing of Convex Two-Dimensional Domains. Acta. Math. (Uppsala), v. 86, 1951, pp. 309–321.
33. Scott, G. D. Packing of Equal Spheres. Nature, v. 188, Dec. 10, 1960, pp. 908–909.
34. ——. Radial Distribution of the Random Close Packing of Equal Spheres. Nature, v. 194, June 9, 1962, pp. 956–957.
35. Segre, B., and K. Mahler. On the Densest Packing of Circles. Am. Math. Monthly, v. 51, May 1944, pp. 261–270.
36. Smith, C. S. Grain Shapes and Other Metallurgical Applications of Topology. Ch. in Metal Interfaces. American Society of Metals, Cleveland, Ohio, 1952, pp. 65–113.
37. ——. Further Notes on the Shape of Metal Grains: Space-Filling Polyhedra With Unlimited Sharing of Corners and Faces. Acta Met., v. 1, May 1953, pp. 295–300.
38. Smith, F. W. The Structure of Aggregates and the Molecular Kinematics of the Viscosity of a Bernal Liquid. Can. J. Phys., v. 42, February 1964, pp. 304–320.
39. Smith, W. O., P. H. Foote, and P. F. Busang. Packing of Homogeneous Spheres. Phy. Rev., v. 34, Nov. 1, 1929, pp. 1271–1274.
40. Sohn, H. Y., and C. Moreland. The Effect of Particle Size Distribution on Packing Density. Can. J. Chem. Eng., v. 46, June 1968, pp. 162–167.
41. Solomon, H. Random Packing Density. Dept. of Statistics, Stanford Univ., Stanford, Calif. Tech. Rept. No. 105, 1965, 138 pp., available as AD 619 420 from the National Technical Information Service, U.S. Department of Commerce, Springfield, Va. 22151.
42. Voronoi, G. F. Nouvelles applications des paramètres continus à la théorie des forms quadratiques (New Applications of Continuous Parameters to the Theory of Quadratic Forms). J. reine angew. Math., v. 134, 1908, p. 198.
43. Westman, A. E. R., and H. R. Hugill. The Packing of Particles. J. Am. Ceram. Soc., v. 13, No. 10, 1930, pp. 767–779.
44. White, H. E., and S. F. Walton. Particle Packing and Particle Shape. J. Am. Ceram. Soc., v. 20, No. 5, 1937, pp. 155–166.
45. Wise, M. E. Dense Random Packing of Unequal Spheres. Philips Res. Rept., v. 7, February 1952, pp. 321–343.

— 2 —

COMPUTER SIMULATION OF DENSE RANDOM COVERINGS OF CIRCLES

by

Lindsay D. Norman

By definition, dense random coverings are formed by particles tangent to all of their nearest neighbors so that no gaps exist between adjacent particles in the system. Densely covered particles are therefore in arrangements quite different from regular lattices and from real particle assemblies in which gaps between particles are known to exist. This difference is particularly evident in their covering densities, which are considerably higher than those observed experimentally. Because of the high densities and the absence of gaps in dense random coverings, these systems are idealizations of real particulate systems in which the most efficient particle arrangement possible has been attained. Thus, the properties of dense random coverings serve as ideal upper bounds for those of more realistic systems.

Whether or not dense, randomly covered systems can be built in practice is only partially known. The model for dense random coverings of equal circles was found years ago in the honeycombs of bees, when it was observed that each hexagonal cell could be inscribed by a circle. It can be easily proven that the covering density and average coordination in these coverings are 0.9069 and 6.0, respectively. Therefore, dense and regular close-coverings are equivalent when equal circles cover an area. The possible existence of dense random coverings of unequal circles is not an easily answered question. If one could witness the construction of a dense random covering before it had progressed too far, sites for additional circles would be formed at which only a specified size could be added and still remain gapless. In the event this size was not available in the circle population in use or if it was too far removed from the site where needed, departures from dense random covering would occur as gaps propagated in the system. The application of the results from the computer simulations of dense random coverings that follow is based on the premise that gapless structures may be considered as ideal upper limits for the more probable arrangements.

COMPUTER SIMULATION MODEL

The ideal situation that exists about any circle when equal or unequal circles form dense random coverings is shown in figure 3. In both of these arrangements, all of the circles surrounding the center circles are tangent to that circle and to their immediate neighbors. Similarly, additional circles placed on the perimeter of these arrangements would also have to be tangent to their immediate neighbors, whether they be located in the same ring of circles or on the interior or exterior of the dense random covering. By connecting the centers of the tangent circles in the two arrangements in figure 3, systems of triangles can be visualized that cover all of the available area around the central circles so that the sum of the angles (expressed as fractions of 2π) subtended at the central circle is unity. Similar systems of triangles can be constructed around any circle in any dense random covering. This makes it possible to calculate the properties of a dense random covering with only the simple geometrical formulas for triangles. This method of calculating covering properties was used exclusively in the dense random covering models developed in this investigation.

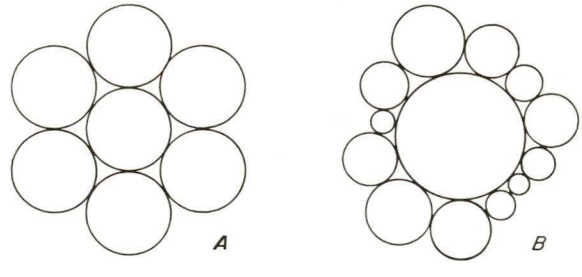

Figure 3.—Dense random coverings of equal (*A*) and unequal (*B*) circles.

Before the computer models for simulating dense random coverings of unequal circles or any other type of random covering or packing of unequal particle sizes could be developed, means of selecting particle radii at random from a sphere or circle distribution had to be formulated. In this investigation the particle radii were chosen at random with a multiplicative congruential pseudorandom number generator (*2*) [1] of numbers between zero and one. For a limited number of radii, such as in a histogram of sizes, the relative frequencies of occurrence of the sphere or circle radii were normalized so that the total probability of occurrence of all the particle sizes was unity. The interval zero to one was then divided into segments whose lengths corresponded to the normalized frequencies of occurrence of the particle sizes. Whenever a random number was generated, its magnitude was compared with the particle radii assignments in the interval zero to one to arrive at the corresponding randomly selected sphere or circle radius.

Selecting radii at random from continuous distributions, such as Gaussian (normal) or log-normal, is more complicated than selecting discrete numbers of radii because the former have an infinite number of sizes. The probability density function in normal distributions of radii is given by

$$f(R)=\frac{1}{\sigma\sqrt{(2\pi)}}\exp\left[-\tfrac{1}{2}(R-\overline{R})^2/\sigma^2\right], \tag{3}$$

where σ is the arithmetic standard deviation, and $\overline{R}$ is the arithmetic mean radius of the distribution. If $F(R)$ is defined so that it represents the fraction of radii less than R, then

$$F(R)=\frac{1}{\sigma\sqrt{(2\pi)}}\int_0^R \exp\left[-\tfrac{1}{2}(R-\overline{R})^2/\sigma^2\right]d(R). \tag{4}$$

Integrated over all possible radii, $F(R)$, or the area under the curve expressed by equation 4, is unity. This fact finds immediate use in assigning radii at random from these distributions. By generating a random number between zero and one and making $F(R)$ equal to it, R in equation 4 can be evaluated from tables of probability integrals. However, in the computer programs, which required randomly selected particle radii, the use of integral tables was not practical. Therefore, a means of using the random numbers that would not involve integral solutions had to be found. As a first step, equation 4 was simplified by changing variables with

$$y=(R-\overline{R})/\sigma\sqrt{2}, \tag{5}$$

and

$$dy=d(R)/\sigma\sqrt{2}. \tag{6}$$

Substituting these back into equation 4 gives

$$F(y)=\frac{1}{\sqrt{\pi}}\int_0^y e^{-y^2}dy. \tag{7}$$

The error function *ERF*, found in most statistical handbooks, is very similar to equation 7 and is given by

$$ERF(y)=\frac{2}{\sqrt{\pi}}\int_0^y e^{-y^2}dy=\frac{2}{\sqrt{\pi}}\left[y-\frac{y^3}{3}+\frac{1}{2!}\frac{y^5}{5}-\frac{1}{3!}\frac{y^7}{7}+\cdots\right].$$

Therefore,

$$F(y)=\tfrac{1}{2}ERF(y),$$

and

$$F(y)=[y-y^3/3+y^5/10-y^7/42+\cdots]/\sqrt{\pi}. \tag{8}$$

In contrast to equation 4, equation 8 can be readily solved with the computer for any value of y. Alternatively, for a given random number, successive iteration of y can be done by the computer until $F(y)$ equals this random number. The final value of y and the known distribution mean and standard deviation are then substituted in equations 5 and 6 to get

$$R=\overline{R}+\sigma\sqrt{2}\,y, \tag{9}$$

which is the radius corresponding to the random number.

Radii are selected at random from a log-normal distribution in a completely analogous fashion. For this type of distribution

$$f(R)=\frac{1}{\log\sigma_g\sqrt{(2\pi)}}\exp\left[-\tfrac{1}{2}(\log R-\log\overline{R}_g)^2/(\log\sigma_g)^2\right], \tag{10}$$

where σ_g and $\overline{R}_g$ now define the geometric distribution parameters. With the same procedure as outlined for normal distributions, the equivalent of equation 9 can be derived for the selection of radii from log-normal distributions:

$$\log R=\log\overline{R}_g+\log\sigma_g\,(\sqrt{2}\,y). \tag{11}$$

Equation 11 and the preceding equations were used throughout this investigation to assign circle and sphere radii from continuous distributions. In most cases, log-normal distributions were employed because they are the most frequently encountered in actual particle technology.

The two-dimensional simulations of dense random coverings began by randomly selecting

[1] Italicized numbers in parentheses refer to items in the list of references at the end of this chapter.

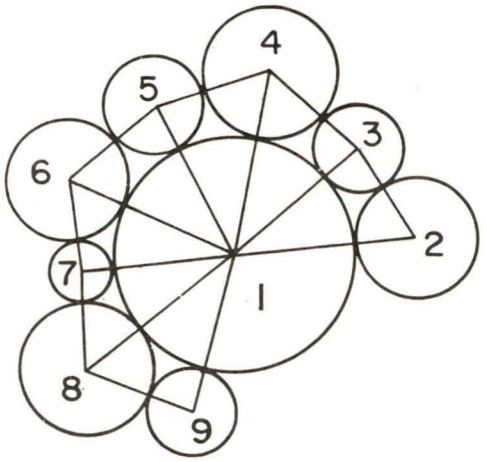

Figure 4.—Construction of dense random covering of unequal circles.

the first circle in the covering and labeling it as the central circle. Second and third circles were selected and made tangent to each other and to the central circle to form the first triangle. Thereafter, each additional circle was made tangent to the central circle and to the last circle added. This construction is shown in figure 4. The condition that all circles must be tangent to their immediate neighbors is satisfied by making the triangle edge lengths equal to the sum of the respective radii of the circles forming the triangle. This is illustrated in figure 5 for the triangle formed by the first three circles in the partial covering shown in figure 4. For this triangle

$$a=R_1+R_2, \tag{12}$$

$$b=R_2+R_3, \tag{13}$$

and

$$c=R_1+R_3. \tag{14}$$

Similar data for every triangle formed in the process of constructing the covering were used to calculate covering properties such as density and pore size. From plane geometry, the area of a triangle can be found in terms of its edge lengths. For the triangle shown in figure 5,

$$\text{Area}=[U(U-a)(U-b)(U-c)]^{1/2}, \tag{15}$$

where $U=(a+b+c)/2$. The covering density within any triangle, defined as the area covered divided by the total area, was found by calculating the total circle sector area within each triangle. For the triangle in figure 5,

$$\text{Area of sectors}=\tfrac{1}{2}(R_1^2B+R_2^2C+R_3^2A), \tag{16}$$

where angles A, B, and C are expressed in radians. These angles were determined using the identity

$$\text{Area of pore}=\text{Area of triangle}-\text{area of sectors.}$$

where U has the same significance as before. Angles B and C were determined in similar fashion. The covering density was given by

$$\Phi=\text{Area of sectors/area of triangle}$$

and the pore area by

$$\text{Area of pore}=\text{Area of triangle}-\text{area of sectors.}$$

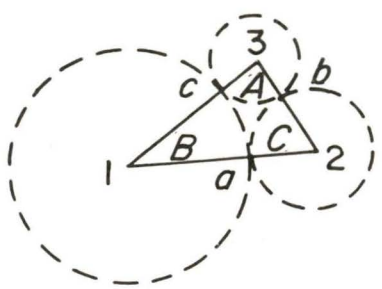

Figure 5.—Dense random covering triangle.

As circles are placed around the central circle, eventually one will overlap a circle already in place. This situation can be visualized in figure 4, where an added circle will eventually overlap circle number 2 unless it has the exact size required to fit tangent to the central circle, the last circle added, and number 2. In a random covering, the random selection of the exact size is extremely unlikely. Furthermore, the required size might not exist in the population from which the circles are randomly drawn. To avoid overlapping, it would be necessary to stop adding circles with the last circle added prior to the overlapping one. However, a gap in the ring about the central circle would inevitable occur and result in a region that was not dense randomly covered. To minimize this problem a central circle was randomly chosen and additional circles were added without concern for overlapping, until 20 complete rings of tangent circles were formed about the central circle. The triangle and sector areas defined by each additional circle were calculated and stored as the simulation progressed. When the sum of the central angles (angle B in figure 5) in all the triangles exceeded or equaled 40π, the circle additions were terminated.

For an integer number of circles to form exactly M rings of dense covering, the sum of the central angles must equal $2\pi M$. Any angle in excess of $2\pi M$ is a measure of the error in assuming gapless packing. The 40π limit was

established by constructing from 15 to 50 rings of dense covering around central circles chosen from different populations. Although adding more circle rings produced smaller errors, for 20 rings of dense covering $40\pi \leq \Sigma B < 40.001\pi$, which was considered an acceptably small error.

The triangle and sector areas were used to calculate the average local density and pore size associated with a dense random covering around a central circle. At this point in the simulation, another circle was randomly selected from the circle population, and the process of adding circles around it was repeated. Up to 50 different central circles were used in each covering simulation. The covering data from each central circle computation were arithmetically averaged to give the overall covering properties of what was considered a dense random covering of circles for the particular circle distribution used.

Nowhere in the preceding discussion has mention been made of fitting a central circle and its neighbors with other central circle combinations. The described simulation merely calculated the properties of many triangles (more than 5,000) typical of those that would have been found in an area-covering arrangement. Because the central circle sizes were present most often in these triangles, the possibility that the calculated covering statistics might have been erroneously weighted toward those associated with these circles could not be immediately discounted. However, by simulating the construction of an equal number of individual triangles formed by randomly selecting three circles at a time, the calculated density and pore size distribution data agreed with the central circle simulation data to within 0.01 percent for all the circle distributions considered in this investigation. This negligible difference in the calculated properties immediately indicated that the central circle radii selected by the random number routine were representative of the entire circle distribution. Although the central circle simulation programs were more complex than those for individual triangles, their use permitted the calculation of the average coordination number of a single circle and of the entire covering. For each central circle computation, the average number of circles contacting the central circle was simply

$$\overline{N} = (I-1)/20, \tag{17}$$

where I was the number of circles required to form the 20 rings of dense covering around the central circle. Because the central circles were random samples of the entire circle population, the coordination number found by averaging the number of contacts for each central circle should be a good measure of the average number of contacts in the entire covering. The fact that the individual units consisting of central circles and their neighbors were not fitted together to form an assembled covering is of no consequence. This fitting together is implicit in the assumption that gapless coverings are possible to construct. In effect, the simulations assumed that a dense random covering having a specific circle distribution had already been assembled. From this covering, many circles were randomly chosen and the covering statistics in the immediate region of these circles were examined. Their properties were then averaged to allow predictions of the overall covering properties.

An additional property of the dense random coverings that was calculated was the interstitial circle distribution. It is the distribution of circles (incircles) that just fit into the pores, or interstices, of the triangles constructed during the simulation. The calculation of these sizes is theoretically of interest to one who wishes to increase the covering density by the inclusion of a secondary circle population in the primary population interstices. The mathematical development of these calculations has been reviewed by Coxeter (*1*), and in this investigation it was reduced to

$$1/r_{int} = 1/r_j + 1/r_k + 1/r_m + 2(1/r_j r_k + 1/r_j r_m + 1/r_k r_m)^{1/2}, \tag{18}$$

where r_{int} is the incircle radius that just fits in the interstice of a triangle formed by three mutually tangent circles of radius r_j, r_k, and r_m.

To illustrate the general types of information that one may obtain from computer simulations of dense random coverings, the results for coverings of equal, uniform, and log-normal circle distributions are presented on the following pages.

DENSE RANDOM COVERING PROPERTIES

Distributions of Equal and Uniform Circle Sizes

A unit radius was used in coverings of equal circles, whereas coverings of uniform circle sizes were constructed from distributions having two to five different radii combined as follows: (1, 2), (1, 2, 3), (1, 2, 3, 4), or (1, 2, 3, 4, 5). These sizes

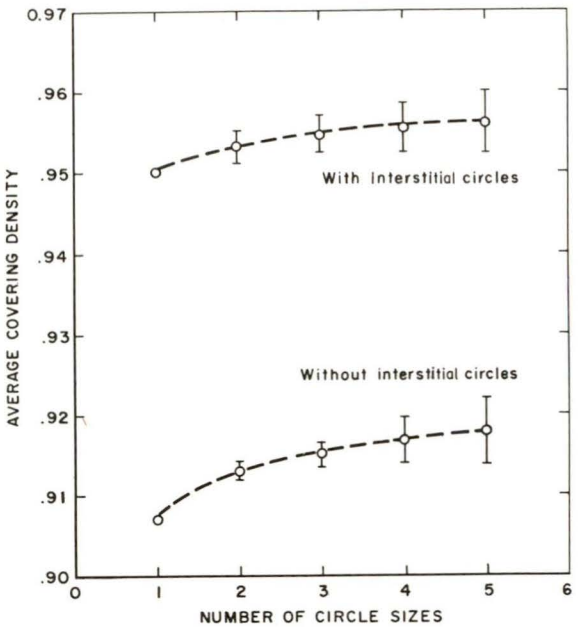

Figure 6.—Covering density in dense random coverings of discrete circle sizes. The vertical bars indicate the deviation in local density around the central circles in each random covering.

and their distributions bore no special relation to practical systems, but were chosen to illustrate the computer simulations.

The predicted average covering densities, with and without interstitial filling, of the dense random coverings of equal and uniform circle sizes are shown in figure 6. The predicted density for a dense random covering of equal circles was 0.9069. This value is exactly the same as that given earlier for dense random and regular close-coverings of equal circles. The increase in density as the number of circle radii increases is intuitively very acceptable, because it reflects the greater covering economy that a range of circle sizes provides. The predicted covering densities of a finite number of circle sizes with interstitial circles included appears to approach an upper limit of less than 0.96. As will be seen later for an infinite number of sizes, this limit eventually approaches the theoretical maximum of 1.0.

The coordination, or average, number of contacting circles around each central circle in the five dense random coverings of uniform circle sizes is shown in figure 7. These data, representing the average local coordination around each circle in the population, were amassed from many central circle computations. Their standard deviation was usually less than 1 percent of the average, indicating that, for systems having only a few circle sizes, the coordination of a single size is definable to within rather narrow limits. The average number of contacts for the entire covering is shown in figure 8. These data also reflect the more efficient covering obtainable as the number of circle sizes is increased. Also shown in figure 8 are the average calculated pore areas and interstitial radii within each of the five coverings. The relatively large deviations in the data for the multisize-circle coverings result from triangular combinations of only large and/or only small circles having widely different pore areas and correspondingly different interstitial radii. Similar large deviations in density were not observed because, for example, the covering density of a triangle of large, equal circles is the same as that of a triangle of small, equal circles.

Distributions of Log-Normal Circle Sizes

Similar dense random covering data were obtained by simulating the construction of coverings from six log-normal distributions of circles. Four of these six distributions are shown in fig-

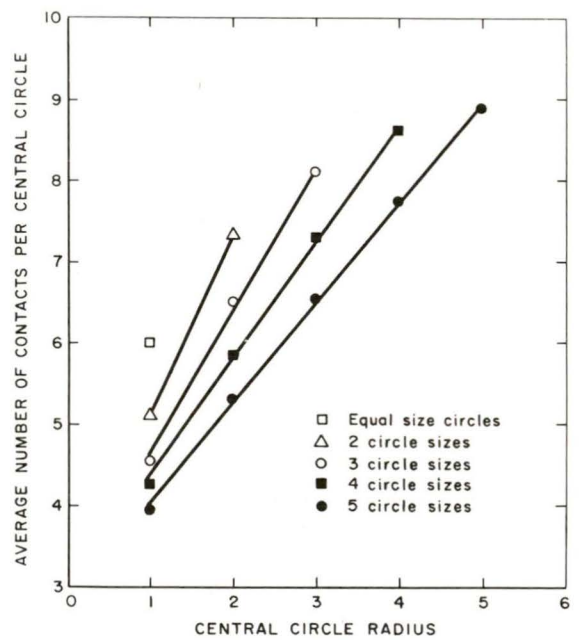

Figure 7.—Contacts per circle in dense random coverings of discrete circle sizes.

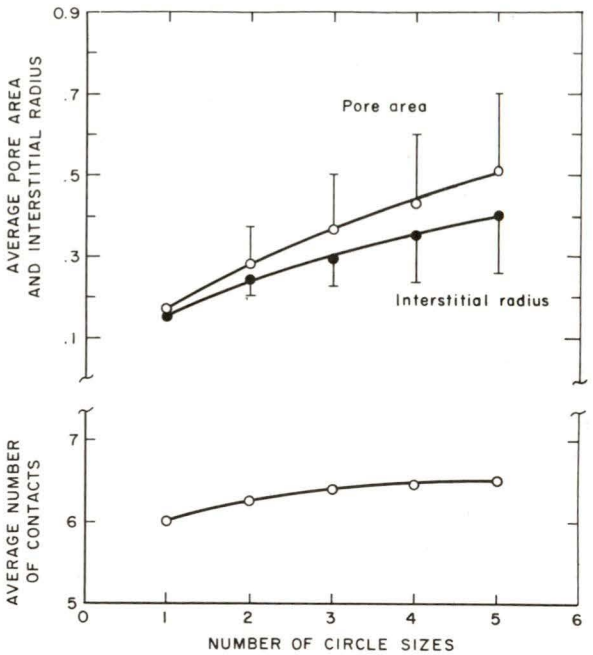

Figure 8.—Average pore areas, contacts, and interstitial radii in dense random coverings of discrete circle sizes. The vertical bars (only half of each is shown) represent 1 standard deviation from the average value.

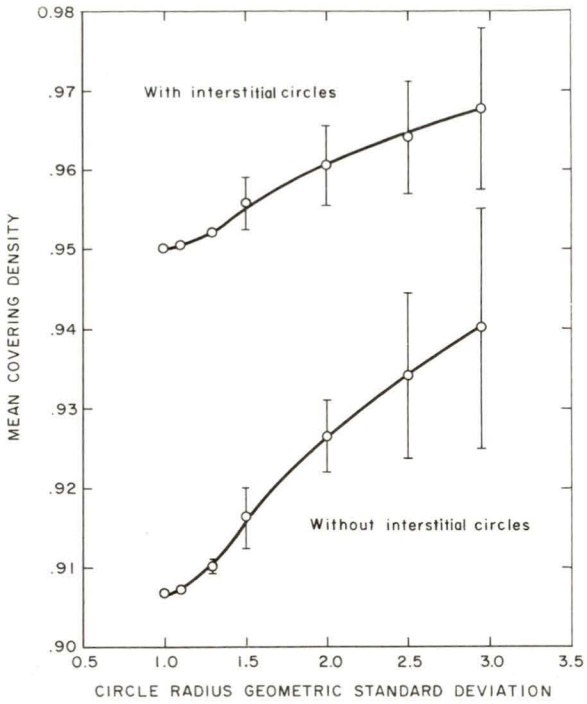

Figure 10.—Log-normal circle dense random covering densities. The vertical bars represent 1 standard deviation from the average value.

ure 9. The log-normal distributions had a geometric mean of 1 and geometric standard deviations σ_g between 1 and 2.96. Each distribution was truncated at $R_g/4\sigma_g$ and $4\sigma_g R_g$, the equivalent in log-normal distributions of ± 4 standard deviations from the mean.

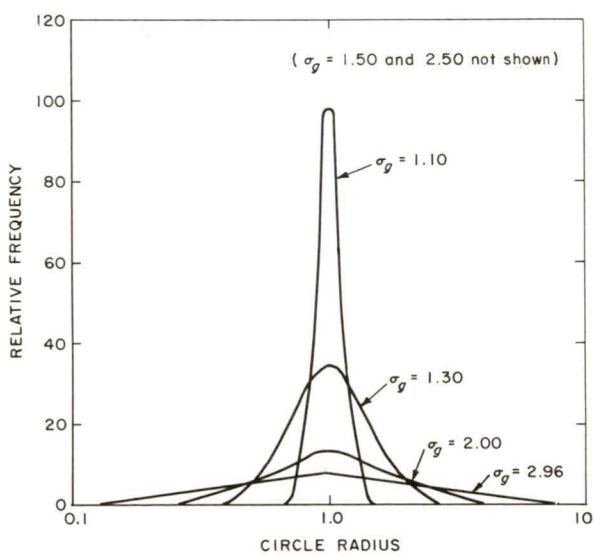

Figure 9.—Log-normal distributions of circles.

The predicted densities of the log-normal coverings and the density of a covering of equal circles having a geometric standard deviation of 1 are plotted in figure 10. The covering density in this case also increased as the number of available circle sizes increased, and, more importantly, as the circle size ratio increased. For the uniform distribution having five discrete sizes, the maximum average density without interstitial filling was 0.918. (See figure 6.) This value corresponds to a maximum/minimum circle size ratio of five. The 0.9403 maximum average density obtained in the log-normal coverings corresponds to a theoretically available size ratio of approximately 140. This parameter controls the maximum density obtainable in dense random coverings. The calculated densities in the log-normal coverings were invariably higher than those of the coverings calculated from a few discrete circle radii. A circle distribution having an infinite standard deviation should theoretically cover to unit density. Moreover, as the number of circle sizes and their size ratio increase, the possible real existence of dense random coverings seems

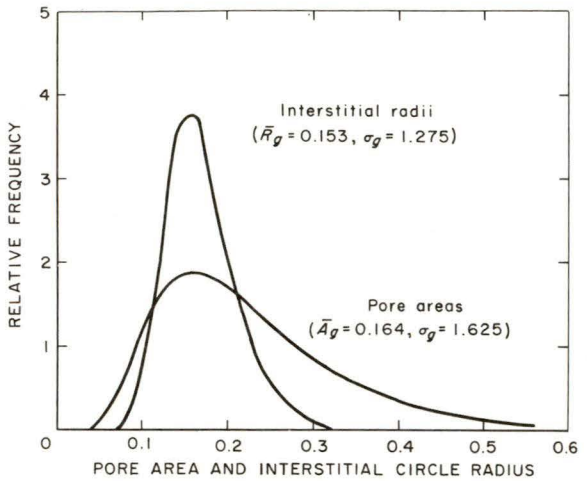

Figure 11.—Typical pore area and interstitial radius distributions in a log-normal dense random covering.

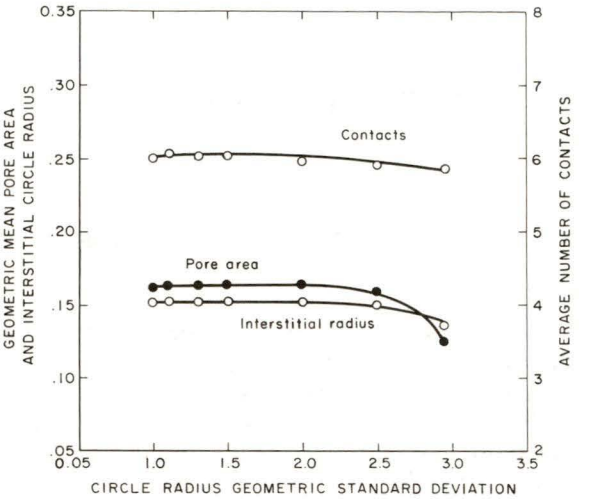

Figure 12.—Average number of contacts, pore areas, and interstitial radii in log-normal dense random coverings.

intuitively more probable, because the likelihood of a particular size being available when needed also increases.

In simulating the construction of dense random coverings of log-normally distributed circles, the pore area and interstitial radius distributions were also found to be log-normal. In figure 11, typical results are shown for the log-normal distribution having a geometric standard deviation of 1.5. These data are based on more than 5,000 triangle calculations. The average number of contacts and the geometric mean pore area and interstitial radius in the six log-normal coverings are shown in figure 12. Each remained relatively constant over most of the range of σ_g. At small σ_g the circle distribution functions were nearly symmetrical about the mean, and the available circle sizes were not too different from one another. Thus, nearly constant numbers of contacts and pore areas and interstitial radii means were to be expected when circles were randomly selected from these distributions. At standard deviations greater than 1.5, the probability of randomly selecting circles of widely different sizes was much greater because of the large size ratios in these distributions. Combinations of a relatively large circle with small or average size circles were very probable triangle arrangements. The mean pore area and interstitial radius decreased because the pores in these types of triangle combinations were considerably smaller than those associated with three average or nearly equal circles. Although the mean sizes decreased slowly at large σ_g, their standard deviations rose quite rapidly. For example, the geometric standard deviation of the mean pore area increased from 1.0 for a circle distribution σ_g of 1.0 to 3.33 in the covering of circles having a standard deviation of 2.96. A similar increase to 1.83 occurred in the geometric standard deviation of the interstitial radius mean. In every dense random covering, a unique relationship appeared to exist between the interstitial radius mean and the circle distribution mean. This can be seen in figures 8 and 12, where the average interstitial radius in all but one of the coverings was 15.0 ± 0.8 percent of the average circle size in the covering.

REFERENCES

1. Coxeter, H. S. M. Introduction to Geometry. John Wiley & Sons, Inc., New York, 1961, p. 11.
2. Hutchinson, D. W. A New Uniform Pseudorandom Number Generator. Comm. ACM, v. 9, June 1966, pp. 432–433.

— 3 —

COMPUTER SIMULATION OF DENSE RANDOM PACKINGS OF SPHERES

by

Lindsay D. Norman, Edwin E. Maust, Jr.,[1] and Leonard P. Skolnick [2]

Dense random packings are formed by particles that are tangent to all of their nearest neighbors so that no gaps exist between adjacent particles in the system. This arrangement is illustrated in fiigure 13. In dense random packing, each sphere added to the system must be tangent to a central sphere and to at least two other surface spheres. Gaps, shown at *G* in figure 13, although present in physically realizable particulate systems, are not allowed in the limiting case of dense random packing. Following a procedure analogous to that adopted in chapter 2 for dense random covering, a system of tetrahedra can be constructed by connecting the centers of tangent surface spheres and the central sphere. The polyhedra so formed will fill all of the available space around the central sphere, and the sum of the tetrahedra fractional solid angles (expressed as fractions of 4π) subtended at the central sphere will be unity.

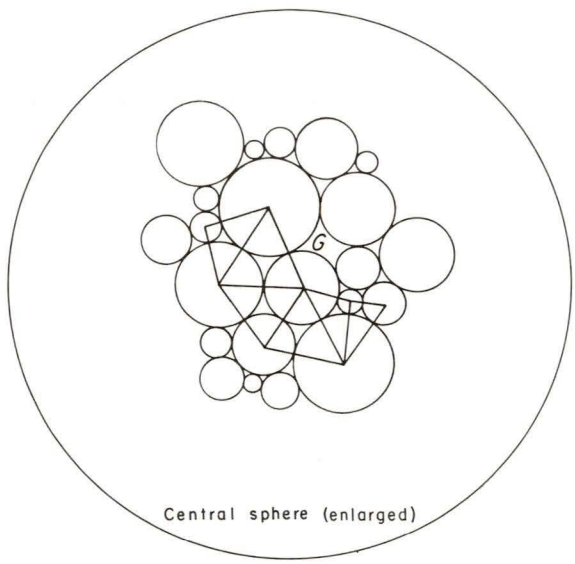

Figure 13.—Dense random packing of spheres. Gaps (*G*) between spheres are present in real particulate systems but are not allowed in the limiting case of dense random packing.

COMPUTER SIMULATION MODEL

In computer simulations of dense random packing, the first, or central, sphere was randomly selected from the sphere distribution by the pseudo-random number generator described in chapter 2. Three additional spheres were randomly selected from the population and made tangent to each other and to the central sphere to form the first dense-packed tetrahedron. Thereafter, each additional sphere was made tangent to the central sphere and to the last two added spheres to form another tetrahedron. In a fashion similar to that used in two dimensions, the tetrahedra edge lengths were made equal to the sum of the respective radii of the spheres forming each tetrahedron. With these data, all of the relevant properties of each tetrahedron could be calculated as it was formed.

A simplified expression for the volume of a tetrahedron formed by four mutually tangent spheres was given by Wise (*6*).[3] For this case,

$$\begin{aligned}\text{Tetrahedron volume} = [&2r_1r_2r_3r_4(r_1r_2+r_1r_3+r_1r_4\\ &+r_2r_3+r_3r_4+r_2r_4)\\ &-(r_1r_2r_3r_4)^2(r_1^{-2}+r_2^{-2}\\ &+r_3^{-2}+r_4^{-2})]^{1/2}/3,\end{aligned} \qquad (19)$$

where the subscripted r's are the radii of the four spheres forming the tetrahedron. To find the packing density, pore volume, etc., in each tetrahedron, the volume occupied by spheres was determined with plane and spherical trigonometry. First, the twelve angles between the tetrahedron edges were calculated from the general equation

$$A_{e\cdot fg} = 2 \arctan [r_f r_g/(r^2_e+r_e r_f+r_e r_g)]^{1/2}, \qquad (20)$$

where $A_{e\cdot fg}$ is the tetrahedron face angle formed at the vertex centered on sphere e having radius r_e, between the tetrahedron edges connecting

[1] Supervisory chemical research engineer, College Park Metallurgy Research Center, Bureau of Mines, College Park, Md.

[2] Professor, engineering materials, University of Maryland, College Park, Md.

[3] Italicized numbers in parentheses refer to items in the list of references at the end of this chapter.

spheres f and g of radius r_f and r_g, respectively. Three tetrahedron faces meet at a vertex; thus there are three $A_{e\cdot fg}$ angles associated with each vertex. For any single vertex in the tetrahedron, these angles, the tetrahedron faces, and the radius of the sphere centered on the vertex define a sphere segment inside the tetrahedron. The surface of the sphere segment within the tetrahedron is a spherical triangle whose sides are the three $A_{e\cdot fg}$ angles calculated from equation 20 for each vertex. Thus, for a tetrahedron constructed from four spheres numbered 1 through 4, the spherical triangle edges associated with the segment of sphere number 1 were identified as $A_{1\cdot 23}$, $A_{1\cdot 34}$, and $A_{1\cdot 24}$. With a similar notation, the angles in the spherical triangle were identified by $\alpha_{1\cdot 23}$, $\alpha_{1\cdot 34}$, and $\alpha_{1\cdot 24}$. Angle $\alpha_{1\cdot 23}$, opposite side $A_{1\cdot 23}$, was defined by the tetrahedron face planes formed by spheres 1, 3, and 4; 1, 2, and 4; etc. The spherical angles were calculated from

$$\alpha_{1\cdot 23}=2 \arctan \{\sin (S_1-A_{1\cdot 34}) \sin (S_1-A_{1\cdot 24})/ [\sin S_1 \sin (S_1-A_{1\cdot 23})]\}^{1/2}, \quad (21)$$

where $S_1=(A_{1\cdot 23}+A_{1\cdot 34}+A_{1\cdot 24})/2$. Angles $\alpha_{1\cdot 34}$ and $\alpha_{1\cdot 24}$ were calculated from the same equation. The area of the spherical triangle A was obtained from

$$A=(\alpha_{1\cdot 23}+\alpha_{1\cdot 34}+\alpha_{1\cdot 24}-\pi)r_1^2.$$

As a fraction of the total surface area of sphere number one, this equation transforms to

$$A'=A/4\pi r_1^2=[(\alpha_{1\cdot 23}+\alpha_{1\cdot 34}+\alpha_{1\cdot 24})/4\pi]-1/4.$$

Therefore, the sphere segment volume of sphere number 1 in the tetrahedron is equal to

$$4\pi r_1^3 A'/3=(\alpha_{1\cdot 23}+\alpha_{1\cdot 34}+\alpha_{1\cdot 24}-\pi)(r_1^3)/3. \quad (22)$$

By an analogous series of calculations, the segment volumes of spheres 2, 3, and 4 in the above example were determined.

When spheres are placed around a central sphere, a point will generally be reached where an additional sphere will overlap one already in place. If it is not added, a gap between surface spheres will result. This situation violates the definition of dense random packing. To reduce the error from this to acceptable levels in the packing simulations, a central sphere was randomly chosen and additional tangent spheres were added without concern for overlapping, until the equivalent of 20 complete shells of spheres or tetrahedra were formed about the central sphere. This limit was reached when the sum of calculated central sphere solid angles in all the tetrahedra exceeded or equaled $20\times 4\pi=80\pi$. This procedure, analogous to the construction of the 20 rings of tangent circles in two dimensions, also resulted in acceptably small errors in three-dimensional packings.

The tetrahedron and sphere segment volumes were calculated for every tetrahedron in the 20 shells. These data were then used to calculate the average local density and pore size associated with a single shell of dense random packing around the central sphere. Up to 50 different central sphere computations were performed, and the results of each were averaged to give the overall dense random packing properties of the sphere population. The validity of the predicted properties rests on the assumption that dense random packing is in fact physically realizable. Considering that on the average over 14,000 spheres were randomly selected from the sphere population to form the dense-packed tetrahedra, the predicted packing statistics should be representative of dense packing if it exists.

The average number of contacts per central sphere was calculated from a knowledge of the number of spheres that had entered into the construction of the 20 shells of tetrahedra. In any single central sphere calculation, the average number of tetrahedra associated with one shell of dense packing was simply

$$\overline{T}=(I-2)/20, \quad (23)$$

where I was the number of spheres required to form 20 shells of dense random packing around the central sphere. A polyhedron constructed from these tetrahedra have triangular faces, a sphere center at each one of its vertices, and the central sphere at its center. For any polyhedron with V vertices, E edges, and Z faces or planes, Euler's theorem states $V=E-Z+2$. For a tetrahedron, $V=4$, $E=6$, $Z=4$, and $E=3Z/2$. All polyhedra built from tetrahedra must be topologically equivalent; thus, $E=3Z/2$ also applies to the polyhedra, and Euler's theorem can be written as $V=\frac{1}{2}Z+2$. Because each tetrahedron contributes one face to the polyhedron in the computer simulations, the average number of vertices or contacting spheres can be calculated from

$$\overline{N}=\frac{1}{2}\overline{T}+2. \quad (24)$$

The mathematical equations for calculating the size of a fifth interstitial sphere in mutual contact with the four spheres in a dense-packed tetrahedron have been developed by Wise (7). These calculations are of interest in three-dimen-

sional dense random packings because of the theoretical possibility of increasing the packing density by the inclusion of these spheres in the tetrahedra interstices. In the computer simulations the interstitial sphere radii were determined from

$$1/r_{int}=\tfrac{1}{2}(1/r_j+1/r_k+1/r_m+1/r_n)+\tfrac{1}{2}(3\rho)^{\frac{1}{2}}, \qquad (25)$$

where

$$\rho=(1/r_j+1/r_k+1/r_m+1/r_n)^2 -2(1/r_j^2+1/r_k^2+1/r_m^2+1/r_n^2)$$

and r_{int} is the insphere radius that will just fit into the interstice of a dense-packed tetrahedron formed by four mutually tangent spheres of radius r_j, r_k, r_m, and r_n.

DENSE RANDOM PACKING PROPERTIES

Distributions of Equal and Uniform Sphere Sizes

Dense random packing simulations were performed on many different types of sphere distributions. Among these were equal, uniform, discrete, and log-normal populations. A unit sphere radius was used in the equal-sphere packings. The same distributions employed in the circle covering simulations described in chapter 2, having radii of (1,2), (1,2,3), (1,2,3,4), and (1,2,-3,4,5), were used in the packings of the uniform sphere size distributions.

The predicted dense random packing densities with and without interstitial filling of the equal- and uniform-sphere packings are shown in figure 14. The predicted density for the equal-sphere packing without interstitial filling was 0.7796. This value is in excellent agreement with the density analytically computed by Boerdijk (*1*) and Rogers (*5*). The higher densities predicted for the packings having more sphere sizes reflect the greater packing economy that a broader range of sphere sizes provides.

The calculated number of contacts and tetrahedra in the equal-sphere packing were 13.4 and 22.8, respectively, which are very close to the theoretical estimates of these properties made by Coxeter (*3*) and others for dense random packings of equal spheres. The average number of contacting spheres around each of the possible central spheres in the five uniform sphere packings is shown in figure 15. These data were similar to those calculated in two dimensions, where the coordination of a single circle was definable to within narrow limits. In the present case, the

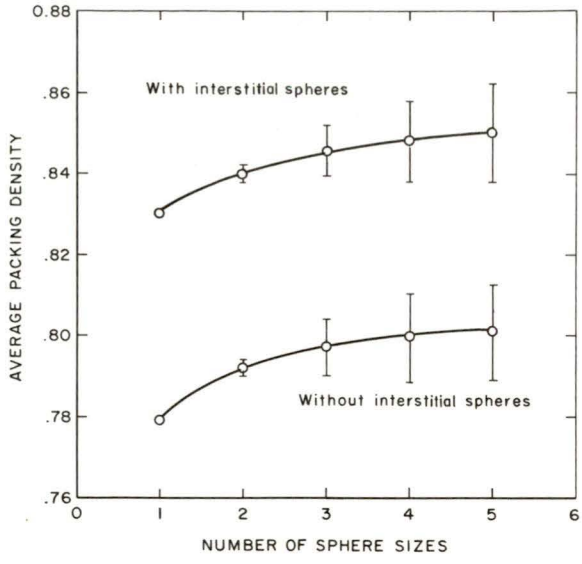

Figure 14.—Packing densities in dense random packings of discrete sphere sizes. The vertical bars indicate the standard deviation in the computed density around the central sphere in each packing.

standard deviation of the average contact numbers was usually less than 3 percent of the average value.

The average number of contacts in each of the uniform sphere distributions is shown in figure 16. The average pore volume and intersti-

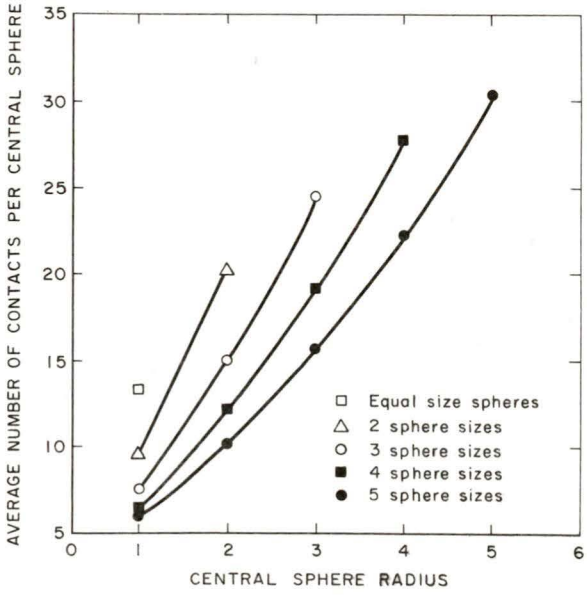

Figure 15.—Contacts per sphere in dense random packings of discrete sphere sizes.

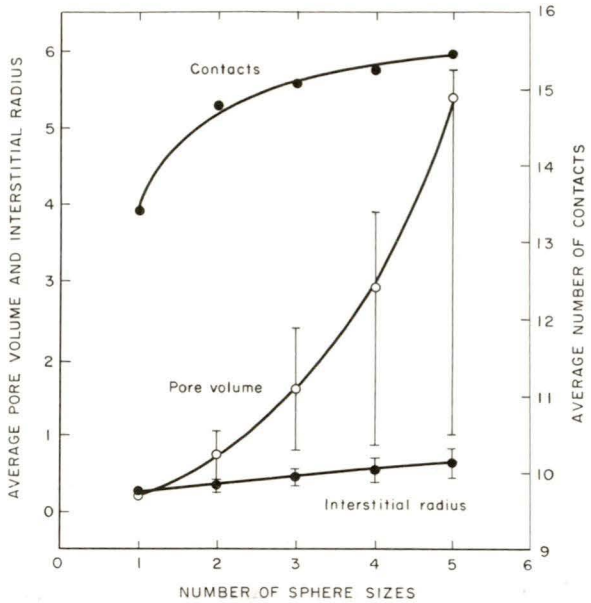

Figure 16.—Average pore volumes, contacts, and interstitial radii in dense random packing of discrete sphere sizes. The vertical bars represent 1 standard deviation from the average value.

tial radius within each of these packings are also shown. The relatively large deviations in the pore volume data result from tetrahedral combinations of only large and/or small spheres or of three spheres of about the same size combined with a much larger or smaller fourth sphere. As was the case in two dimensions, similar large deviations in the density data were not observed. For example, the packing density of a tetrahedron of large, equal spheres is the same as that of a tetrahedron of small, equal spheres because the ratio of pore volume to tetrahedron volume is the same in each case.

Discrete Sphere Size Distributions

The dense random packings of four discrete sphere size distributions were simulated, corresponding to those reported by Hogendijk (*4*). In an attempt to simplify the log-normal dense random packing work done by Wise (*6*), Hogendijk approximated Wise's continuous distribution with two, three, four, and five different radii whose occurrence in the packing corresponded to frequency ratios that roughly typified a log-normal distribution with a mean sphere radius of 1.205 and a geometric standard deviation of 1.685. Dense-packed tetrahedra were analytically constructed from these radii, and their packing statistics were examined. The radii frequency ratios in these tetrahedra are listed in table 3. With these data, Hogendijk made numerical estimates of the packing density with and without interstitial filling (Φ_i and Φ), the number of tetrahedra per sphere averaged over the total number of spheres (T), and the average interstitial sphere radius (R_{int}) and then compared his results with the data obtained by Wise. Hogendijk's results are listed in table 4. In general, his data showed reasonable agreement with those reported by Wise (who also reduced the log-normal distribution to a few discrete sizes in order to obtain numerical results). In the present study, packing simulations of the four distributions in table 3 were made to test the validity of Hogendijk's data. The results of these simulations, also presented in table 4, were not too different from those estimated by Hogendijk, but they reflect the improved statistics obtainable when dealing with greater numbers of tetrahedra (over 10,000) randomly constructed from these discrete distri-

Table 3.—Radii frequencies in Hogendijk's tetrahedron packings [1]

Radii	Frequency ratios	$\bar{R}$
1,2	2.02:1	1.33
1,2,3	2.18:2.86:1	1.80
1,2,3,4	1.78:4.97:2.47:1	2.17
1,2,3,4,5	1.15:5.98:4.32:1.89:1	2.69

[1] From (*4*), p. 112.

Table 4.—Hogendijk's sphere distribution dense random packing properties

Radii	Φ	$\bar{T}$	Φ_i	$\bar{R}_{int}$	$\bar{V}_p$
		HOGENDIJK (*4*)			
1,2	0.7947	5.360	0.8423	0.272	.....
1,2,3	.8017	5.135	.8496	.372	.....
1,2,3,4	.7996	5.100	.8476	.457	.....
1,2,3,4,5	.7978	5.110	.8458	.543	.....
		COMPUTER SIMULATION			
1,2	0.7948	5.419	0.8424	0.291	0.482
1,2,3	.7954	5.161	.8435	.371	1.037
1,2,3,4	.7949	5.105	.8430	.484	2.266
1,2,3,4,5	.7961	5.120	.8440	.588	4.060

butions. The calculated average pore volumes (V_p) for the simulated packings are also presented in table 4. More accurate predictions of the dense random packing properties of the log-normal distribution mentioned above were made by simulating the construction of the packing from the entire sphere population. These results and those obtained by Wise are presented in the following discussion of the log-normal dense random packings.

Log-Normal Distributions of Sphere Sizes

Although computer simulations of dense random packing were made with many different types of sphere distributions, of greater interest were those done with log-normal distributions because these are most often encountered in multisize-particle populations. Seven different log-normal distributions were used in the dense random packing simulations. The geometric mean sphere radius in each distribution was 1, and the geometric standard deviations were 1.0, 1.10, 1.30, 1.50, 1.74, 2.00, 2.50, and 2.96. Initially, the seven log-normal distributions were truncated at the sphere radii equivalent to ± 4 standard deviations from the mean sphere radius.

The log-normal distribution curve with a geometric standard deviation of 1.5 is shown in figure 17. The numbers of tetrahedra and intersphere contacts, calculated from equations 23 and 24, are plotted for a representative sample of central sphere radii in the dense random packing of this distribution. Similar data were obtained

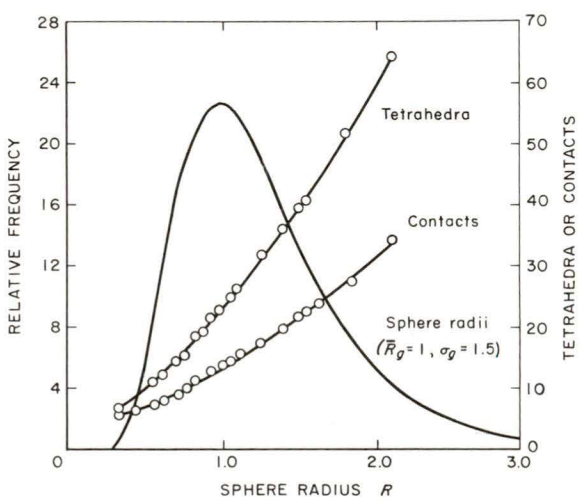

Figure 17.—Tetrahedra and contacts per sphere in a typical log-normal dense random packing.

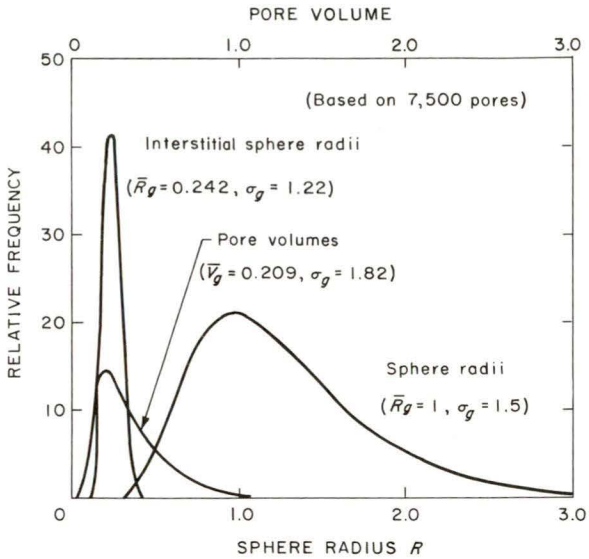

Figure 18.—Pore volume and interstitial radius distributions in a typical log-normal dense random packing.

for all of the log-normal dense random packings.

In figure 18, the calculated pore volume and interstitial sphere distribution curves are plotted for the same population shown in figure 17. These data, based on more than 7,500 tetrahedra calculations, were also found to be log-normally distributed. The mean interstitial radius remained relatively constant at 0.23 ± 0.02 of the mean sphere radius for $\sigma_g \leqq 2$. At larger standard deviations, slightly smaller mean interstitial radii were calculated. The mean pore volume also decreased at higher σ_g, but it remained relatively constant at approximately 0.21 (or about 5 percent of $4\pi/3$, the volume of a sphere with mean radius) for standard deviations of less than 2. Over the range of σ_g, the geometric standard deviations of the mean values increased from 1 to 1.66 and 4.68, respectively. At standard deviations of 1.5 or less, the sphere distribution functions were nearly symmetrical and the available size ratio was less than 30, so that when compared to the higher σ_g distributions, the available sphere sizes were not too different from one another. Thus the pores and interstitial radii in tetrahedra constructed from these distributions were closely grouped about the mean, as evidenced by the relatively small standard deviations shown in figure 18 for the sphere population with a σ_g of 1.5. At standard deviations greater than 1.5, tetrahedra of spheres of widely different radii were much more probable, and this led to

smaller mean pore volumes and interstitial radii than were observed for $\sigma_g \leq 1.5$. However, when compared with the two-dimensional dense random covering data in chapter 2, the relative decrease in the mean values was much less. The mean pore area and interstitial radius in the dense random coverings decreased from their nearly constant values by approximately 22 and 9 percent, respectively, over the range of σ_g for which the covering simulations were done. The corresponding decreases in the three-dimensional packings were 13 and 2 percent, respectively.

For the log-normal distribution shown in figure 18, there were very few spheres in the primary sphere population small enough to go into the interstices. However, as the standard deviation of the primary sphere distribution increased above 1.5, the overlap between the two sphere radii distribution curves became much greater and thus increased the probability that a sphere chosen from the primary distribution would fit into one of the interstices. When this occurred, it was geometrically impossible to construct this tetrahedron in a dense-packed configuration because all four spheres could not be made mutually tangent. As an example, consider a triangle of three rather large tangent spheres to which a fourth sphere is to be added to form a dense-packed tetrahedron. If the fourth sphere is small relative to the other three, it might fall through the triangular hole formed by the large spheres because it can not be made mutually tangent to all three. Hence, a tetrahedron of these four spheres would be geometrically impossible to construct in a dense-packed fashion. In the initial packing simulations of these distributions, whenever an invalid tetrahedron was encountered, the small sphere was discarded and another that could be made tangent to the other three was randomly selected. However, this procedure had obvious disadvantages. At the larger sphere standard deviations, the sphere distribution in the final dense random packing was considerably different from that of the initial sphere distribution, because tetrahedra of large spheres or of small spheres only were preferred.

At sphere radii standard deviations greater than 1.5 it became necessary to truncate the sphere distributions so that the size range was less than ± 4 standard deviations. For a large sphere population, the truncation limits required were dependent on the tetrahedron geometry and only slightly dependent on the distribution parameters. In this investigation, a size ratio of about 9.0 was adequate to reduce the number of invalid tetrahedra in 7,000 attempts to less than 0.05 percent when packing spheres with a geometric standard deviation less than or equal to 2.96. For distributions with larger standard deviations, the limiting size ratio approached 6.46. Thus it should be noted that only those distributions having sphere radii within well-defined limits can be packed in conformance with the definition of dense random packing. The mean pore volumes and interstitial radii decreased less than the analogous covering means because of these more restrictive truncation limits. Although more sphere sizes distant from the mean were chosen as the sphere radius standard deviation increased, the extreme sizes were not available because of the smaller size ratios imposed by the new truncation limits. The additional large or small spheres decreased the mean pore volume and interstitial radius in the packings, but not to the same extent that the extreme sizes did in the dense random coverings.

The mean dense random packing densities with and without interstitial filling of the log-normal packings and of an equal-sphere packing are shown in figure 19. These data are similar to those observed in the dense random coverings and in the discrete dense random packings of spheres, where greater particle size ratios resulted in more efficient packing and thus higher densities. However, above a sphere radius standard deviation of 1.5 the density in figure 19 approached a limiting value because of the truncation limits that were necessary to eliminate

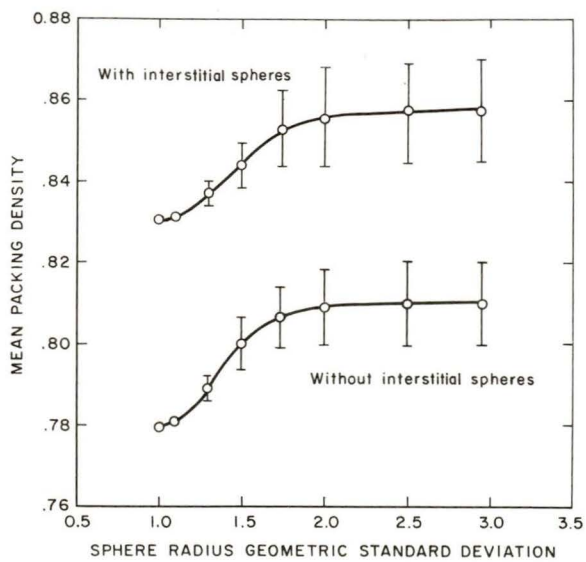

Figure 19.—Log-normal sphere dense random packing densities.

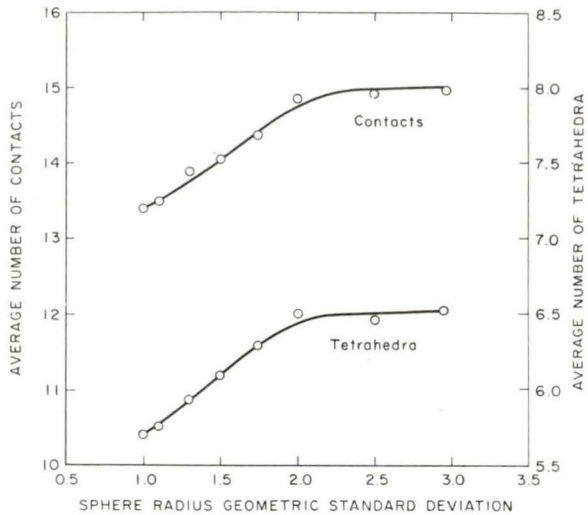

Figure 20.—Contacts and tetrahedra in log-normal dense random packings.

invalid terahedra in these packings. This limiting density (0.81) represents the dense random packing of a uniform distribution of spheres with a maximum size ratio of 6.46.

In figure 20, the number of tetrahedra and intersphere contacts per sphere of mean size are plotted for each log-normal distribution. The positive slope on the initial segments of these curves also reflects the improved packing obtainable as the allowable sphere size range is increased. However, when the probability of picking spheres near the truncation limits is no longer negligible (specifically, at large standard deviations), the number of contacts and tetrahedra also approach the values for a uniform distribution of spheres.

Among the other log-normal distributions whose dense random packings were simulated, one was reported by Wise (*6*) as having a mean radius of 1.205 and a standard deviation of 1.685. The density (Φ) and the numbers of contacts (N) and tetrahedra (T) associated with a sphere of mean size were estimated by Wise for a dense random packing of this distribution and are listed in table 5. By a complicated mathematical analysis of the tetrahedra that could be formed from this population, Wise was able to deduce the rough estimates shown in table 5 from the corresponding properties of the weighted averages of the 15 possible tetrahedra formed by spheres with radii of $\frac{1}{2}R_g$, R_g, and $2R_g$. With the same three sphere radii the properties of over 5,000 individual tetrahedra randomly selected in

Table 5.—Dense random packing properties of Wise's log-normal sphere distribution

Source	Φ	$\overline{N}$	$\overline{T}$
M. E. Wise (*6*)	0.802	12.2	20.0
Individual tetrahedra simulation	.8018	11.943	19.886
Distribution simulation	.8057	12.650	21.300

accordance with Wise's tetrahedron frequency function were calculated and averaged to give the packing properties shown in table 5 for individual tetrahedra. As expected, these data are very similar to those obtained by Wise, except they are statistically better because of the greater number of tetrahedra that were considered in their calculation. A more accurate prediction of the dense random packing properties of this distribution was made by simulating the construction of the packing from the entire sphere population. These results, also shown in table 5, were larger than those given above because all of the available sphere size range was considered. As noted before, when the sphere size ratio is increased, the spheres pack more efficiently to produce higher densities, more tetrahedra, and more contacting spheres.

The question of whether dense random packings of spheres can be obtained experimentally has been tentatively answered in experimental investigations of particle compaction at the Bureau.[4] In this research, an attempt was made to use the Cooper-Eaton relationship (*2*),

$$V = A_1 e^{-k_1/P} + A_2 e^{-k_2/P}, \qquad (26)$$

to correlate powder compaction data obtained in a double-acting die. V in this equation is the relative compaction of the powder, P is the compacting pressure, and k_1 and k_2 are empirically determined constants. The first exponential term in equation 26 is purported (*2*) to represent the compaction that occurs by rearrangement of particles, and the second, the compaction that occurs by brittle fracture. The coefficients A_1 and A_2 represent the maximum extent of densification achievable by the respective mechanisms. Several compaction experiments with multisize powders that were nearly perfect spheres were made by the Bureau in the belief that the coeffi-

[4] The authors are indebted to Dr. D. A. Stanley of the Bureau of Mines College Park Metallurgy Research Center, College Park, Md., for suggesting the experimental approach outlined here.

cient A_1 corresponds to the density of dense random packing for the powder used. A_1 was calculated in each of these experiments and compared with the density predicted by the dense random packing simulation of the same sphere distribution. For example, the density predicted for one of the experimental powders was 0.805, whereas the values of A_1 calculated during several compaction experiments on the same powder were 0.80 ± 0.01. Thus, the preliminary results indicate that the packing density predicted by the computer model is very nearly identical with the ultimate density achievable by particle rearrangement during compaction. These observations are intuitively very acceptable, because if one assumes that some elastic deformation of the particles is possible during compaction, it seems quite probable that the particles will be forced to assume a dense-packed structure, at least in some regions of the packing.

REFERENCES

1. Boerdijk, A. H. Some Remarks Concerning Close-Packing of Equal Spheres, Philips Res. Rept., v. 7, January 1952, pp. 303–313.
2. Cooper, A. R., and L. E. Eaton. Compaction Behavior of Several Ceramic Powders. J. Am. Ceram. Soc. v. 45, 1962, pp. 97–101.
3. Coxeter, H. S. M. Close Packing and Froth. Ill J. Math., v. 2, No. 4B, 1958, pp. 746–758.
4. Hogendijk, M. J. Random Dense Packing of Spheres With a Discrete Distribution of the Radii. Philips Res. Rept., v. 18, March 1963, pp. 109–126.
5. Rogers, C. A. The Packing of Equal Spheres. Proc. London Math. Soc., v. 8, 1958, p. 609.
6. Wise, M. E. Dense Random Packing of Unequal Spheres. Philips Res. Rept., v. 7, February 1952, pp. 321–343.
7. ———. On The Radii of Five Packed Spheres in Mutual Contact. Philips Res. Rept., v. 15, April 1960, pp. 101–106.

— 4 —

COMPUTER SIMULATION OF LOOSE RANDOM COVERINGS OF CIRCLES

by

Lindsay D. Norman and Edwin E. Maust, Jr.

COMPUTER SIMULATION MODEL

In all the simulations of loose random coverings of circles, the pseudo-random number generator described in chapter 2 was used to randomly select circle radii from specified circle populations. The computer program developed for constructing loose random coverings utilized a two-dimensional Cartesian coordinate system, or x–y grid, in the computer memory on which all calculations of distances and circle coordinates were made and in which the area occupied and the locations of circles present in the covering were stored. The latter feature allowed for rapid surveys of the area covered by circles at any time during the construction of the covering and for the examination of any region of the covering such as the outer boundary. Because the computer programs were designed to simulate actual construction of circle coverings, this ability to map the area covered by circles as the covering grew simplified the problem of deciding where each new circle should be placed at each step of the construction progess.

The x–y grid was reserved in the computer memory with a two-dimensional array of the form $XY(x,y)$ having dimensions of 140 by 140. This array effectively established a square area with 140 units on a side on which the covering was constructed. Each grid point in this area had an array location in memory; thus, whenever a circle was placed anywhere on this area, the grid points on or within the circle were effectively reserved by changing the value of the XY variable for these array points to any convenient number that indicated the reserved or covered condition. The major disadvantage of using the point array was that the number of memory locations available to the user on most computers limits the number of circles or the size of the covering that can be constructed. However, in this investigation the aforementioned array dimensions, requiring 19,600 memory locations, provided a sufficiently large area for simulating the construction of coverings with 200 or more circles having radii less than or equal to 5 units.

The computer-simulated construction of a loose random covering began by random selection of the first circle, which was placed at the center of the coordinate system. The second and third circles were placed tangent to the first, but separated from each other by a specified angle Ψ, between the lines joining each of their centers with the center of the first circle. The arrangement of the first three circles formed the nucleus upon which the remainder of the covering was constructed. Beginning with the fourth and every one thereafter, each successive circle was placed tangent to at least two existing circles on the boundary of the covering. Of the many possible positions on the boundary where the new circle could be placed tangent to two existing circles, the one closest to the center of the covering was chosen. This procedure was equivalent to subjecting the circle additions to a radial gravitational field; hence, the computer models for constructing the coverings may be thought of as radial gravitational models. As each circle was added, the list of the coordinates of each of the grid points in the XY array lying on the perimeter or within the circle was updated to indicate that area of the coordinate plane was now occupied by a circle. For a circle of radius r having its center at the coordinates h and k, the x–y grid points on or within this circle are all the integral solutions of the equation

$$(x-h)^2+(y-k)^2\leq r^2. \tag{27}$$

The value of the XY array at each of these grid points was set equal to the circle number within

or on which they lay so that, at any stage of the covering construction, the particular circles that formed any portion of the covering were immediately specified by the values of XY at the x–y locations in that portion of the covering.

When a circle was to be added to the covering, the list of covered grid points was searched to find the boundary site closest to the center of the covering and the existing circles in the vicinity of that site. The new circle was then placed tangent to the two existing circles closest to the chosen boundary site. The center coordinates (a,b) of the new circle were calculated by simultaneously solving the equations

$$(a-h_1)^2+(b-k_1)^2=(r_1+r)^2 \tag{28}$$

and

$$(a-h_2)^2+(b-k_2)^2=(r_2+r)^2, \tag{29}$$

where (h_i, k_i) and r_i are the center coordinates and radii, respectively, of the two existing circles, and r is the radius of the new circle. For each pair of existing circles, equations 28 and 29 give two solutions for (a,b), one on each side of the line connecting the centers of these circles. In the computer simulations, the center site furthermost from the center of the covering was selected as a potential center for the new circle. The new circle was placed in this position and tested to insure that it did not overlap any existing circle in the covering. If it did, other combinations of two boundary circles in the vicinity of the chosen site were used to compute another potential center. When no overlap existed, the location was accepted, the list of covered grid points updated, and the entire process was repeated for the next circle.

The centers of all mutually tangent circles were considered to be connected by straight lines at each stage of the covering construction so that the covering defined a network of area-covering, n-sided polygons whose vertices were circle centers. Figures 21 and 22 show typical loose random coverings of equal circles and of a uniform distribution of circles (R=2, 4, 6, and 8), respectively, whose construction was simulated by the computer. Several of the polygons whose edges connect tangent circle centers are drawn. In all of the circle coverings constructed in the manner just described, the number of edges of any polygon in the covering was always $3 \leq n \leq 6$. These four general types are shown in figure 23. For n=3, triangles were formed that were equivalent to those considered in the dense random coverings described in chapter 2. At n=4, parallelograms or a square was possible. Because a new

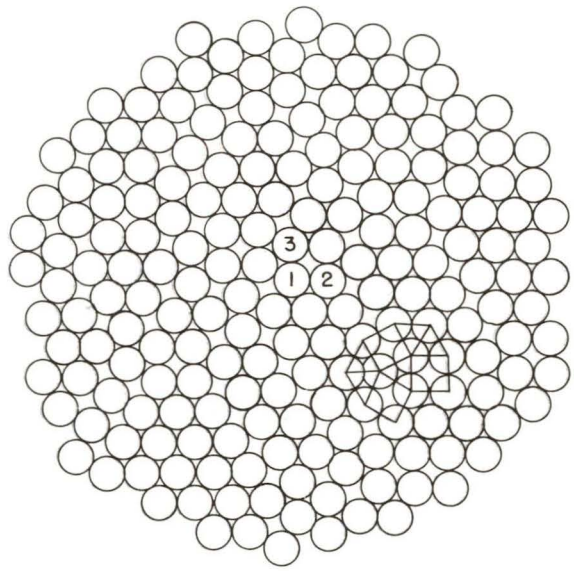

Figure 21.—Loose random covering of equal circles. The first three circles selected during construction of the coverings are labeled.

polygon was formed with each circle added to the covering after the first three, the total area, the area covered by circles, and the uncovered pore area within each new polygon could be calculated as the construction progressed. After the

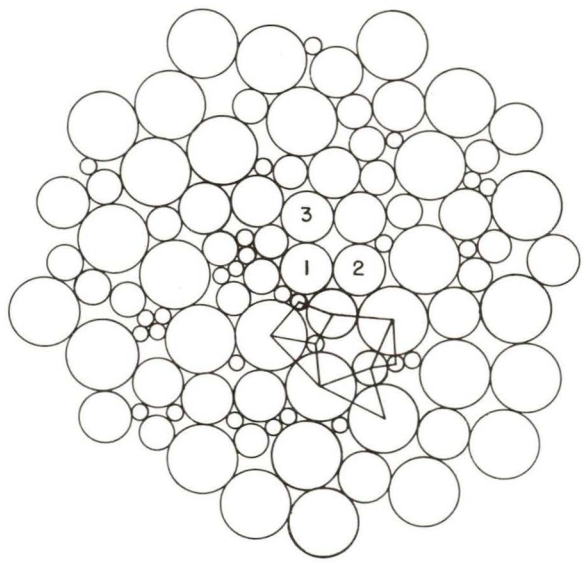

Figure 22.—Loose random covering of a uniform distribution of four circle sizes. The first three circles selected during construction of the covering are labeled.

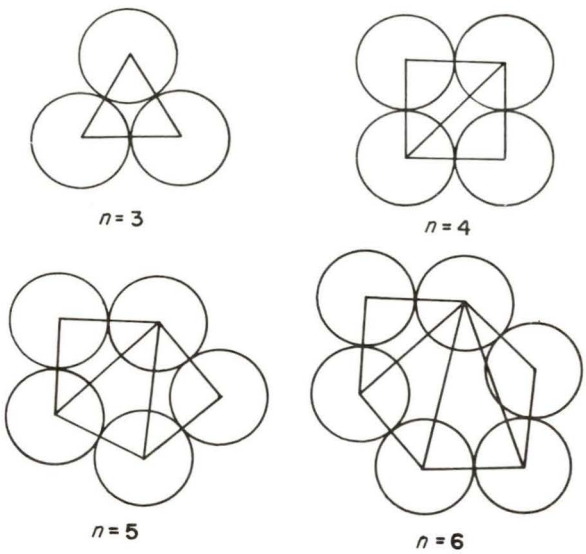

Figure 23.—Polygon types in loose random coverings.

last circle had been added, the covering density and pore size distribution were calculated from these data, obtained for all of the polygons in the covering. In order to calculate these areas, every time a circle was added to the covering, the computer determined the type of polygon that the new circle had just completed. For polygons with $n>3$, a system of $(n-2)$ triangles was constructed within each polygon as shown in figure 23. The total area of each of the $(n-2)$ triangles was found by calculating the lengths of their three edges (a, b, and c) and substituting these data in equation 15,

$$\text{Area of triangle}=[U(U-a)(U-b)(U-c)]^{1/2},$$

where $U=(a+b+c)/2$. The covering density within any single triangle, defined as the area covered divided by the total area, was found by calculating the total circle sector area within each triangle. For a triangle with vertices centered on circles of radii R_1, R_2, and R_3, the total area of sectors is given by equation 16:

$$\tfrac{1}{2}(R_1^2A+R_2^2B+R_3^2C),$$

where angles A, B, and C, expressed in radians, are the angles in the triangle defining the sectors of the circles of radius R_1, R_2, and R_3, respectively. The covering density was given by

$$\Phi=\text{Area sectors/area triangle}$$

and the pore area by

$$\text{Pore area}=\text{Areas of triangle}-\text{Area of sectors.}$$

Although triangles were used exclusively in the calculation of the covering density, the numbers and types of polygons formed by tangent circles were important in interpreting the statistical geometry in these systems. Thus, in all of the covering simulations, records of the numbers of each kind of polygon and their size and edge length distributions were maintained as the construction progressed. Once the covering was completed, the center-to-center distances between the first 50 circles that were placed in the covering and between all the other circles were calculated to provide data for plotting the radial distribution function. More importantly, these data were also used to calculate the average number of contacts in the covering.

LOOSE RANDOM COVERING PROPERTIES

Computer simulations of loose random coverings were performed with many different circle populations, such as equal, discrete, and uniform distributions. The objectives of these simulations were to provide a body of data for use in developing the statistical geometry of circle coverings and to develop means for predicting covering properties from circle sizes or some other property of the covering. However, the majority of the computer simulations were done with equal circles because the properties of these coverings were more amenable to statistical analysis and many of the empirical observations made on them were found to apply to the unequal-circle coverings as well. The uniform-circle coverings were constructed from distributions having two to four different circle radii combined as follows: (1,2), (1,2,3), and (1,2,3,4).

For equal circles, the requirement that each new circle added to the covering had to be tangent to at least two existing circles placed a lower limit of 0.7854 on the covering density that could be obtained. This value is the density of a regular square array of equal circles. In effect, the tangency requirement insured that only mechanically stable coverings would be constructed. By removing this restriction and by allowing circles to be placed in the covering at any portion of the bounadry, so that the additional requirement of only placing circles at the boundary site nearest to the center of the covering was removed, coverings that were looser than the square array could have been built. However, this lower limit on the density was believed to be well below that

of any realistic system that might be of interest in this investigation. Moreover, by retaining the tangency requirement, no pores in any covering were large enough to admit another circle. Hence, this requirement produced the two-dimensional analog of Bernal's (*1*) [1] proposition on the nature of real loose random packings of equal spheres, specifically, no holes large enough to admit another sphere.

In each of the equal-circle coverings, different configurations of the first three circles in the covering were used to examine their effect on the covering properties. The angle (Ψ) separating the second and third circles was specified at the beginning of each simulation at either 70°, 80°, or 90°. For $\Psi=\pi/3$, a regular close-covering or dense random covering was constructed. For $\pi/2<\Psi<\pi$, the resulting covering was identical to that constructed with the supplement of Ψ. In figures 21 and 22, the first three circles selected during construction of the coverings are labeled. The starting angle in each of these coverings is $\pi/2$. This angle was also employed in the loose random coverings of multisize-circle populations having from two to four different radii.

Some of the loose random covering properties calculated for the equal and uniform circle distributions are listed in table 6. The calculated properties of the equal-circle coverings were independent of circle size. Moreover, the similarity between calculated density (Φ) and average number of contacts ($\overline{N}$) in each covering indicated that the starting angle (Ψ) had only a slight effect on the final properties of each covering.

In an attempt to simulate the construction of lower density coverings, the position of the fourth circle was specified at the outset of two different simulations. Its position was chosen to maximize the distances between the first four circles so that the loosest possible construction nucleus would be used. In each case, the second and third circles were placed at an angle of $\pi/2$ to one another, and the center of the fourth circle was placed at the angle Ψ' from the x-coordinate axis. The covering data from these simulations, also tabulated in table 6, were not too different from those calculated when the position of the fourth circle was not specified. All of these observations suggest that the density and average number of contacts in a loose random covering of equal circles, believed to have maximum mechanical stability, are approximately 0.85 and 5.0,

[1] Italicized numbers in parentheses refer to items in the list of references at the end of this chapter.

Table 6.—Loose random covering properties of equal and uniform circle distributions

$\overline{R}$	Ψ(°)	Ψ'(°)	$\overline{N}$	Φ	$\overline{A_p}$	Number of circle sizes
			EQUAL CIRCLES			
3	60	—	6.000	0.9069	1.451	1
3	70	—	5.360	.8724	2.678	1
3	80	—	5.024	.8525	3.187	1
3	90	—	5.000	.8516	3.112	1
4	90	—	5.054	.8546	5.322	1
3	Square array	—	4.000	.7854	7.722	1
3	90	−110	4.827	.8442	3.710	1
4	90	−100	4.890	.8461	6.399	1
			UNIFORM CIRCLE DISTRIBUTION			
1.5	90	—	5.022	0.8558	1.839	2
2.0	90	—	4.925	.8488	3.837	3
3.69	90	—	4.880	.8444	6.273	3
2.5	90	—	4.721	.8402	7.208	4

respectively. For equal circles the actual average density and number of contacts, calculated from all but the dense random covering ($\Psi=60°$) and regular square array data in table 6, are 0.8536 and 5.026, respectively. If the hypothesis of maximum stability is correct, the above values of Φ and $\overline{N}$ are those defining a random close-covering of equal circles. A covering with these properties would be the two-dimensional analog of Scott's (*3*) random close-packing of equal spheres, also having maximum stability.

The radial distribution calculated for the covering in figure 21 is plotted as a histogram in figure 24. Very similar data were obtained in all

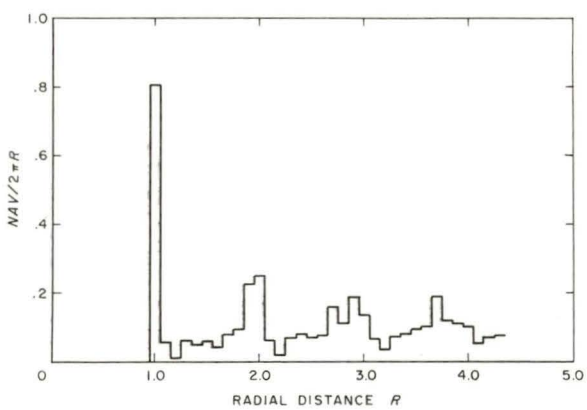

Figure 24.—Radial distribution curve in a loose random covering of equal circles.

of the loose random coverings of equal circles. In figure 24, NAV is the average number per circle of intercircle distances of size R, where R is the radial distance in circle diameters from the center of any one of the 50 different reference circles used in this calculation to any other circle in the covering. The average number of intercircle distances at $R=1.0$ is also the average number of contacts in each covering. Data similar to that shown in figure 24 have been given elsewhere (*2*) for several experimentally produced loose random circle coverings. The radial distribution data presented herein agree very well with these data. Although the computer predictions were based on artificially produced coverings of circles, the agreement of the radial distribution data indicates that the properties predicted for the simulated coverings are probably representative of those that one would obtain for experimentally produced coverings.

The contact and average pore area ($\overline{A}_p$) data in table 6 were plotted against the covering density in figure 25 to determine if there was any significant dependency between them. To remove any dependence upon circle size, the average pore area was plotted as a fraction of the area of a circle having the average radius in the covering. The corresponding data calculated for the dense random coverings of discrete numbers of

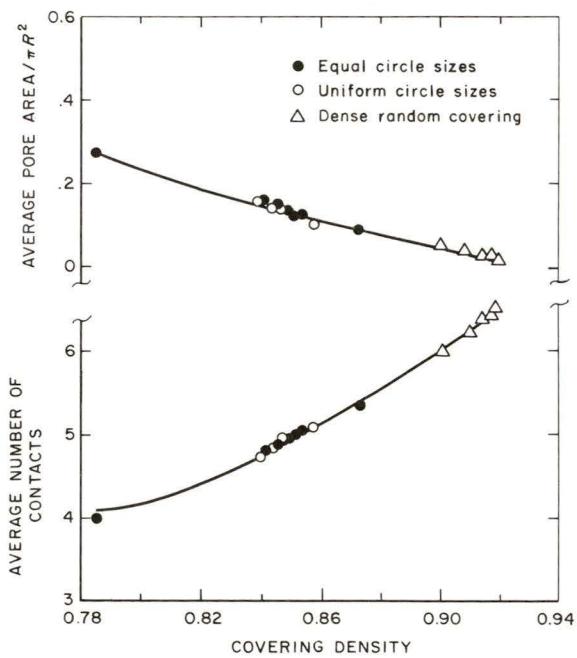

Figure 25.—Average number of contacts and pore area in loose random coverings.

circle sizes are also shown in figure 25. From a purely empirical treatment of these data, the equations

$$\overline{N}=0.291e^{3.34\phi} \tag{30}$$

and

$$A_p'=\overline{A}_p/\pi R^2=0.983-0.159\Phi-\Phi^2 \tag{31}$$

were found satisfactory for expressing the observed relationship between the covering density and the average number of contacts and average pore area, respectively.

In the equal-circle coverings, analysis of the pore sizes and types in the networks of polygons showed that only two kinds of polygons existed in these coverings. These were equilateral triangles and parallelograms; the acute angles of the latter were identical to the angle Ψ specified for the first three circles. In the two coverings where Ψ' was specified, polygons of the type in figure 23 with $n=5$ were formed, but in each case they accounted for less than 0.8 percent of the total number of polygons. The remainder were equilateral triangles and parallelograms with acute angles of 70°, 80°, and 90°, all occurring with different frequencies. When the position of the fourth circle was not specified and the starting angle was $\pi/3<\Psi\leq\pi/2$, only equilateral triangles and parallelograms having just the acute anle Ψ were propagated as the covering grew. This situation can be seen in the covering in figure 21 in which Ψ was $\pi/2$. Only equilateral triangles and squares would be present in this covering after connecting all the tangent circle centers. When $\Psi=\pi/3$, the trivial case of dense random or regular close-covering resulted, where the polygon network consisted entirely of equilateral triangles.

To a good approximation, it was found that the covering properties of all the equal-circle coverings were predictable by taking suitable weighted averages of the corresponding properties of just four polygons: an equilateral triangle, parallelograms having acute angles of 70° or 80°, and a square. The edge lengths of the polygons in all cases were equal to twice the circle radius. In table 7 the covering area and density for each of the four polygons constructed from circles of radius R are listed. By considering these four polygons as the only ones present in a covering, the density can be formulated in terms of the relative frequency of occurrence and properties of each polygon and is given by

$$\Phi=\frac{1.571[f_1+2(f_2+f_3+f_4)]}{1.732f_1+3.759f_2+3.939f_3+4f_4}, \tag{32}$$

Table 7.—Covering properties of four types of polygons in loose random coverings of equal circles

Polygon	Acute angle	Polygon area	Pore area	Density
Equilateral triangle	60°	$\sqrt{3}R^2$	$(\sqrt{3}-\frac{1}{2}\pi)R^2$	0.9069
Parallelogram	70°	$4R^2 \sin 70°$	$(4 \sin 70°-\pi)R^2$	.8358
Do	80°	$4R^2 \sin 80°$	$(4 \sin 80°-\pi)R^2$	.7975
Square	90°	$4R^2$	$(4-\pi)R^2$	.7854

where f_1 is the normalized frequency of triangles and f_2, f_3, and f_4 are the normalized frequencies of 70°, 80°, and 90° parallelograms, respectively. Different coverings correspond to different frequency distributions. The normalized frequency of occurrence is defined such that

$$f_1+f_2+f_3+f_4=1. \tag{33}$$

Hence, in a dense random covering of equal circles, where all the polygons are triangles, f_2, f_3, and f_4 are zero, and the covering density predicted by equation 32 is $1.571/1.732=0.907$, as expected.

Euler's law in two dimensions, $P-E+C=1$, relates the number of polygons (P), edges (E), and apices or corners (C) in any area-covering arrangement of polygons and is not altered by any topologically continuous distortion. The polygon network formed by circle centers in the simulated coverings had to conform to this law. In these coverings, each polygon with n sides contributes $n/2$ edges to the covering, except at the boundary where some of the polygon edges are not shared. Therefore, the total number of edges in each covering is

$$E=\tfrac{1}{2}\left(\sum_n nP_n+E_b\right)$$

where P_n is the number of n-sided polygons and E_b is the number of edges on the covering boundary. On the average, N edges met at each corner so that

$$C=2E/\overline{N},$$

because each edge joins two circle centers. Substituting these relations in Euler's law gives

$$\sum_n P_n-\tfrac{1}{2}\left(\sum_n nP_n+E_b\right)+\left(\sum_n nP_n+E_b\right)/\overline{N}=1,$$

which was first simplified to

$$\sum_n P_n+\left(2-\overline{N}\right)\left(\sum_n nP_n+E_b\right)/2\overline{N}=1,$$

and finally to

$$n_1+n_2+n_3+n_4+(2-\overline{N})[3n_1+4(n_2+n_3+n_4)+E_b]/2\overline{N}=1, \tag{34}$$

where n_1 is the number of triangles and n_2, n_3, and n_4 are the numbers of 70°, 80°, and 90° parallelograms, respectively, in the covering. When a covering approaches infinite size, ΣP_n or Σn_i approaches infinity, $\overline{N}$ remains constant, and E_b increases, but at a much slower rate than ΣP_n. Thus, equation 34 can be simplified by dividing each term by ΣP_n and discarding all terms that are negligible or zero in an infinite covering. This simplification gives

$$(\overline{N}-2)[3f_1+4(f_2+f_3+f_4)]/2\overline{N}=1$$

or

$$\overline{N}=\frac{6f_1+8(f_2+f_3+f_4)}{f_1+2(f_2+f_3+f_4)}, \tag{35}$$

where the f_i's have the same meaning as before. Equation 35 could have also been derived by considering the average interior angle α between polygon edges in the covering. For an infinite covering, $\alpha(°)=360/\overline{N}$. In any covering of the four special polygons,

$$\text{Total number of angles}=3n_1+4(n_2+n_3+n_4),$$

and

$$\text{Total angle sum }(°)=180n_1+360(n_2+n_3+n_4).$$

Thus,

$$\alpha(°)=180[f_1+2(f_2+f_3+f_4)]/[3f_1+4(f_2+f_3+f_4)]=360/\overline{N},$$

which, when solved for $\overline{N}$, gives the same expression as equation 35. This equation or equation 35 is a consequence of area-covering and together with equation 33, evidently embodies a restriction on the polygon distributions that are allowed in coverings of various densities constructed from the four kinds of polygons.

For a specified value of f_1 in equation 33, the equation represents a plane in a three-dimensional space in which f_2, f_3, and f_4 are the three coordinates. The normal to the general plane $Ax+By+Cz+D=0$ has direction numbers $[A,B,C]$, regardless of the particular value of D. Hence, equation 33 implies that, for any specified value of f_1, the direction numbers of the normal to the specified plane in f_2–f_3–f_4 space are [1,1,1]. Equation 33 thus represents a family of parallel planes, each member representing a different value of f_1.

Inspection of equation 35 in conjunction with 33 indicates that $\overline{N}$ is a function of f_1 only. Hence, in a family of parallel planes, each member must also be a plane of constant coordination number. However, in view of equation 32, the planes are not planes of constant density. These facts, and the fact that empirical equation 30 adequately represents the observed relationship between $\overline{N}$ and Φ, imply that, of the various polygon distributions which can possibly satisfy space-filling requirements, only special distributions corresponding to some particular surface in f_2–f_3–f_4 space were encountered in the computer models. If strict analytical consistency prevailed, this surface would be the locus of all points simultaneously satisfying both equations 32 and 35 and would further be the surface on which $\overline{N}$ and Φ were everywhere related by equation 30. That this is not the case and that, therefore, equation 30 must be an approximation, is easily demonstrated. Equations 32 and 35, having been derived from basic principles, can be considered irrefutable in the present context. Inasmuch as $\overline{N}$ is a function only of f_1 but Φ is not, there can be no relationship between them in which all f-dependence vanishes, such as indicated by equation 30. This equation, being merely an empirical fit to observed results, is clearly an approximation and, for strict analytical consistency, should include some dependence upon polygon distribution parameters. The fact that equation 30 fits the data satisfactorily as it stands implies that the dependence of the correct relationship between $\overline{N}$ and Φ upon polygon distribution must be a very weak one.

The surface in f_2–f_3–f_4 space corresponding to the polygon distributions encountered in the computer models was found by a numerical-graphical procedure, as follows: Values for f_1 and for many f_2, f_3, and f_4 combinations consistent with equation 35 were assumed, and then the density for each combination was calculated from equation 34. These data provided a density contour map for the given f_1 plane. In triangular coordinates, the f_1=0.7 plane is shown in figure 26, along with several calculated densities for this case. From equation 35, $\overline{N}$ was found to be 5.077 and from equation 30 Φ should be 0.8568. The line shown in figure 26 is the locus of points satisfying all these conditions and represents the ranges of f_2, f_3, and f_4 occurring in space-filling arrangements of equilateral triangles and 70°, 80°, and 90° parallelograms, in which the triangles constitute 70 percent of the polygons present. Repetition of this procedure for other f_1

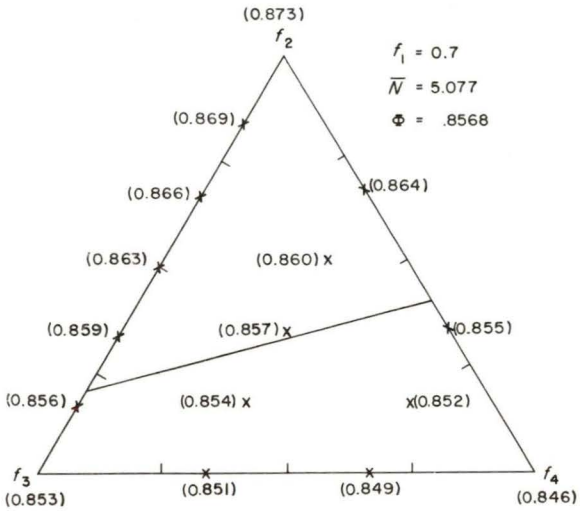

Figure 26.—Density map of an area-covering array of equilateral triangles and parallelograms.

planes (f_1=0.1, 0.2, . . . , 0.9) permitted development of the surface shown in figure 27. The allowed ranges of f_2, f_3, and f_4 for each case are summarized in table 8.

These data, together with equations 30 through 35, summarize in all essential detail the polygon distributions in, and the properties of, the equal-circle coverings generated in this study. Starting angles (Ψ) other than those used here would lead to coverings that contained parallelograms having acute angles other than 70°, 80°, and/or 90°, and these coverings could be analyzed in a similar fashion.

Analysis of the data on coverings of unequal circles was not as straightforward as that of the coverings of equal circles. Empirical equations

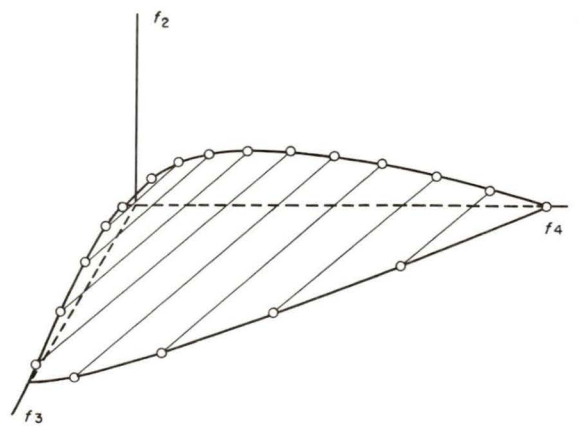

Figure 27.—Parallelogram frequencies in equal-circle coverings.

Table 8.—Allowed polygon frequencies in equal-circle coverings

f_1	f_2	f_3	f_4
0.0	0.0	0.0	1.0
.1	0.0 –0.041	0.0–0.171	0.729–0.959
.2	.0 – .076	.0– .313	.487– .724
.3	.0 – .103	.0– .424	.276– .597
.4	.0 – .122	.0– .500	.100– .478
.5	.012– .131	.0– .488	.0 – .369
.6	.043– .131	.0– .357	.0 – .269
.7	.060– .119	.0– .240	.0 – .181
.8	.059– .094	.0– .140	.0 – .106
.9	.040– .055	.0– .060	.0 – .045
1.0	0.0	0.0	0.0

30 and 31 are equally applicable to these data. However, at first inspection the density and contact data in table 6 indicate that a situation existed in these coverings that was opposite to that observed in the unequal-circle random covering data in chapter 2. Intuitively one would expect the density and contacts to become greater as the number of circle sizes or the size range increased, regardless of the type of random covering considered. The data in table 6 indicate that the opposite effect occurred. The source of this anomaly was discovered on inspecting the mappings of circles that were drawn from the circle coordinate and radius data that were printed out by the computer at the end of each covering simulation. For example, when the covering in figure 22, which was constructed from four circle sizes having a size ratio of four, is compared to that shown in figure 28, having two circle sizes and a size ratio of two, the two-size covering appears to be mechanically more stable. In the four-size covering, there are many small circles that could move within an adjacent pore and in so doing allow outlying circles to move closer to the center of the covering. This would result in more stable and denser circle configurations. Thus, if each of these coverings were subjected to some restraining force aimed at increasing the mechanical stability of each, the two-size covering in figure 28 would change very little because of the limited latitude for movement of any of its circles, whereas the covering in figure 22 would have many possible ways of rearranging itself to increase its stability. If it were possible to perform this rearrangement, the density and number of contacts in this covering would undoubtedly be higher than that calculated for the two-size covering. This difference would then conform to all of the previous observations on the effect of size ratio on the covering properties. The fact that the most stable coverings were not constructed from the higher size ratio circle populations was merely in artifact of the manner in which these coverings were constructed. Whereas the equal-circle loose random coverings were believed to be random close-coverings having maximum mechanical stability, it appears that the unequal circles merely formed loose coverings in which small rearrangements would have produced the analogous close-covering condition of maximum stability. This situation is analogous to Scott's (*3*) observations on equal-sphere packing, where spheres poured into a container assumed random structures with densities of about 0.60, but when the container was shaken, sphere rearrangement increased the packing densities to approximately 0.64.

Analysis of the polygon networks in the unequal-circle coverings was complicated by the diversity of polygon shapes and sizes that exist in these coverings. For example, in a covering of m circle sizes there are

$$Q=[m(m+1)(m+2)]/3!$$

different possible triangles. The number of different equilateral triangles is equal to m, whereas $Q-m$ is the number of different scalene triangles that may exist in the covering. The unequal-cir-

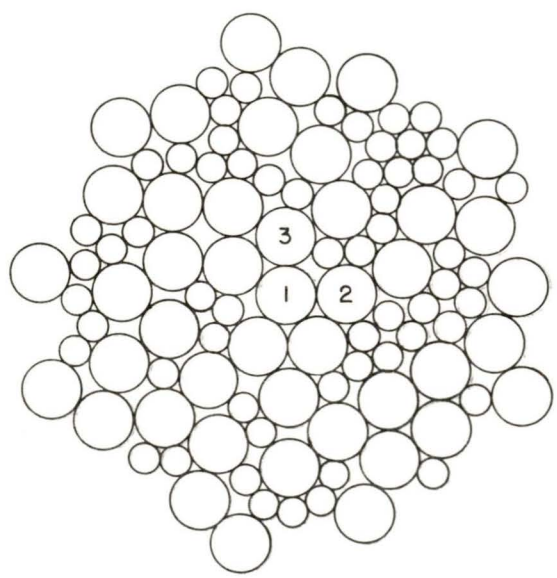

Figure 28.—Loose random covering of a uniform distribution of two circle sizes. The first three circles selected during construction of the covering are labeled.

cle polygon networks were further complicated by the fact that five- and six-sided polygons occurred quite often in these coverings. Moreover, no particular types or sizes of polygons were propagated as these coverings grew, which made it impossible to pursue the same type of development that was used to obtain equation 32, relating the density and polygon frequencies in equal-circle loose coverings.

Although the complexity of the polygon networks in the unequal-circle coverings precluded the development of any density–polygon frequency relation, these coverings had to conform to Euler's law. The number of edges and corners in these coverings were calculable from the same equations used in the equal-circle coverings, except that the index on ΣnP_n in the edge calculation went to six instead of four, to account for the presence of five- and six-sided polygons. Substituting E and C in Euler's law and simplifying the resulting expression for an infinite covering produced the following expression:

$$(\overline{N}-2)(3F_3+4F_4+5F_5+6F_6)/2\overline{N}=1,$$

where F_n ($n=3$, 4, 5, or 6) is the normalized frequency or fraction of n-sided polygons in the covering. When solved for $\overline{N}$, this equation reduced to

$$\overline{N}=\frac{6F_3+8F_4+10F_5+12F_6}{F_3+2F_4+3F_5+4F_6}, \tag{36}$$

which is the unequal-circle covering analog of equation 35. The polygon frequencies were formulated so that

$$F_3+F_4+F_5+F_6=1. \tag{37}$$

Hence, this equation also represents a family of planes in a three-dimensional space in which F_4, F_5, and F_6 are the three coordinates, and different values of F_3 correspond to different planes in the family. However, a detailed analysis of the polygon frequencies that would permit area-covering was not possible in the unequal-circle coverings, because inspection of equation 36 reveals that $\overline{N}$ is no longer a function of F_3 alone.

REFERENCES

1. Bernal, J. D. A Geometrical Approach to the Structure of Liquids. Nature, v. 183, Jan. 17, 1959, pp. 141–147.
2. Guadagno, J. R. A Compressible Sphere Theory of Liquid Structure. 97th Annual Meeting, AIME, New York, Feb. 26, 1968.
3. Scott, G. D. Packing of Equal Spheres. Nature, v. 188, Dec. 10, 1960, pp. 908–909.

— 5 —

COMPUTER SIMULATION OF LOOSE RANDOM PACKINGS OF SPHERES

by

Lindsay D. Norman and Edwin E. Maust, Jr.

Loose random packings of particulate systems are considerably different from dense random arrangements because gaps may exist between neighboring particles. This situation leads to lower densities, smaller coordinations, and more complex particle geometries than exist in dense random particle assemblies. In this investigation, the loose random arrangements were of greatest interest because they describe the arrangements formed by real particles. Therefore, in three dimensions, the validity of packing property predictions made by any computer simulation that might be developed could easily be tested for several different particle populations because of the existence of much of this data in the literature. Probably the greatest benefit to be derived from the development of loose random packing models is the prediction of particulate system properties that have heretofore escaped experimental determination or whose determination has been subject to considerable experimental error. Furthermore, these properties could be determined for systems comprised of any distribution of particles, provided the population could be analytically described.

COMPUTER SIMULATION MODELS

In the early stages of this investigation, it was considered advisable to base the development of the loose random models on the techniques and information that had been gained in simulating the dense random packings described in chapter 3. Because the properties of dense random particle arrangements are considered ideal upper bounds for the less dense, loose random systems, it seemed appropriate as a first step to modify the dense random models to account for the presence of gaps. However, it soon became apparent that this procedure could, at best, only approximate the properties of the looser assemblies. The lack of information on the particle geometry in loose random packings made it impossible to precisely identify the types and numbers of gaps that had to be incorporated into the dense random models (having one type of particle geometry) to produce loose packings of particles (having completely different geometrical arrangements). Thus, it became necessary to independently model the loose random packings by simulating the actual construction of these systems from a chosen sphere distribution.

The details of the computer programs developed for simulating the construction and for calculating the properties of loose random systems are presented in the following discussion. In addition, some of the data obtained by modifying the three-dimensional dense random packing model to produce looser packings are presented. Throughout these discussions, regular sphere arrangements are referred to frequently to provide understanding and a means of comparing the predicted packing properties to information that is widely known. Most of these data can be found in the packing literature (*9, 15, 18, 22*),[1] in geometry texts (*7*), or in almost any general presentation of crystallography.

Modified Dense Random Packing Model

Dense random packings of spheres are ideal assemblages and, in general, cannot be obtained experimentally by randomly putting spheres into a container. The properties predicted for dense random packings are considered ideal upper bounds for those of the looser or more realistic systems. For this reason, before an attempt was made to construct loose random packings with the computer in a fashion analogous to that used in two dimensions (chapter 4), the dense random packing models were modified to allow for the presence of gaps between spheres. In this manner,

[1] Italicized numbers in parentheses refer to items in the list of references at the end of this chapter.

it was hoped that new insights into the geometry of loose packings and into their gap distributions would be realized. Moreover, if real loose random packings could be constructed by this procedure, a unified solution for all types of random packings based on the relatively simple geometry of dense random packing would evolve from these endeavors.

Before the dense random packing models could be modified to produce loose packings, realistic means for adding gaps to the dense-packed structure had to be devised. It was assumed that the gaps in loose packings had some probability distribution function of their sizes, so that, in general, there were three parameters that had to be specified prior to adding gaps to the dense-packed structure. These were the gap size distribution mean and standard deviation and the frequency with which the gaps were to be added. Once these parameters were established, the packing property calculations were performed where the chosen gap size(s) was added at the specified frequency to one or more of the tetrahedron edges normally constructed during the dense random packing simulation.

To find the packing density and pore volume in each tetrahedron, the tetrahedron volume and the volume occupied by spheres were determined with plane and spherical trigonometry. First, the plane angles (A, B, and C) on each face of the tetrahedron were calculated from the general equation

$$A=2 \arctan [(U-b)(U-c)/U(U-a)]^{1/2}, \qquad (38)$$

where $U=(a+b+c)/2$ and a, b, and c are the three tetrahedron edges defining any given face. The same calculation was made for angles B and C. Three tetrahedron faces meet at a vertex; thus there are three plane angles associated with each vertex. For any single vertex in the tetrahedron, these angles, the tetrahedron faces, and the radius of the sphere centered on the vertex, define a sphere segment inside the tetrahedron. The surface of the sphere segment within the tetrahedron is a spherical triangle whose sides are angles A, B, and C calculated from equation 38 for each vertex. Thus, for a tetrahedron constructed from four spheres numbered 1 through 4, the spherical triangle sides associated with the segment of sphere number 1 were $A_{1\cdot23}$, $A_{1\cdot34}$, and $A_{1\cdot24}$, where the angle $A_{i\cdot jk}$ is the tetrahedron face angle formed at the vertex centered on sphere i, between the tetrahedron edges connecting spheres j and k. With a similar notation, the angles in the spherical triangle were identified by $\alpha_{1\cdot23}$, $\alpha_{1\cdot34}$, and $\alpha_{1\cdot24}$. Angle $\alpha_{1\cdot23}$, opposite side $A_{1\cdot23}$, was defined by the tetrahedron face planes formed by spheres 1, 3, and 4; 1, 2, and 4; etc. The spherical angles were calculated from equation 21,

$$\alpha_{1\cdot23}=2 \arctan \{\sin (S_1-A_{1\cdot34}) \sin (S_1-A_{1\cdot24})/ [\sin S_1 \sin (S_1-A_{1\cdot23})]\}^{1/2},$$

where $S_1=(A_{1\cdot23}+A_{1\cdot34}+A_{1\cdot24})/2$. Angles $\alpha_{1\cdot34}$ and $\alpha_{1\cdot24}$ were calculated from the same equation. The area of the spherical triangle θ was obtained from

$$\theta=(\alpha_{1\cdot23}+\alpha_{1\cdot34}+\alpha_{1\cdot24}-\pi)r_1^2 ,$$

where r_1 is the radius of the sphere centered on vertex number 1. As a fraction of the total surface area of this sphere, this equation transforms to

$$\theta'=\theta/4\pi r_1^2=[(\alpha_{1\cdot23}+\alpha_{1\cdot34}+\alpha_{1\cdot24})/4\pi]-1/4.$$

Therefore, the segment volume of the sphere centered on vertex number 1 is

$$4\pi r_1^3\theta'/3=(\alpha_{1\cdot23}+\alpha_{1\cdot34}+\alpha_{1\cdot24}-\pi)(r_1^3)/3. \qquad (39)$$

By an analogous series of calculations, the segment volumes of spheres 2, 3, and 4 in the above example were determined.

The volume of any tetrahedron can be expressed in terms of the lengths of its six edges by a five-by-five determinant:

$$\text{Volume}=\frac{1}{12\sqrt{2}}\begin{vmatrix} 0 & E_{12}^2 & E_{13}^2 & E_{14}^2 & 1 \\ E_{12}^2 & 0 & E_{23}^2 & E_{24}^2 & 1 \\ E_{13}^2 & E_{23}^2 & 0 & E_{34}^2 & 1 \\ E_{14}^2 & E_{24}^2 & E_{34}^2 & 0 & 1 \\ 1 & 1 & 1 & 1 & 0 \end{vmatrix}^{1/2} \qquad (40)$$

where E_{ij} (i and j=1, 2, 3, or 4) is the six tetrahedron edge lengths that connect vertices i and j. When tangent spheres define the tetrahedron edge, E_{ij} is equal to the sum of the radii of spheres i and j. If a gap is present, E_{ij} is equal to this sum plus the length of the gap. When expanded, equation 43 reduces to

$$\begin{aligned}\text{Volume}=\frac{1}{12}\ [&-(E_{12}^4E_{34}^2+E_{12}^2E_{34}^4+E_{13}^2E_{24}^4+E_{13}^4E_{24}^2 \\ &+E_{14}^2E_{23}^4+E_{14}^4E_{23}^2) \\ &+E_{12}^2(E_{23}^2E_{34}^2+E_{14}^2E_{23}^2+E_{13}^2E_{24}^2 \\ &+E_{24}^2E_{34}^2+E_{13}^2E_{34}^2+E_{14}^2E_{34}^2) \\ &+E_{13}^2(E_{23}^2E_{24}^2+E_{14}^2E_{24}^2+E_{14}^2E_{23}^2+E_{24}^2E_{34}^2) \\ &+E_{14}^2(E_{23}^2E_{24}^2+E_{23}^2E_{34}^2) \\ &-E_{12}^2(E_{31}^2E_{23}^2+E_{14}^2E_{24}^2) \\ &-E_{34}^2(E_{13}^2E_{14}^2+E_{23}^2E_{24}^2)]^{1/2}.\end{aligned}$$

In each tetrahedron, the packing density Φ is given by

$$\text{Total segment volume/tetrahedron volume}$$

and the pore volume V by

$$\text{Tetrahedron volume—total segment volume.}$$

The remainder of the property calculations were identical to those described for the dense random packings.

Initially, gaps were added between either every fifth or every other surface sphere and the last sphere to be added around the central sphere. This situation corresponded to a gap-to-surface sphere ratio in the packing of 1:5 or 1:2, respectively. In each of these cases, only equal spheres of radius R were considered. The gaps were randomly chosen with a random number routine from a uniform size distribution of from zero to R. The packing properties, density and contacts, were calculated in these simulations. However, these data were not very different from those predicted for the gapless packing. Therefore, if the packings were to approach real particulate systems, more drastic modifications had to be made in the dense packing model. This was accomplished by adding more gaps to the structure (in one case the gap-to-surface sphere ratio as as high as 4:3), by allowing gaps to exist between the central sphere and the surface spheres, by making the gap lengths greater than R, or by combinations of all of these. In addition to equal spheres, uniform and log-normal sphere distributions were used, as were equal, discrete, and log-normal gap distributions. All of the sphere and gap combinations that were employed in constructing modified dense random packings are summarized in table 9. Also listed are the density (Φ) and average number of contacts ($\overline{N}$) calculated for each of these packings.

Although some of the equal-sphere data in table 9 very nearly approximates the known packing density and number of contacts in real packings, the manner in which they were obtained was artificial, and the gap sizes and frequencies in no way related to the corresponding properties of real particulate systems. However, the behavior of the density and contact data bore a resemblance to that observed for circle coverings in chapter 4. To determine if $\overline{N}$ was functionally related to Φ in the three-dimensional packings, the data in table 9 were plotted in figure 29 together with some of the dense random packing data. The additional points in figure 29 were obtained by plotting the experimentally measured density and contact data of Bernal, Finney, and Mason (*3–4*), Scott (*16*), Smith, Foote, and Busang) (*20*), and Meissner, Michaels, and Kaiser (*14*), and of the regular packings of equal spheres. For $\Phi \geqq 0.5$, an empirical expression was found that fitted these data very well. This equation, represented by the solid portion of the curve in figure 29, is

$$\overline{N}=1.126e^{3.196\phi}. \tag{41}$$

This equation provides a much better fit to the experimental data in figure 29 than the equation, $\overline{N}=26.493-10.729/\Phi$, obtainable from Smith, Foote, and Busang's (*20*) empirical equations.

Table 9.—Modified dense random packing results

Sphere distribution	Gap distribution	Gap frequency [1]	Gap position in tetrahedron	Φ	$\overline{N}$
Equal (R=1)	Uniform (0→R)	1:5	Surface edges	0.7701	13.08
Do	do	1:2	do	.7558	12.59
Do	do	1:5	Any edge	.7603	12.80
Do	do	1:2	do	.7306	11.88
Do	do	1:1	do	.6744	9.94
Do	do	2:3	do	.5894	6.92
Do	Uniform (0→1.5R)	1:1	do	.6734	9.80
Do	do	2:3	do	.5420	5.90
Do	Discrete (0.9R or 0.45R)	2:3	do	.5839	7.66
Do	Discrete (0.5R or 0.25R)	2:3	do	.6116	8.86
Do	Discrete (0.4R or 0.2R)	2:3	do	.6356	8.99
Do	Discrete (0.5R or 1.R)	4:3	do	.5796	7.19
Do	Log-normal (G_g=0.25, σ_g=3)	1:2	Surface edges	.7622	12.89
Uniform (0.5→1.5	Uniform (0→1)	1:1	Any edge	.6900	10.70
Log-normal (R_g=1, σ_g=1.5)	Log-Normal (G_g=0.25, σ_g=3)	1:2	Surface edges	.7845	13.66

[1] Ratio of gap to surface spheres.

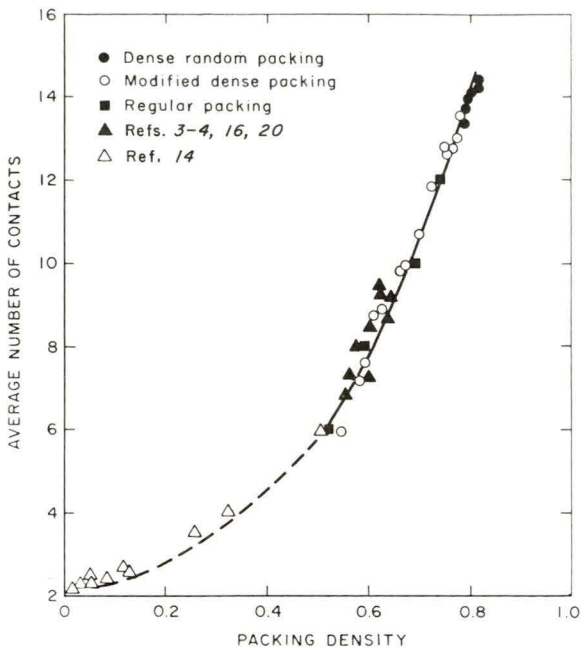

Figure 29.—Average number of contacts in loose random packings.

Although Meissner's data was obtained from ultralow density agglomerates that did not exactly correspond to the random hard-sphere concept used throughout this investigation, its inclusion in figure 29 provided the basis for formulating the equation

$$\overline{N}=1.126e^{3.196\phi}+0.860e^{-3.50\phi}, \tag{42}$$

which expresses the observed relationship between contacts and density over the entire range of densities that are physically realizable in particulate systems, or in the case of dense random packing, theoretically realizable.

It is remarkable that a single functional relationship between density and contacts as simple as equation 41 or 42 holds for all packings. However, the data in figure 29 for dense random packings of log-normal and discrete spheres; loose random packings of equal, discrete, uniform, and log-normal spheres; regular sphere packings; and irregular particle agglomerates clearly indicates that, if the density of a packing is known, the average number of contacts can, to a good approximation, be empirically predicted. This result should be of considerable value to many individuals working with particulate systems, because although packing densities can usually be obtained accurately and easily, at present there are no easy or accurate experimental techniques for determining the average number of contacts in an irregular or random packing.

The simple dependency of $\overline{N}$ on Φ implies that a unique gap structure or sphere-gap distribution dependency may exist in any packing of spheres that is an irrevocable result of the geometry of three-dimensional packing. However, unless the actual gap size distribution were known in a real packing, this dependency, if it exists, cannot be determined from the data obtained from the artificially produced loose random packings. Therefore, in the discussion that follows, computer models are described for simulating the acutal construction of physically realizable loose random packings.

Loose Random Packing Model

The computer programs that were initially developed for simulating the construction of three-dimensional loose packings were completely analogous to those used in constructing loose random circle coverings. A three-dimensional Cartesian coordinate system and listings of reserved grid points were used. This latter feature of the computer programs was accomplished with a three-dimensional array in the computer memory of the form $XYZ(x,y,z)$ with dimensions of 26 by 26 by 26. The array of x-, y-, and z-coordinates defined a cubical volume with 26 units on a side, in which the packing construction was simulated.

The packing simulation began by randomly selecting three spheres from the specified population and placing them at the center of the grid system so that they were mutually tangent. These spheres formed the nucleus upon which the remainder of the packing was constructed. As was the case in two dimensions, each additional sphere was always placed at the boundary site nearest to the center of the packing. However, a new sphere had to be tangent to three existing spheres, because this was the only stable position possible. The list of the coordinates of each grid point in the XYZ array lying on or within each sphere was updated whenever a sphere was added. For a sphere of radius r having center coordinates of (h,k,l), the values of the XYZ array locations whose indices satisfied the equation

$$(x-h)^2+(y-k)^2+(z-l)^2\leq r^2 \tag{43}$$

were redefined to signify that space in the coordinate system was now occupied by a sphere.

In two dimensions the center coordinates of each new circle added to the covering were calculated by simultaneously solving two equations to get a simple quadratic, which could then be solved for the two possible circle-center positions. In three dimensions the calculation was more complex because the analogous equations,

$$(a-h_1)^2+(b-k_1)^2+(c-l_1)^2=(r_1+r)^2, \tag{44}$$

$$(a-h_2)^2+(b-k_2)^2+(c-l_2)^2=(r_2+r)^2, \tag{45}$$

and

$$(a-h_3)^2+(b-k_3)^2+(c-l_3)^2=(r_3+r)^2, \tag{46}$$

could not by themselves be simultaneously solved to get the center coordinates (a,b,c) of the new sphere of radius r in terms of the center coordinates (h_i,k_i,l_i) and radii (r_i) of the three spheres that formed the new site, because the above three equations are not independent of one another. Therefore, it was necessary to develop an indedendent fourth equation that would permit the solution of equations 47, 48, and 49 for (a,b,c). This development follows.

There are only two solutions for (a,b,c) that satisfy equations 44, 45, and 46. Each defines a potential sphere center on opposite sides of the plane formed by the centers of the three existing spheres. Because the centers of these three spheres are never collinear, the equation of the plane they define can be written as

$$\begin{vmatrix} x & y & z & 1 \\ h_1 & k_1 & l_1 & 1 \\ h_2 & k_2 & l_2 & 1 \\ h_3 & k_3 & l_3 & 1 \end{vmatrix} =0. \tag{47}$$

The three existing spheres define a triangle lying in this plane whose edges are the lines connecting the three centers. This triangle also serves as the common face for two identical tetrahedra whose fourth vertices are the unknown sphere centers (a,b,c), each on opposite sides of the plane. Therefore, the unknown sphere centers are $\pm H$ from the base plane containing the other three centers, where H is the altitude of the tetrahedra. A well-known theorem in solid geometry states that "the volume of any pyramid is equal to one-third the product of the base area and the altitude." Thus the altitude of the tetrahedra of spheres is given by $H=3V/B'$, where V is the tetrahedron volume and B' is its base area. V can be calculated from equation 40, and

$$B'=\tfrac{1}{2}\left[\begin{vmatrix} k_1 & l_1 & 1 \\ k_2 & l_2 & 1 \\ k_3 & l_3 & 1 \end{vmatrix}^2 + \begin{vmatrix} l_1 & h_1 & 1 \\ l_2 & h_2 & 1 \\ l_3 & h_3 & 1 \end{vmatrix}^2 + \begin{vmatrix} h_1 & k_1 & 1 \\ h_2 & k_2 & 1 \\ h_3 & k_3 & 1 \end{vmatrix}^2\right]^{\frac{1}{2}}, \tag{48}$$

which is the three-point form for calculating the area of a triangle. An additional theorem states that "the directed distance d from the given plane $Ax+By+Cz+D=0$ to the given point P(u,v,w) is obtained by the formula

$$\mathrm{d}=\frac{Au+By+Cw+D}{\pm[A^2+B^2+C^2]^{\frac{1}{2}}}."$$

For the case of the two tetrahedra, if the tetrahedra base plane is the given plane and d equals H, then two (u,v,w) solutions are the unknown sphere centers (a,b,c). Therefore, the above equation can be recast as

$$Aa+Bb+Cc+D=\pm H(A^2+B^2+C^2)^{\frac{1}{2}}, \tag{49}$$

where A, B, C, and D are now the coefficients of the terms in the expansion of equation 47. Equation 49 defines two planes that contain the unknown sphere center coordinates and that are parallel to the tetrahedra base plane and distance $\pm H$ from it. When taken individually, the equation of each of these planes served as the additional independent expression needed to simultaneously solve equations 44, 45, and 46 for the coordinates of each of the unknown sphere centers.

In the computer simulations, the center furthermost from the center of the packing was selected. The new sphere placed at this site was tested before another sphere was added to insure that it did not overlap any existing sphere in the packing. If overlapping had occurred, the center site was rejected and other combinations of three boundary spheres in the same vicinity of the packing were used to compute a new sphere center until finally an acceptable site was found.

Although the computer model just described was completely operational, it could not be used to construct loose random packings of more than about 40 equal spheres, because the computer memory required to store the necessary listings of reserved grid points for larger packings exceeded the capacity of the IBM 7094. Therefore, complete analogy with the two-dimensional models was not practical because packings of several hundred spheres were believed required if meaningful statistics of packing geometry were to be obtained. Several computer models were developed that did not require a precise knowledge of the packing surface contours or occupied space, thus eliminating the need for the XYZ array. Each point of interest in the three-dimensional coordinate system was tested as the need arose to determine if it lay outside, inside, or on

the surface of any sphere already in the packing. In this fashion, the boundary site for an additional sphere nearest to the center of the packing and the existing spheres in the vicinity of that site were found. The remainder of the packing construction techniques were identical to those described for the models that employed the listings of reserved grid points. The required calculations were considerably more time consuming than those used when the occupancy state of any grid point could be read directly from the computer memory. However, the vastly reduced memory requirements for these programs resulted in the capability to pack any number of spheres of any size, thus offsetting the increased expense of executing them.

Listings of the sphere radii, the coordinates of each sphere center in the packing, and the three spheres that formed the tangent site for each new sphere were part of the computer output. The latter data permitted the physical construction of ball models of the packings. These were essential for visualizing the geometrical relationships required for the property calculations and also served as a check on the computer simulations to insure that the packings were physically realizable and contained no flaws. The ball model for an equal-sphere packing containing 250 spheres is shown in figure 30. It was constructed from ping-pong balls and silicon rubber adhesive. The light weight of the balls and the short curing time of the adhesive permitted the construction of models with 200 or fewer spheres in less than a day.

Although the packing properties, such as density and contacts, were of primary interest in developing the computer simulations, an interesting byproduct of the packing constructions was the ability to define the appearance of any two-dimensional section passed through the packing from the listings of the sphere center coordinates and their radii. For example, if one assumes that the desired sectioning plane is perpendicular to one of the coordinate axes, such as the z-axis, then the equation of this plane is $z=\text{constant}=Z$, where Z is simply the value on the z-axis intersected by the plane. If the coordinates of the center of the ith sphere are (a_i, b_i, c_i) and its radius is r_i, then the only spheres that intersect the chosen sectioning plane are those for which

$$\left| Z-c_i \right| \leq r_i. \qquad (50)$$

Whenever a section was to be made in the simulated packings, a list of intersecting spheres that satisfied the condition set forth by equation 50 was formulated. For any one of these spheres, its intersection with plane Z was given by

$$(x-a_i)^2+(y-b_i)^2=r_i^2-(c_i-Z)^2,$$

which is the equation of a circle having its center at (a_i, b_i) and a radius of

$$R_i=[r_i^2-(c_i-Z)^2]^{1/2}.$$

Therefore, the corresponding circle-center coordinates and radii for all the intersecting spheres are all one needs in order to draw the chosen cross section of the packing. One of these cross sections is shown in figure 31, calculated for the plane $Z=102$ in the packing shown in figure 30. Other cross sections were similarly obtainable for any plane of interest in every packing.

Cross sections of the type just described may be of value in random sampling experiments that investigate the relation between the size distribution of grains or particles and the distribution of dimensions of planar and linear intercepts of the particles. Although many metallurgical investigations (*8, 11*) of this nature have been performed, quantitative microstructural analysis in many applications remains a statistical art in which one or more simplifying geometrical assumptions are usually required that do not always accurately represent the particle sample.

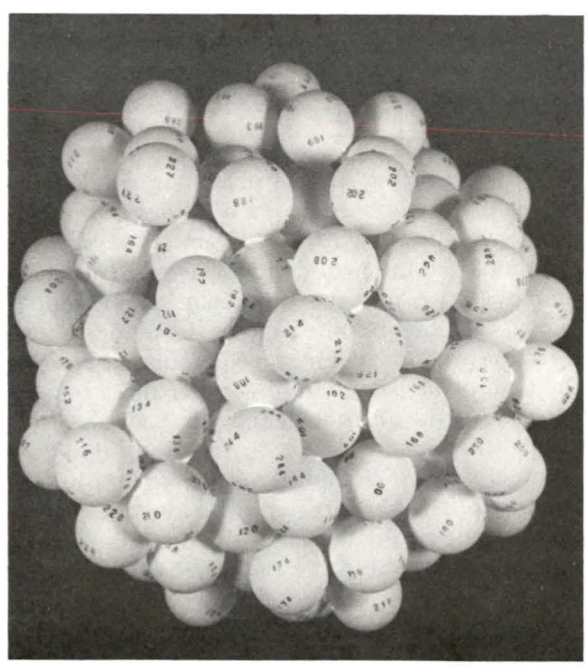

Figure 30.—Loose random packing of 250 equal spheres.

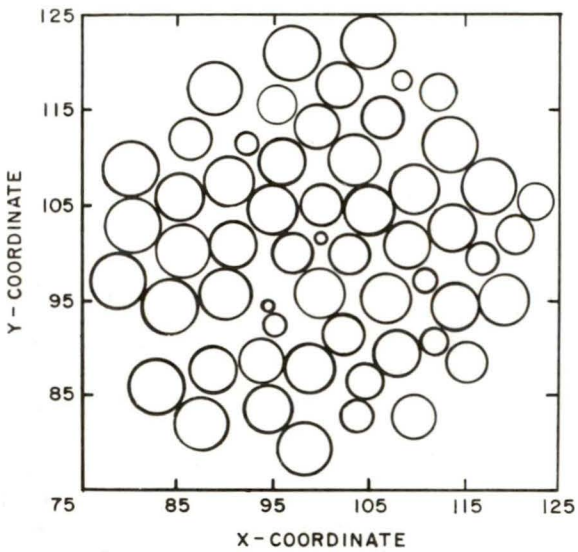

Figure 31.—Packing cross section in loose random packing of equal spheres.

Because the computer models can perform the reverse analysis, that is, predict the cross section from a knowledge of the particle distribution, they could conceivably be used to improve the counting statistics in these analyses and might yield important relationships that would permit better estimates of the geometric properties of three-dimensional structures from plane section measurements. These estimates might be superior to any that currently exist, because the positions of the particles in the packing or of the circles on any sectioning plane are unequivocably defined by the computer models. Therefore, statistical studies such as those performed by Higuti (*10*) on random packings or by Blum and Wilhelm (*5*) on homogeneous packed-bed devices might benefit from these data.

The ball model shown in figure 30 and larger packings having up to 400 equal spheres, bear a striking resemblance to experimental sphere packings described in the literature. Of these, those reported by Bernal (*1–2*) most closely resemble the ping-pong ball models. Bernal found that five general types of polyhedrons existed in all loose random packings of equal spheres. He defined these polyhedra in his experimental packings by connecting the centers of tangent or nearly tangent spheres. However, a variation or deformation of the edge lengths in the five different polyhedra of up to 15 percent was required to fill space with them. This deformation he was able to visually account for by dissecting his experimental packings. The five polyhedral types reported by Bernal were clearly present in the ball models constructed from the computer-calculated data. In addition, the predicted average coordination number in these packings agreed moderately well with that reported by Bernal.

These observations led to investigating the possibility that the properties and topology of the simulated packings could be determined by dissecting them into the five unique Bernal polyhedra and then calculating the density, pore size, and other properties of interest in each of these. Furthermore, this approach could conceivably lend itself to an analysis similar to that done in chapter 4, where only a limited number of polygon types were found to exist in each equal-circle covering. In two dimensions, every time a circle was added it defined or completed a closed area in the covering so that the pore that was formed was completely surrounded by tangent circles. This permitted convenient definition of the pores and of the polygons surrounding them and for their dissection into triangles when calculating the density and other relevant covering properties. However, the same approach in three dimensions leads to considerable ambiguity because of the open structure that exists in loose random heaps of spheres. It is not possible to define similar pores or their equivalent polyhedra of tangent spheres in three dimensions, because examination of the ball models reveals that this type of pore only exists in the dense-packed tetrahedra in the packing The remainder of the void space in the packing is not enclosed by tangent spheres, but can be reached from any other pore that is not dense-packed by moving through the nontriangular openings between neighboring spheres. These observations were equivalent to Bernal's when he stated that the edges of his five minimal-volume polyhedra had to be distorted or extended in order to fill space with them, which, in the ping-pong ball models, would have permitted the formation of polyhedra of tangent spheres. Although visual account of the polyhedra edge deformation could have been taken if the ball models were physically dissected, it would be nearly impossible to program the computer to chose the correct polyhedra edges to form only the Bernal polyhedra because of the many other types of polyhedra that might be defined in these packings by simply changing the manner with which the polyhedra edges were assigned. Moreover, even if the equal-sphere packings could be reduced by the

computer to the Bernal polyhedra, the operations required would be useless for the unequal-sphere packings. Therefore, more general techniques that would be amenable to computer programing had to be found for calculating the packing properties.

The method that was finally developed was first suggested in an article by Smith (*19*), who described how the Bernal polyhedra could be divided to form the simplicial graph of equal-sphere packings. The simplicial graph of any aggregate of particles is formed by first constructing the Dirichlet region, or Voronoi polyhedron, around each sphere in the packing. All the space surrounding a selected sphere that is closer to that sphere than to any other defines the Voronoi polyhedron of the selected sphere. It takes the form of a convex polyhedron bounded by planes that are perpendicular bisectors of the lines joining the sphere with each of its neighbors. The three-dimensional array of Voronoi polyhedra in a packing also define an inverse array whose zero-, one-, two-, and three-dimensional elements correspond, respectively, to the three-, two-, one-, and zero-dimensional elements of the Voronoi polyhedra. This inverse array is known as the simplicial graph, or Delaunay simplex, of the packing and consists of a system of space-filling tetrahedra (simplices) whose edges connect all the sphere centers. For any single sphere in a packing, its center is the vertex of a number of simplicial tetrahedra formed by connecting the centers of spheres that gave rise to a face on the surrounding Voronoi polyhedron with the central sphere and with each other. Taken in its entirety, the simplicial graph around a sphere can therefore be combined to form a convex polyhedron of tetrahedra having triangular faces and vertices that are neighboring sphere centers. Because the simplicial graph is a unique construction for any array of equal or unequal spheres, its use was considered the best approach to solving the problem of reducing the simulated packings to manageable geometric units whose properties could be calculated using simple geometrical formulas. Furthermore, the ability to construct a set of unique tetrahedra for any packing would undoubtedly find use in interpreting the statistical geometry of that packing.

The vertices of each Voronoi polyhedron surrounding a sphere must be exactly equidistant from at least three spheres in addition to the central sphere. This, in principle, allows one to calculate the Voronoi polyhedra in any packing. Once the Voronoi polyhedra are defined, the spheres that gave rise to each Voronoi vertex can be connected with each other and with the surrounded sphere in all the Voronoi polyhedra to form the simplicial graph of tetrahedra for the packing. Therefore, in order to obtain the sphere combinations required to subdivide the simulated packings into their simplicial graphs, work was initiated on the development of a computer program for constructing the Voronoi polyhedra in these packings. This resolved to considering all the neighbors around each sphere that were within a certain distance, Rc, and calculating the potential vertices of each Voronoi polyhedron by simultaneously solving many center-to-center distance equations. The set of vertices that defined the minimum volume polyhedron around each sphere would then define the Voronoi polyhedron of that sphere. As a result of similar work found in the literature (*3*), Rc was initially fixed at 1.6 sphere diameters in the equal-sphere packings. Upon examination of the radial distribution curve calculated in the above investigation, this distance was found to roughly correspond to the beginning of the second coordination shell. Intuitively this observation was very acceptable, because no other neighbors than those in the first coordination shell should enter into the construction of a sphere's Voronoi polyhedron and consequently form the Delaunay simplex around that sphere. For this reason it was possible to reduce the number of neighbors that had to be considered around any given sphere, which in turn led to an entirely different approach to determining the Delaunay, or simplicial, graph of a packing. By listing only those spheres that lay within the first coordination shell of a given sphere, determined from the radial distribution curve of the packing, a procedure was developed and programed that forms the simplicial graph of a sphere-packing directly, without having to deal with the Voronoi polyhedra.

The computer program that was used to calculate the packing properties of loose random packings of equal spheres began by formulating lists of the neighbors within a distance Rc for each of the first 350 spheres that had been added to the heap. By trial and error, an Rc of 1.63 sphere diameters was found to adequately insure that all of the space around any given sphere would be accounted for when the packing was broken into tetrahedra. The neighbor lists were arranged in order of increasing distance from the given sphere or in order of increasing sphere number for the set of contacting spheres. If tetra-

hedra were to be first constructed around sphere number 1, the lists for each of its neighbors were revised so that only those spheres common to the list for sphere 1 remained and were in the same sequential order as existed on the neighbor listing for sphere number 1. The tetrahedra construction began by selecting the first neighbor on the list for sphere 1 and then the first sphere on that neighbor's list. The listings for the two neighboring spheres were then searched for the first sphere common to each. The centers of these three spheres, together with sphere number 1, the reference sphere, constituted the first tetrahedron between sphere centers. Similarly, additional tetrahedra were formed by searching the neighbor listings for triads of spheres that included the reference sphere and that were already associated with a tetrahedron face, until a sphere common to all three lists was found. This sphere's center was then taken as the fourth vertex of a new tetrahedron. These operations were repeated until all of the available space around the reference sphere had been assigned to tetrahedra for up to 100 different reference spheres in the packing. In effect, this procedure reduced the packing to a set of minimum-volume, space-filling tetrahedra around the 100 reference spheres. This result was a natural consequence of the listing procedure, which prejudiced the computer to attempt to form tetrahedra from contacting or close neighbors before using spheres more distant from the reference sphere. Because the simplicial graph of a sphere packing represents the inverse of the Voronoi polyhedra, it must be constructed from minimum-volume tetrahedra. Thus, it was for this reason that the computer-generated tetrahedra were considered equivalent to those that would have been formed by a Voronoi analysis of the packing.

Occasionally in very loose regions of some packings, when the sphere lists were being searched to find an additional geometrical neighbor for use as a fourth vertex of a new tetrahedron, the sphere required to continue the proper simplicial division of the packing was either out of sequence as a result of the listing procedure and thus could not be chosen via the selection rules, or it was absent from one or more of the three lists that were being searched. This latter problem arose whenever the needed sphere was located at a distance greater than the chosen Rc used in formulating the lists. However, this problem was usually insignificant compared to the former one. Whenever either situation was encountered, the computer program was written so that a new triad of spheres, specifically, a new tetrahedron face, was considered. Fortunately, in most of these cases the required sphere was usually selected in combination with another tetrahedron face, so that space-filling around the reference sphere was ultimately accomplished. In order to determine where and to what extent, if any, incomplete space-filling had occurred, running sums of the fractional solid angles, subtended at each reference sphere by all the simplicial tetrahedra in which the sphere was a part, were kept during the simplicial calculations. In most of the packings these sums were unity or very nearly so. However, in some of the unequal-sphere packings, in which very large pores or low-density regions were often encountered, space-filling around an occasional reference sphere was not accomplished. The number of such spheres in any single packing was usually less than 10 percent of the total number of reference spheres considered. Moreover, in almost all cases the lack of complete space-filling was shown to be attributed to one or, at most, two tetrahedra that should have been constructed, but were not. Because the final packing properties were calculated from the individual properties of 700 to 1,000 tetrahedra, the effect of the few missing tetrahedra on the final values of these data was not considered significant enough to warrant the effort that would have been required to resolve these problems.

Once the loose random packing had been dissected into tetrahedra, the tetrahedron pore volume and hence the density; the average number of tetrahedra and geometrical, or Dalaunay, neighbors per sphere; and the tetrahedron edge length distribution were calculated. All of the properties calculated from the sphere center coordinates in the loose random packing of equal spheres are presented in the following discussion. Where available in the literature, experimental data on equal-sphere packings are also included.

LOOSE RANDOM PACKING PROPERTIES

Packings of Equal Sphere Sizes

The calculated distribution of contacting spheres in the loose random packing of equal spheres is shown in figure 32. Also shown are similar data obtained exeprimentally by Bernal and Mason (*4*) and Levine and Chernick (*12*). The predicted frequency distribution agrees only superficially with these data. However, for a

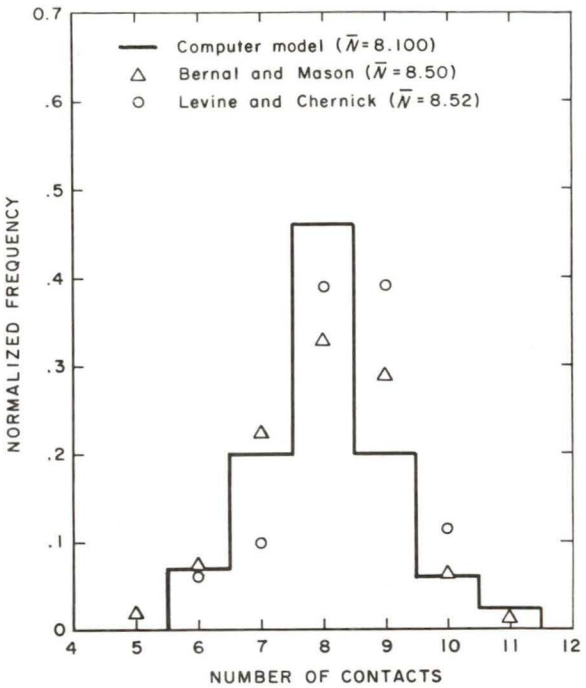

Figure 32.—Contact frequency distribution in loose random packing of equal spheres.

random close-packing of equal spheres, which will be subsequently shown to have been simulated by the computer, the calculated data may be more accurate than the experimental data. Whereas the density of random close-packing is 0.63 to 0.64, the experimental data in figure 32 were measured in packings having densities from 0.60 to 0.62. The calculated average number of contacting spheres and its standard deviation in the simulated packing were 8.100 and 1.229, respectively. This result is less than the 8.5 measured by Bernal and Mason because of their inability to differentiate experimentally between contacting spheres and those that were separated by 1.0 to 1.05 sphere diameters. The latter cases were considered contacting; thus, the average number of contacting spheres measured in their experiments was necessarily high. In Levine and Chernick's numerical model of random packing, spheres were randomly introduced around central spheres until there was no room for additional spheres. The properties of each central-sphere cluster were then calculated. However, the absence of contact calculations on second, third, and higher order neighbors, and forcing a sphere to be tangent to the central sphere if room existed for it, resulted in calculated average numbers of contacts higher than actually exists in real loose random packings. Thus it appears that in a random close-packing of equal spheres the average number of contacting spheres is 8.10 and the contact frequency distribution ranges from 6 to 11 and is fairly symmetrical at about eight contacts per sphere.

The radial distribution histogram for the loose packing of equal spheres is shown in figure 33. The experimental data of Scott (*17*) and that of Bernal (*2*), calculated from measurements with an optical comparator on 25 centers in a loose packing of ball bearings, are included in this figure. All of these data are in substantial agreement, indicating that the same or very nearly the same packing had been considered in this investigation and in theirs. However, the data predicted from the packing model may be statistically better because it was determined from 50 sphere centers. Furthermore, the experimental measurements were very tedious and subject to error because of the inherent difficulties in making accurate measurements of radial distances and of sphere center coordinates in actual three-dimensional heaps of spheres. Conversely, it was possible to calculate distances and coordinates to any desired degree of accuracy in the simulated packing.

The average number of geometrical neighbors was defined by Bernal (*1*) as the average number of spheres located within 1.414 of the distance of closest approach of any sphere. In the simulated packing, the average number of geometrical neighbors so defined (calculated from the radial distribution data) was 13.567, which is in excellent agreement with the 13.6 obtained by Bernal from his experiments and the 13.564 Coxeter (*6*) calculated from his theoretical model. In any

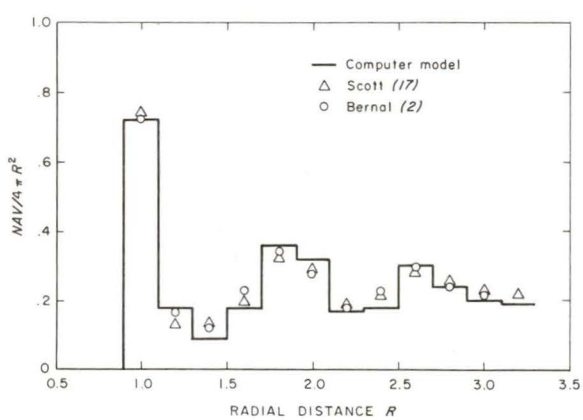

Figure 33.—Radial distribution curve in loose random packing of equal spheres.

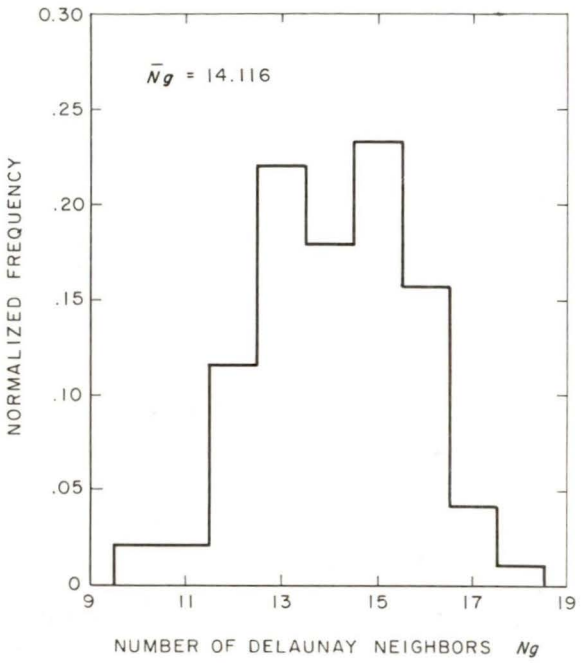

Figure 34.—Delaunay neighbor frequency in loose random packing of equal spheres.

sphere packing, the average number of geometrical neighbors also define the average number of faces on the Voronoi polyhedra. This number was calculated by recording the number of spheres, or Delaunay neighbors, used in the construction of the simplicial graph around each reference sphere. For 100 reference spheres, the Delaunay neighbor frequency in the equal-sphere packing is plotted as a histogram in figure 34. The average number of Delaunay neighbors was 14.116, which agrees fairly well with the 14.28 calculated in one of Bernal and Finney's (*3*) models, but is considerably higher than the number of geometrical neighbors presented above. However, inspection of the lists of Delaunay neighbors around each reference sphere and the distance each neighbor was separated from its reference clearly showed that spheres more distant from the reference sphere than 1.414 of the distance of closest approach would have contributed faces and/or vertices to the Voronoi polyhedra if they had been constructed. These faces would have existed in regions of low density and been very small, thus explaining why they may have gone uncounted in Bernal's earlier experimental model. Furthermore, in any real packing, there are regions where spheres are not packed in the densest possible fashion; thus, positive departures from the average number of geometrical neighbors predicted by Coxeter's model are to be expected. If one were at liberty to always place the spheres in a packing so that the tightest possible irregular grouping around each sphere was achieved, then there probably would be about 13.56 Delaunay neighbors, or Voronoi faces, associated with that sphere. However, in a looser packing of equal spheres, such as that obtained in the present work, this number is closer to 14.12 and includes neighboring spheres that are separated from the reference sphere by as much as 1.63 of the distance of closest approach.

The properties of 990 different tetrahedra were calculated during the construction of the simplicial graph in the equal-sphere packing. From these data the calculated bulk packing density was 0.6374, which may be identical to the 0.63 calculated by Scott (*16*) for random close-packings of equal spheres. Thus, judging from this agreement and that found in the radial distribution data in figure 33, the computer programs appear to have successfully simulated the construction of random close-packing, which is by far the most interesting of all equal sphere random loose packings because it has the maximum obtainable density. The entire distribution of tetrahedron densities is shown in figure 35 together with similar data reported by Mason (*13*). The cal-

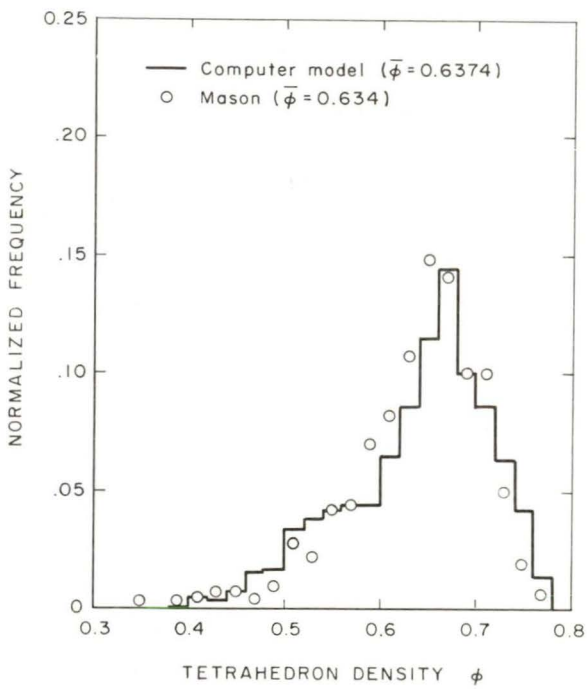

Figure 35.—Tetrahedron density frequency in loose random packing of equal spheres.

culated data in this figure are statistically more significant because they were calculated for a packing that had 90 percent more spheres and 36 percent more tetrahedra than the one considered by Mason. Both sets of data clearly indicate that the porosity of the tetrahedra, defined as unity minus the density, may to a good approximation be represented by a log-normal distribution. The geometric mean porosity and geometric standard deviation calculated from the computer data were 0.3641 and 1.2317, respectively.

The tetrahedron pore volumes were represented by a log-normal distribution having a geometric mean volume of $0.3535R^3$ and geometric standard deviation of 1.522, where R is the radius of the spheres in the packing. A histogram of pore volume frequencies is shown in figure 36, where the pore volume V is plotted as $3V/4\pi R^3$ to eliminate sphere-size dependence. The pore data in figure 36 should not be confused with that normally measured experimentally in real sphere or particle packings, for it represents only the unoccupied space in individual tetrahedra constructed during the simplicial division of the packing.

The tetrahedron edge length distribution in terms of the reduced coordinate of sphere diameters was also calculated during the simplicial division of the equal-sphere packing. There were 910 different tetrahedron edges associated with the 990 tetrahedra whose properties were calculated. The average reduced edge length ($\overline{E'}$) was

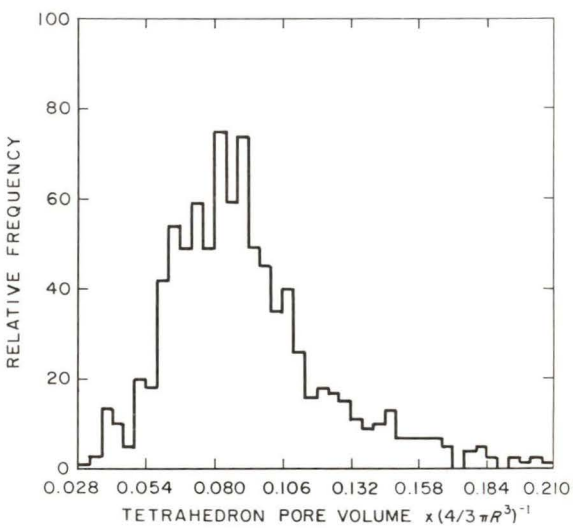

Figure 36.—Tetrahedron pore volume frequency in loose random packing of equal spheres.

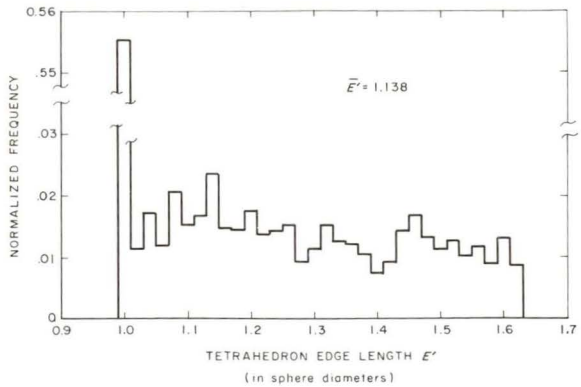

Figure 37.—Tetrahedron edge length distribution in loose random packing of equal spheres.

1.138 sphere diameters, and it had a standard deviation of 0.197. The majority of the edges (55.6 percent) were formed by tangent spheres ($E'=1.0$), whereas the remaining edges were almost evenly distributed between $1.0<E'\leq 1.63$. These features are illustrated in figure 37. The data in this figure for $E'>1.0$ can be approximated by a uniform distribution of edge lengths at the average frequency of 0.0143. This observation agrees qualitatively with that made earlier in the attempt to construct loose random packings by modifying the dense random packing model. The data in figure 37 indicate that the use of uniform gap distributions in those simulations very nearly approximated the type of distribution that exists in real packings of equal spheres.

Packings of Unequal Sphere Sizes

Computer programs that were nearly identical to those used to simulate the construction and calculate the properties of loose random packings of equal spheres were also employed for uniform and log-normal distributions of sphere radii. The same unequal-sphere populations, whose dense random packing properties were presented in chapter 3, were employed in these simulations. The only exception was in the log-normal distributions, which were truncated at ± 4 standard deviations from the mean sphere size in the loose random packing simulations. These truncation limits could not be used to simulate dense random packings, because of the limiting size ratio required to pack spheres in conformance with the gapless requirements of this type of packing.

The calculated properties of all the loose pack-

Table 10.—Loose random packing properties of unequal spheres.

Sphere distribution	Φ	$\overline{N}$	$3\overline{V}/4\pi R^3$	$\overline{E}'$
Uniform (R=2,4)	0.6520	8.425	0.1074	1.116
Uniform (R=2,4,6)	.6846	9.420	.1065	1.091
Uniform (R=2,4,6,8)	.6966	9.580	.1083	1.083
Log-normal (σ_g=1.3)	.6572	8.587	.....	1.111
Log-normal (σ_g=1.5)	.6892	9.541	.....	1.099

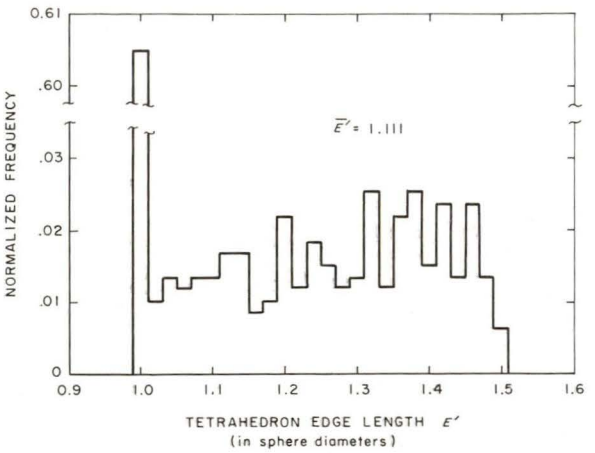

Figure 38.—Tetrahedron edge length distribution in log-normal loose random packing of spheres.

ings of unequal spheres were very similar to those of the equal-sphere packings. These data are listed in table 10. The numbers of contacting spheres were log-normally distributed in the log-normal sphere packings, whereas the uniform distribution packings showed fairly symmetrical peaks in the contact frequency curves similar to that found in figure 32 for equal spheres. Each peak corresponded to a different sphere size in the population. The number frequency curves of geometrical, or Delaunay, neighbors behaved in much the same manner. The tetrahedron porosities and pore volumes were also found to be log-normally distributed in all of the unequal-sphere packings.

Very little information exists in the literature enabling one to validate the calculated data presented in table 10 for unequal-sphere packings. However, the densities predicted for the two log-normal distributions compare very favorably with the recent experimental measurements reported by Sohn and Moreland (*21*), who claim to have achieved the condition of random close-packing in their particle assemblies. With the equivalent condition having been attained in the equal-sphere packing, the agreement in the unequal sphere density data suggests that for all sphere populations the computer models successfully simulated the construction of by far the most interesting of the random loose packing modes, that of the maximum density and thus maximum stability.

The reduced tetrahedron edge length distributions in the unequal-sphere packings confirmed the earlier observation that uniform gap distributions were applicable when describing real packings. When plotted in terms of sphere diameters, these distributions differed from the one shown in figure 37 for an equal-sphere packing only with respect to the fraction of tangent tetrahedron edges (at E'=1) and the maximum edge length required to complete the simplicial division of the packing. This difference can be readily seen in the tetrahedron edge length distribution calculated for the log-normal packing with σ_g=1.3, illustrated in figure 38. In this packing, the maximum reduced edge length was 1.5 sphere diameters, meaning an Rc equal to 1.5 for any pair of sphere radii was adequate to insure complete space filling during the construction of the minimum-volume simplices around the reference spheres. Greater numbers of tangent edges and smaller maximum edge lengths were always observed whenever higher density packings were simulated, regardless of the distribution of spheres used. The ability to visualize these changes is a direct consequence of plotting the tetrahedron edges in terms of sphere diameters. However, this method also obscures the true nature of the edge distributions in the unequal-sphere packings, where all the tangent edges, regardless of their actual length, are plotted at E'=1.

REFERENCES

1. Bernal, J. D. A Geometrical Approach to the Structure of Liquids. Nature, v. 183, Jan. 17, 1959, pp. 141–147.
2. ———. The Structure of Liquids. Proc. Roy. Soc. (London), Ser. A, v. 280, No. 1382, July 28, 1964, pp. 299–324.
3. Bernal, J. D., and J. L. Finney. Random Close-Packed Hard Sphere Model. II. Geometry of Random Packing of Hard Spheres. Disc. Faraday Soc., No. 43, 1967, pp. 62–69.
4. Bernal, J. D., and J. Mason. Coordination of Randomly Packed Spheres. Nature, v. 188, Dec. 10, 1960, pp. 910–911.
5. Blum, E. H., and R. H. Wilhelm. A Statistical Geometric Approach to Random-Packed Beds. AIChE-IChE Sym. Ser. No. 4, 1965, pp. 21–27.
6. Coxeter, H. S. M. Close Packing and Froth. Ill. J. Math., v. 2, No. 4B, 1958, pp 746–758.
7. ———. Introduction to Geometry. John Wiley & Sons, Inc., New York, 1961, p. 11.
8. DeHoff, R. T. Quantitative Microstructural Analysis. Am. Soc. Testing Mater. Spec. Tech. Pub. 430, 1968, pp. 63–95.
9. Graton, L. C., and H. J. Fraser. Systematic Packing of Spheres, With Particular Relation to Porosity and Permeability. J. Geol., v. 43, November–December 1935, pp. 785–909.
10. Higuti, I. A Statistical Study of Random Packing of Unequal Spheres. Ann. Inst. Stat. Math. (Tokyo), v. 12, 1961, pp. 257–271.
11. Hilliard, J. E. Direct Determination of the Moments of the Size Distribution of Particles in a Opaque Sample. Trans. AIME, v. 242, 1968, pp. 1373–1380.
12. Levine, M. M., and J. Chernick. A Numerical Model of Random Packing of Spheres. Nature, v. 208. Oct. 2, 1965, pp. 68–69.
13. Mason, G. Disc. Faraday Soc., No. 43, 1967, pp. 75–76.
14. Meissner, H. P., A. S. Michaels, and R. Kaiser, Crushing Strength of Zinc Oxide Agglomerates. I & EC Process Design Develop., v. 3, July 1964, pp. 202–205.
15. Rogers, C. A. The Packing of Equal Spheres. Proc. London Math. Soc., v. 8, 1958, p. 609.
16. Scott, G. D. Packing of Equal Spheres. Nature, v. 188, Dec. 10, 1960, pp. 908–909.
17. ———. Radial Distribution of the Random Close Packing of Equal Spheres. Nature, v. 194, June 9, 1962, pp. 956–957.
18. Segre, B., and K. Mahler. On the Densest Packing of Circles. Am. Math. Monthly, v. 51, May 1944, pp. 261–270.
19. Smith, F. W. The Structure of Aggregates and the Molecular Kinematics of the Viscosity of a Bernal Liquid. Can. J. Phys., v. 42, February 1964, pp. 304–320.
20. Smith, W. O., P. H. Foote, and P. F. Busang. Packing of Homogeneous Spheres. Phy. Rev., v. 34, Nov. 1, 1929, pp. 1271–1274.
21. Sohn, H. Y., and C. Moreland. The Effect of Particle Size Distribution on Packing Density. Can. J. Chem. Eng., v. 46, June 1968, pp. 162–167.
22 Westman, A. E. R., and H. R. Hugill. The Packing of Particles. J. Am. Ceram. Soc., v. 13, No. 10, 1930, pp. 767–779.

— 6 —

COMPUTER SIMULATION OF SIMPLICIAL TETRAHEDRA IN LOOSE RANDOM PACKINGS OF SPHERES

by

Lindsay D. Norman, Edwin E. Maust, Jr., and Leonard P. Skolnick

In the computer model for simulating loose random packings described in the preceding chapter, the calculation of volume-dependent properties such as density was based on procedures for dividing up an assembled sphere packing into a simplicial graph of tetrahedra whose vertices were defined by sphere centers. The simplicial graph, or Delaunay simplex, is a unique construction for any irregular or regular array of points and consists of a system of space-filling tetrahedra formed between each of the geometrical neighbors of each point in the packing. In the loose random packing model, certain calculations were performed for each individual tetrahedron, and the results of these operations were stored so that, at the end of the computations, summations and suitable overall averages of the packing properties for the entire sphere packing could be calculated. The procedures required to construct a packing and then analytically dissect it into simplicial tetrahedra were quite lengthy and involved. Moreover, the complexity of the computer programs were such that, even with an IBM 7094 computer, there was an upper limit on the size of the heap that could be realistically treated. It was pertinent, therefore, to consider whether or not an alternative procedure could be developed.

ANALYSIS OF SIMPLICIAL TETRAHEDRA EDGE LENGTHS

The edge length distribution of tetrahedra resulting from the simplicial division of the computer-simulated loose random packings was nearly identical when the edges were presented in terms of the reduced coordinate of sphere diameters. Moreover, the gaps in the non-tangent edges of these tetrahedra were to an excellent approximation representable by a uniform distribution of gap sizes or lengths. Space-filling was implicit in these edge length distributions. Therefore, if one were able to predict the appropriate tetrahedron edge length distribution in a space-filling array of any sphere population, it should be possible to predict loose packing properties by dealing exclusively with individual tetrahedra whose edges are selected from the predicted edge length distribution. This approach to determining particulate system properties is very appealing because it offers a number of advantages lacking in the previous loose packing model. Foremost among these advantages is the possibility of obtaining more accurate statistical information on the packing parameters than what had been realistically obtainable with the previous models. In order to obtain adequate numbers of spheres in the simulated packings and thus insure meaningful results, it had been necessary to expend large amounts of computer time for the execution of the programs. However, if means could be developed for predicting the same properties by dealing exclusively with individual tetrahedra, the calculations required should be shorter, simpler, and more economical of computer time for a given packing size. Therefore, the equivalent of much larger packings could be analyzed.

The general type of simplicial tetrahedron edge length distribution observed for all loose random sphere packings is illustrated in figure 37. This particular distribution was calculated for an equal-sphere packing with a packing density of 0.6374. The average reduced edge length $\overline{E'}$ was 1.138 sphere diameters. The majority of the edges (55.6 percent) were formed by tangent spheres ($E'=1.0$), whereas the remaining edges were almost uniformly distributed between $1.0<E'\leq 1.63$. When plotted in terms of sphere diameters, the edge length distributions in uniform, discrete, and log-normal sphere packings differed only with respect to the fraction of tangent tetrahedron edges (at $E'=1$) and the maxi-

mum edge length $(1+G')$ required to complete the simplicial division of each packing. This observation provided the starting point for this analysis.

If one assumes from these observations that any gap length between zero and G', the maximum reduced edge length minus one, is equally probable, then all the tetrahedron edge length distributions were completely specified by the fraction of tangent edges at $E'=1$ and the maximum edge length. Intuitively the form of these distributions is very acceptable because, in a stable random array of noninteracting particles, it seems quite probable that all gap sizes up to some upper limit would exist. The problem resolved to finding means of predicting the fraction of tangent tetrahedron edges (H) and the upper limit on the permissible edge lengths $(1+G')$ for any distribution of particles and packing density. With this information the distribution and the frequency of occurrence of gaps in any packing would be specified and thus the construction and the determination of the properties of individual tetrahedra would be possible. The fraction of tangent tetrahedron edges in any packing is simply related to the number of neighbors that are used in the construction of the simplicial graph of that packing. For all the spheres or particles in a packing, this relationship is

$$H=\overline{N}p/\overline{N}g, \tag{51}$$

where $\overline{N}_p$ and $\overline{N}_g$ are the average number of physical, or contacting neighbors, and the average number of geometrical neighbors, respectively. Although the physical significance of the quantity H is clear, equation 51 is of little value for predictive purposes in the absence of the assembled packing because $\overline{N}_p$ and $\overline{N}_g$ cannot, in general, be found otherwise. Similarly, the physical significance of G' is clearly the maximum gap which exists between a sphere and its most distant Delaunay neighbor, divided by the sum of the two radii, but this is not generally known a priori.

In order to assign values of H and G' at any packing density, it is necessary to rely on empirical observations made during the loose random packing simulations. The data from these simulations indicated that the fraction of tangent tetrahedron edges in any packing was uniquely determined by the packing density (Φ) and that the value of G' was similarly set by H for any packing, regardless of the sphere population used in its construction. If this behavior of H and G' was universally valid for all loose packings, then comparable data calculated for the regular packings had to conform to the observed behavior as well. In order to test this assumption, H and G' values were calculated for three regular packings: simple cubic, cubical-tetrahedral, and rhombohedral.

The fraction of tangent tetrahedron edges in each regular array was calculated with equation 54, where $\overline{N}_g$ was determined by constructing the Voronoi polyhedron characteristic of each packing and by counting the number of faces on this body, specifically, each face on a Voronoi polyhedron arising from a Delaunay, or geometrical, neighbor. Once the Voronoi polyhedron was known for each of the three regular structures, one-half the maximum gap length $(\frac{1}{2}G')$ was taken as the maximum center-to-vertex distance in the Voronoi polyhedron minus the sphere radius in the packing. The data calculated for the three regular packings are listed in table 11. An additional H and G' were used in formulating the empirical expressions that follow by considering dense random packing as the upper limit of loose packing. For this ideal case, the fraction of tangent tetrahedron edges and the maximum reduced gap size are by definition unity and zero, respectively. The calculated H and G' data for the regular packings, those predicted by the loose packing model, and the values unique to dense random packing are plotted in figure 39. Empirical equations were fitted by least-squares to these points, and this gave very satisfactory agreement with the observed data. The resulting equations, represented by the curves in figure 39 were

$$H=2.487-8.020\Phi+7.836\Phi^2 \tag{52}$$

and

$$G'=1.090-0.841H-0.234H^2. \tag{53}$$

Thus, over the range of densities normally ascribed to the loose mode of packing or, $0.5<\Phi<$(dense random packing), if the density of a packing is specified, the reduced tetrahedron

Table 11.—Properties of regular packing simplices

Packing	$\overline{N}p$	$\overline{N}g$	H	G'	Φ
Cubical	6	14	0.4286	0.7321	0.5236
Cubical-tetrahedral	8	16	.5000	.5275	.6046
Rhombohedral	12	14	.8571	.2247	.7405

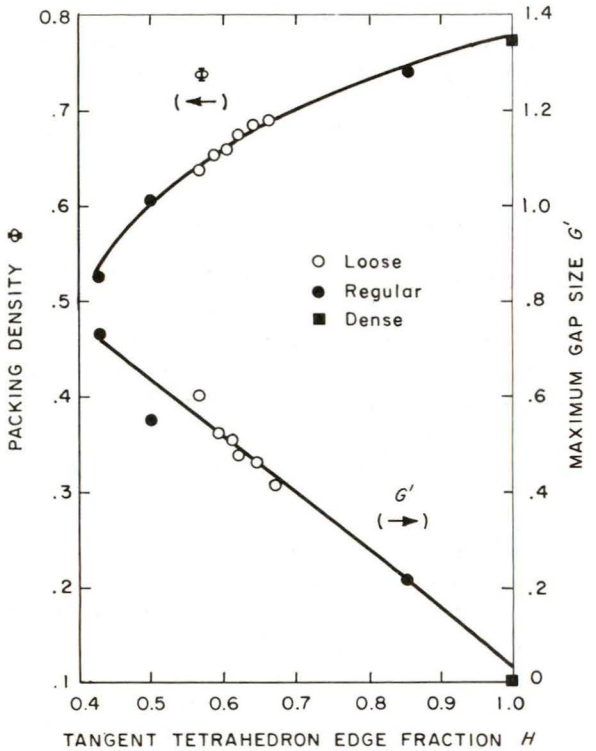

Figure 39.—Tangent edge fractions and maximum gap sizes in loose packings.

edge distribution in the simplicial graph of that packing can be completely determined from equations 52 and 53.

COMPUTER MODEL FOR SIMULATING SIMPLICIAL TETRAHEDRA

Once it was possible with the aid of empirical equations 52 and 53 to predict the reduced tetrahedron edge length distribution in the simplicial graph of any loose random sphere packing, consideration was given to constructing individual tetrahedra by randomly selecting six edges at a time from the edge distribution whose cumulative packing properties properly describe the corresponding packing. The success of this approach rested on the assumption that the population of tetrahedra obtained in this fashion could be made to fill space. In order to test the applicability of using individual tetrahedra, the edge length distribution variables, H and G', were calculated for each of the packing densities obtained in chapter 5. If the assumptions involved were valid, the calculated packing properties resulting from the simulation of individual tetrahedra would agree with those predicted by the loose random packing model.

Loose Random Packings of Equal Sphere Sizes

Initially, loose random packing of equal spheres was simulated with individual tetrahedra. The length of each of the six edges of a tetrahedron was assigned by generating a pseudorandom number between zero and one, which was compared with the value of H calculated by equation 52. If the random number RX was less than H, that edge was considered to be composed of two tangent spheres so that $E=2R$. If $RX>H$, the length of the edge was assigned by

$$E=2R[1+(G')(RX')],$$

where G' was calculated by equation 53 and RX' was a new random number between zero and one. This calculation assumes that any reduced gap size from zero up to the maximum value G' is equally probable, as implied by the uniform distribution of nontangent edges observed earlier. The density and pore volume of the tetrahedron were calculated. These operations were repeated for 20,000 tetrahedra. Records of each tetrahedron edge length, density, and pore volume were kept during the simulation to allow for the calculation of the distribution parameters of each of these when the simulation was completed. The average numbers of physical and geometrical neighbors were found by calculating the average solid angle (A) subtended at the $4(20{,}000)=80{,}000$ vertices of all the tetrahedra. The average number of tetrahedra around an average sphere was then found from $T=1/A$. Because these tetrahedra were assumed to be the equivalent of Dalaunay simplices, the number of tetrahedron vertices on the simplicial graph around any sphere is by definition equal to the number of geometrical neighbors, or by Euler's law

$$\overline{N}g=\tfrac{1}{2}T+2=1/(2A)+2. \qquad (54)$$

The number of physical neighbors was then calculated from equation 51.

Loose Random Packings of Unequal Sphere Sizes

The operations required to simulate individual space-filling tetrahedra from unequal-sphere populations were complicated by the fact that a tangent tetrahedron edge could be any one of three or more lengths depending on the number of sphere sizes in the population. Moreover, ac-

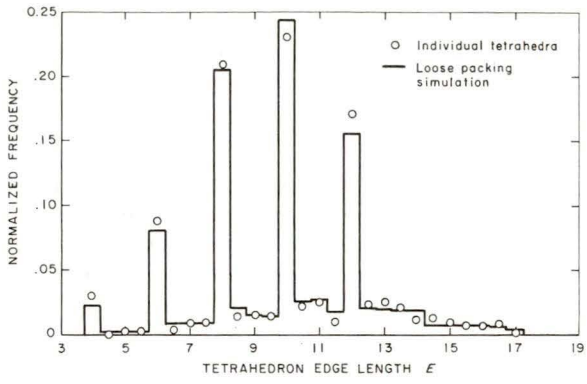

Figure 40.—Tetrahedron edge length distribution in a loose random packing of uniform sphere sizes.

count had to be made for the presence of the larger spheres in more of the individual tetrahedra, because there would always be more simplicial tetrahedron edges associated with a large sphere than with a smaller sphere. The actual distribution of tetrahedron edges in a packing of three uniformly distributed sphere sizes (R=2, 4, 6) is shown by the histogram in figure 40. It is easy to see from this figure that plotting these data in terms of the reduced coordinate of sphere diameters to yield a histogram of the form shown in figure 37 or 38 can lead to an oversimplification of the observed distribution. This observation is particularly true for the log-normal packings in which the true edge distributions were log-normal. However, plotted in terms of the reduced coordinate of sphere diameters, the log-normal edge distributions also reduced to the form shown in figure 38.

In order to predict the edge distributions in unequal-sphere packings, it is necessary to first predict the relative frequency of occurrence of each of the possible tangent edge lengths that can exist from the simplicial division of a packing constructed from unequal sphere sizes. Then, by assuming the gap sizes are uniformly distributed, the entire tetrahedron edge length distribution can be predicted. Alternatively, one can formulate a modified sphere distribution that reflects the change from the original unequal-sphere population required to account for the presence of larger spheres in more tetrahedra. The latter procedure is more worthwhile, because once the actual distribution of sphere radii in the simplicial tetrahedra is known, four sphere sizes can be selected at random from this distribution and the tetrahedron edge lengths in individual tetrahedra can then be assigned in a fashion identical to that used for equal spheres. In addition to the uniform gap size assumption, both of the above approaches to simulating individual tetrahedra require that the probability of finding a gap in any given tetrahedron edge, expressed by $(1-H)$, is independent of the size of the spheres associated with that edge. This assumption was tested by calculating the average fraction of tangent tetrahedron edges, H_i, associated with each of the spheres of radius R_i in one of the uniform distribution packings whose properties were calculated in chapter 5. For each assembled packing, the H_i values were nearly the same and were closely grouped around the overall H observed for the entire packing. Hence, the assumption that H is independent of sphere size appears to be justified.

In the current study, equal, uniform, and log-normal distributions of spheres were considered. The uniform distributions had sphere radii of (2, 4), (2, 4, 6), and (2, 4, 6, 8), whereas the log-normal distributions had geometric standard deviations of 1.3 and 1.5. For the case of uniform distribution of three sphere sizes having radii of 2, 4, and 6, the spheres can form tangent edges by the following combinations:

(2, 2)(4, 2)(6, 2)
(2, 4)(4, 4)(6, 4)
(2, 6)(4, 6)(6, 6).

If all of the possible edges are equally probable and if space-filling is neglected, the normalized frequencies of occurrence of tangent edges of lengths 4, 6, 8, 10 and 12 are 1/9, 2/9, 3/9, 2/9, and 1/9, respectively. However, the edges are not equally probable in tetrahedra that are constructed to represent the space-filling simplicial graph, because the edges containing the larger spheres must be weighted toward more combinations than the smaller spheres. In order to arrive at the appropriate weighted distributions of edge lengths in all the unequal-sphere packings, recourse was made to the dense random packings of these distributions. Because dense random packing properties are assumed to be upper limits for those of looser packings, the relative behavior of these properties as a function of sphere size should at least approximate the behavior one would expect to find in the looser assemblies of the same sphere population. On this assumption, the distributions of tangent tetrahedron edges in the loose packings were predicted by considering the number of contacts as a function of sphere size in dense random packings of each

of the sphere populations whose loose packings were simulated by the loose random packing model. The number of contacts N_i associated with a sphere of size R_i was usable because, by definition in a dense random packing, N_i defines the average number of tangent tetrahedron edges in which R_i is a part; specifically, all the edges in dense random packing are formed by tangent spheres. For the previous example of the uniform distribution of three sphere sizes, the number of contacts per sphere of radii 2, 4, and 6 in the dense random packing are 7.521, 15.04, and 24.58, respectively. (See figure 15.) The normalized fraction of edges N_i' associated with each sphere size is therefore given by

$$N_i'=N_i/\Sigma N_i,$$

which for the above N_i data gives N_i' values of 0.160, 0.319, and 0.521, respectively. Therefore, in a dense random packing of this sphere distribution, 16 percent of all the tetrahedron edges connecting tangent sphere centers would have a sphere of size 2 associated with these edges, etc. Taken one at a time, each sphere in the above distribution can combine with itself or with one of the other two sizes to form a tangent edge. For example, for a sphere with radius equal to 6, (R_6) can be a part of edges of length 8, 10, or 12, by combining with spheres of radius R_2, R_4, and R_6, respectively. Because the N_i data essentially describe a modified distribution of sphere radii in the simplicial tetrahedron edges, the probability of having an edge of length $2R_6=12$ or of selecting two R_6 spheres from this distribution to form an edge of length 12 in the assembled packing is simply $(N_6')^2$. Similarly, the probability of forming other tangent edge lengths can be found from the N_i' data by calculating the combined probabilities of all sphere radii whose sums equal the edge length in question. Thus, for the above uniform distribution of three sphere sizes, the tangent edge length probabilities are

$E_4=(N_2')^2=(0.16)^2=0.025.$

$E_6=(N_2'N_4')+(N_4'N_2')=2[(0.16)(0.319)]=0.102.$

$E_8=(N_4')^2+(N_2'N_6')+(N_6'N_2')=(0.319)^2+2[(0.16)(0.521)]=0.268.$

$E_{10}=(N_4'N_6')+(N_6'N_4')=2[(0.319)(0.521)]=0.333.$

$E_{12}=(N_6')^2=(0.521)^2=0.272.$

The corresponding data obtained by actual count of the tetrahedra edges in the loose packing of this sphere distribution that was simulated by the model described in chapter 5 were 0.029, 0.106, 0.313, 0.372, and 0.179, respectively. Similar agreement between the counted and calculated tangent edge fractions was obtained for the other uniform distributions. Thus, this simple procedure yields the distribution of tangent edges in a loose packing of uniform spheres. In fact, the predicted tangent edge fractions are more accurate than those obtained from the simulated packing, because the latter data were based on limited statistics from only 100 spheres in the packing.

The preceding development has shown how the tangent edge length distributions in loose random packings of uniform spheres can be predicted. The entire distribution of tetrahedron edges was simply obtained by adding the uniform gap distribution predicted by empirical equations 52 and 53 to the tangent edge distribution. In each case, the fraction of edges having gaps was $(1-H)$, and the maximum edge length was $(1+G')$ multiplied by the maximum tangent edge length in the packing. Analogous distributions for log-normal or discrete sphere populations were also developed by modifying the preceding steps to account for the nonuniform frequencies of occurrence of the sphere sizes in these populations.

The distributions of sphere radii in the individual tetrahedra constructed to represent the simplicial tetrahedra in an assembled packing were approximated in a fashion similar to that used in calculating the tangent edge distributions. However, the sphere radii calculations were considerably easier. For any given sphere population, the modified sphere distribution in the simplicial graph of the packing of the original spheres is directly calculable from a knowledge of the number of tetrahedra t_i associated with each sphere of radius R_i in the dense random packing of the original sphere distribution. By definition, the t_i data for any dense random packing are the number of tetrahedra in which spheres of size R_i are a part. Therefore, these data define the modified sphere distributions in dense-packed tetrahedra. The present problem is to determine the analogous distributions in looser packings. However, if one again assumes that the relative behavior of the dense random packing properties typifies the loose packing properties, the modified sphere distributions in the simplicial graphs of the loose packings would be identical to those calculated from the t_i data for a dense random packing of the same original sphere population. For the uniform distribution of three sphere sizes, the number of tetrahedra associated with each sphere of radius 2, 4, and 6

is 11.04, 26.08, and 45.16, respectively. The normalized fraction of tetrahedra U_i associated with each of these sphere sizes is given by

$$U_i = t_i / \sum_i t_i, \tag{55}$$

which for the above t_i data gives U_i values of 0.134, 0.317, and 0.548, respectively. Hence, in a random packing of this sphere distribution, equation 55 predicts that 13.4 percent of all the tetrahedron vertices are located at the centers of spheres of radius 2, etc. For the other two uniform distributions whose loose random packings were simulated on the computer equation 55 predicted the following sphere radii fractions in the Delaunay simplices of these packings:

$$R_2:R_4 = 0.292:0.708$$

and

$$R_2:R_4:R_6:R_8 = 0.077:0.178:0.298:0.447.$$

These data compared favorably with those actually counted in the assembled packings. For example, the counted fractions of sphere radii in the simplicial tetrahedra in the three-size loose packing were

$$R_2:R_4:R_6 = 0.173:0.337:0.490.$$

By a similar analysis, the frequencies of occurrence of sphere radii in simplicial tetrahedra constructed from discrete distributions or from log-normal distributions that have been reduced to a finite number n of sphere sizes are given by

$$U(R_i) = [P(R_i)t(R_i)] / [\sum_{i=1}^{n} P(R_i)t(R_i)], \tag{56}$$

where $P(R_i)$ is the frequency, or probability of occurrence, of a sphere with radius R_i in these distributions. For the two log-normal distributions whose loose random packings were simulated by the computer, the distributions of sphere radii obtained after modifying the original distributions with equation 56 were also log-normal. In fact, the only significant change in the two distributions having geometric mean radii of 6 and standard deviations of 1.3 and 1.5 was a shift of the mean sizes to larger radii. The geometric standard deviations were nearly unchanged at 1.304 and 1.501, whereas the corresponding means were 7.038 and 8.782.

Once the sphere radii distributions in the simplicial tetrahedra of the loose packings of unequal spheres were known, individual tetrahedra were constructed by selecting four spheres at random from these distributions. The determination of the location of gaps in the six edges of each tetrahedron and the size of each gap was identical to that used in the equal-sphere individual tetrahedron simulations. Similarly, records of the edge lengths, densities, and pore volumes of 20,000 individual tetrahedra were kept. The average numbers of geometrical and physical neighbors were also calculated in an analogous fashion, except the number of tetrahedra around a sphere was calculated as a function of the sphere's size, or

$$T(R_i) = 1/A(R_i).$$

Hence, the neighbor distributions as a function of sphere size were readily available from equation 51 and 54. The corresponding number of geometrical neighbors for the entire packing was predicted from

$$\bar{N}_g = \left\{ \sum_{1}^{n} [(\tfrac{1}{2}T(R_i)+2)P(R_i)] \right\} \Big/ \sum_{1}^{n} P(R_i), \tag{57}$$

where n is again the number of sizes in the sphere population.

LOOSE RANDOM PACKING PROPERTIES OF INDIVIDUAL TETRAHEDRA

The packing properties predicted by the individual tetrahedron simulations of the equal-and unequal-sphere packings are presented in table 12. In each simulation, the density Φ predicted by the loose random packing model for that sphere distribution was used to calculate empirical H and G' values from equations 52 and 53. These data, together with the modified sphere populations in the case of the unequal-sphere simulations, were the only required input into the individual tetrahedron computer programs. In table 12 the loose packing results from chapter 5 for these distributions are also included to permit comparison with the individual tetrahedron results. V in this table is the predicted average tetrahedron pore volume.

It is obvious from the data in table 12 that the use of individual tetrahedra for calculating bulk packing properties leads to a good approximation of the properties that would be measured on the assembled heap. Moreover, the packing statistics from the individual tetrahedron simulations may actually be more representative of packings of these sphere distributions. The packing size, the number of spheres used in the simplicial graph of each packing, and the effects of the starting sphere configuration on the calculated properties may have limited the significance of the packing

Table 12.—Individual tetrahedron packing results

Sphere distribution	Loose packing model				Individual tetrahedron model			
	Φ	$\overline{N}$	V	$\overline{E}'$	Φ	$\overline{N}$	V	$\overline{E}'$
Equal (R=3)	0.6374	8.100	10.287	1.138	0.6205	7.811	11.529	1.120
Uniform (R=2,4)	.6520	8.425	12.999	1.116	.6522	8.542	14.408	1.103
Uniform (R=2,4,6)	.6846	9.420	29.442	1.091	.6895	9.295	28.956	1.068
Uniform (R=2,4,6,8)	.6966	9.580	60.160	1.083	.6890	8.764	64.845	1.076
Log-normal (R_g=6, σ_g=1.3)	.6572	8.587	.....	1.111	.6564	8.601	38.134	1.098
Log-normal (R_g=6, σ_g=1.5)	.6892	9.541	.....	1.099	.7053	9.612	19.180	1.064

statistics calculated for these packings by the previous loose packing model. However, very few differences were noted in the tetrahedron density and edge length distributions calculated by the different simulations for all the sphere distributions. The degree to which the individual tetrahedron model was able to simulate the same tetrahedron edges as the loose packing model is shown, for the three-size uniform distribution, by the points in figure 40. Without exception, similar or even better agreement between the two simulations was achieved for all the sphere distributions.

The ability to use individual tetrahedra to arrive at bulk packing properties offers much new insight into the statistical geometry of loose random packings. Besides the distributions of tetrahedron edges, gaps, densities, and pore sizes that are predictable for space-filling individual tetrahedra by the methods developed in this investigation, other statistical geometry properties could have been calculated. Thus, for any packing of any particle size distribution, a unique method now exists for studying almost all the relevant packing parameters influencing the packing behavior of that particulate system. The uniqueness arises from the fact that the individual tetrahedra simulate the simplices in the Delaunay, or simplicial, graph of a packing, which by definition is a unique construction for any packing. Moreover, the method described can be easily performed on any computing machine, and it requires only an introductory knowledge of computer programing.

☆ U.S. GOVERNMENT PRINTING OFFICE: 1971 O—423-411